AD-A131 462 YC-15 EBF (EXTERNALLY-BLOWN FLAP) STOL (SHORT TAKEOFF AND LANDING) AIRPLA..(U) AIR FORCE WRIGHT AERONAUTICAL LABS WRIGHT-PATTERSON AFB OH V R MILLER MAY 83 1/1

UNCLASSIFIED AFWAL-TM-83-170-FIBE F/G 1/3 NL

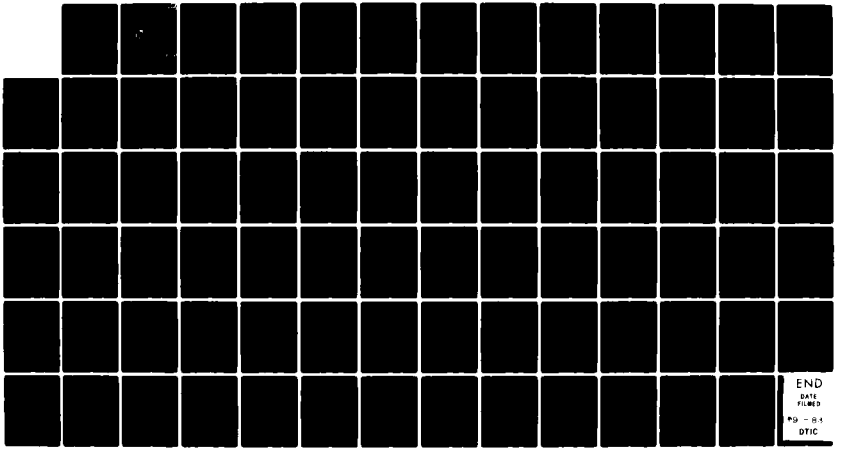

END

DATE FILMED

8 - 83

DTIC

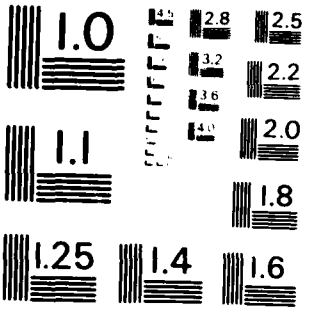

AFWAL-TM - 83 - 170 - FIBE

YC-15 EBF STOL AIRPLANE FUSELAGE AND INTERIOR NOISE ENVIRONMENT

V.R. Miller

May 1983

Approved for public release; distribution unlimited

FLIGHT DYNAMICS LABORATORY
AIR FORCE WRIGHT AERONAUTICAL LABORATORIES
WRIGHT-PATTERSON AIR FORCE BASE, OHIO 45433

NOTICE

When Government drawings, specifications, or other data are used for any purpose other than in connection with a definitely related Government procurement operation, the United States Government thereby incurs no responsibility nor any obligation whatsoever; and the fact that the government may have formulated, furnished, or in any way supplied the said drawings, specifications, or other data, is not to be regarded by implication or otherwise as in any manner licensing the holder or any other person or corporation, or conveying any rights or permission to manufacture use, or sell any patented invention that may in any way be related thereto.

This report has been reviewed by the Office of Public Affairs (ASD/PA) and is releasable to the National Technical Information Service (NTIS). At NTIS, it will be available to the general public, including foreign nations.

This technical report has been reviewed and is approved for publication.

VINCENT R. MILLER
Project Engineer
Acoustics & Sonic Fatigue Group

HOWARD F. WOLFE
Technical Manager
Acoustics & Sonic Fatigue Group

DAVEY L. SMITH, Chief
Structural Integrity Branch

"If your address has changed, if you wish to be removed from our mailing list, or if the addressee is no longer employed by your organization please notify AFWAL/FIBE, *W-PAFB, OH 45433 to help us maintain a current mailing list".*

Copies of this report should not be returned unless return is required by security considerations, contractual obligations, or notice on a specific document.

Unclassified

SECURITY CLASSIFICATION OF THIS PAGE (When Data Entered)

REPORT DOCUMENTATION PAGE		READ INSTRUCTIONS BEFORE COMPLETING FORM
1. REPORT NUMBER AFWAL-TM-83-170-FIBE	2. GOVT ACCESSION NO. AD-A131462	3. RECIPIENT'S CATALOG NUMBER
4. TITLE (and Subtitle) YC-15 EBF STOL Airplane Fuselage and Interior Noise Environment		5. TYPE OF REPORT & PERIOD COVERED Final Report October 1931-February 1983 6. PERFORMING ORG. REPORT NUMBER
7. AUTHOR(s) V.R. Miller		8. CONTRACT OR GRANT NUMBER(s)
9. PERFORMING ORGANIZATION NAME AND ADDRESS Flight Dynamics Laboratory AFWAL/FIBE Wright-Patterson AFB OH 45433		10. PROGRAM ELEMENT, PROJECT, TASK AREA & WORK UNIT NUMBERS 24010146
11. CONTROLLING OFFICE NAME AND ADDRESS		12. REPORT DATE May 1983 13. NUMBER OF PAGES 80
14. MONITORING AGENCY NAME & ADDRESS(if different from Controlling Office)		15. SECURITY CLASS. (of this report) Unclassified 15a. DECLASSIFICATION DOWNGRADING SCHEDULE

16. DISTRIBUTION STATEMENT (of this Report)

Approved for Public Release; Distribution Unlimited.

17. DISTRIBUTION STATEMENT (of the abstract entered in Block 20, if different from Report)

18. SUPPLEMENTARY NOTES

19. KEY WORDS (Continue on reverse side if necessary and identify by block number)

YC-15	Noise Reduction	Jet/Flap Interaction Noise
STOL	Externally Blown Flaps	
Acoustic Loads	Powered Lift Noise	
Aircraft Interior Noise	Structural Vibration	

20. ABSTRACT (Continue on reverse side if necessary and identify by block number)

The purpose of this effort was to investigate the exterior fuselage and interior noise of the USAF/McDonnell-Douglas YC-15 Advanced Medium-Range Short-Takeoff- and Landing Transport airplane. This aircraft employs an under-the-wing, externally-blown-flap powered lift system designed to create augmented lift, which creates an intense acoustic environment. The blowing of the flap produces higher noise levels at lower frequencies than does the jet alone, increasing the acoustic environment on the fuselage

DD FORM 1 JAN 73 1473 EDITION OF 1 NOV 65 IS OBSOLETE

Unclassified

SECURITY CLASSIFICATION OF THIS PAGE (When Data Entered)

Block #20 (cont')

and inside the cabin. A combination of exterior flush-mounted microphones, accelerometers, interior centerline and sidewall microphones were used during this investigation. Test conditions analyzed included takeoff, cruise, landing, taxi, and ground static over the full range of operating conditions. The effects of different flight parameters are displayed in the form of the octave, one-third octave, and narrowband plots and are compared to the changes on the acoustic environment.

FOREWORD

This work was performed by the Acoustics and Sonic Fatigue Group, Structures and Dynamics Division, Flight Dynamics Laboratory, Air Force- Wright Aeronautical Laboratories, Wright-Patterson AFB, Ohio. The work was performed under Project 2401, "Flight Vehicle Structures and Dynamics Technology," Work Unit 24010146, "Acoustics and Sonic Fatigue Research".

The work was performed by V.R. Miller of the Structural Integrity Branch. The author wishes to extend his appreciation to L.P. Vaughn, Capt L.G. Peck, and R.M. Shimovetz, who assisted or made valuable comments on this effort. Special acknowledgement is due Mmes. C. Spahr and B. Hudson for careful typing of the manuscript.

The manuscript was released in May 1983, as a technical memorandum.

TABLE OF CONTENTS

LIST OF FIGURES

LIST OF TABLES

I. INTRODUCTION

The YC-15 was one of the first Short Takeoff and Landing (STOL) airplanes to employ the use of the Under-the-Wing (UTW) Externally-Blown Flap (EBF) powered lift concept. It was recognized that the integration of the airframe with this type of propulsive concept, would require an extensive research program. As a part of this program, the noise/vibration environment of the structure of such an airplane needed to be explored. Part of the program included noise/vibration measurements on a full-scale vehicle. Testing included both ground (static) and flight test measurements. Part of the results have been published (Ref. 1 through 5), and include data on the pressure, temperature, and acoustic environments, as well as engine inlet acoustics and exterior fuselage and interior acoustic levels.

The purpose of this report was to investigate the exterior fuselage and the interior noise levels of the YC-15 airplane. This includes identifying the controlling sources of exterior and interior noise, the effects of speed and altitude on interior noise, and the noise reduction of the sidewall.

A description of the YC-15 airplane is contained in Section 2. Sections 3 and 4 discuss the data acquisition and reduction systems. The ground and flight test configurations and conditions that were conducted are given in Section 5. The results of the exterior and interior noise measurements are given in Section 6 with conclusions presented in Section 7.

II. AIRPLANE DESCRIPTION

The YC-15 (Figures 1 and 2) is a wide-bodied, high-wing, T-tailed military transport airplane. Four Pratt and Whitney JT8D-17 engines, rated at 16,000 lbs (71,168 N) thrust at sea level under static conditions, are mounted in a forward position just under the wing. The unswept wing embodies supercritical aerofoil technology. The high-lift system consists of a large chord, two-segment flap and full-span, leading-edge devices. The flaps are designed to penetrate the engine exhaust and deflect the engine efflux downward at the same angle as the flap. This is accomplished by a double four-bar linkage. The spoilers ahead of the flap are drooped to maintain a slot between the forward flap and the wing upper lip (spoiler trailing edge). The required lift is achieved from the deflected thrust and increased wing circulation.

The engines are installed in nacelles (no acoustic treatment) that are positioned such that the engine exhaust nozzles are forward of and just below the wing leading edge. The external mixer nozzle arrangement promotes good mixing of fan and primary exhaust air with freestream air to produce rapid temperature and velocity reduction. This spreads the exhaust wake over a large span of the flap.

The fuselage is a standard aircraft with mechanically riveted rib stringer construction. The airplane used did not contain interior acoustic absorptive material. A more detailed description of the airplane can be found in the flight test plans (Ref 6 and 7).

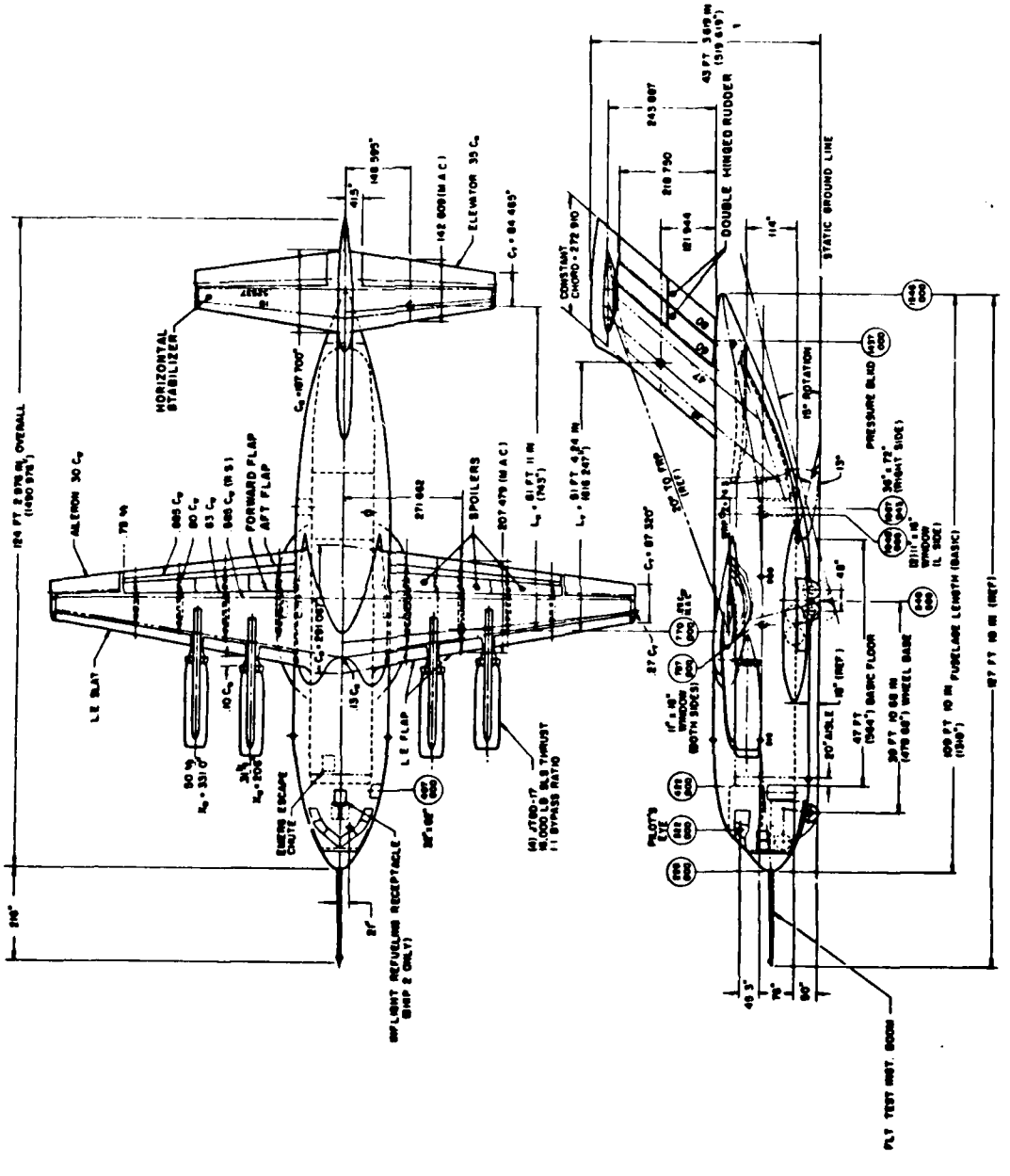

FIGURE 1 YC-15 AIRPLANE

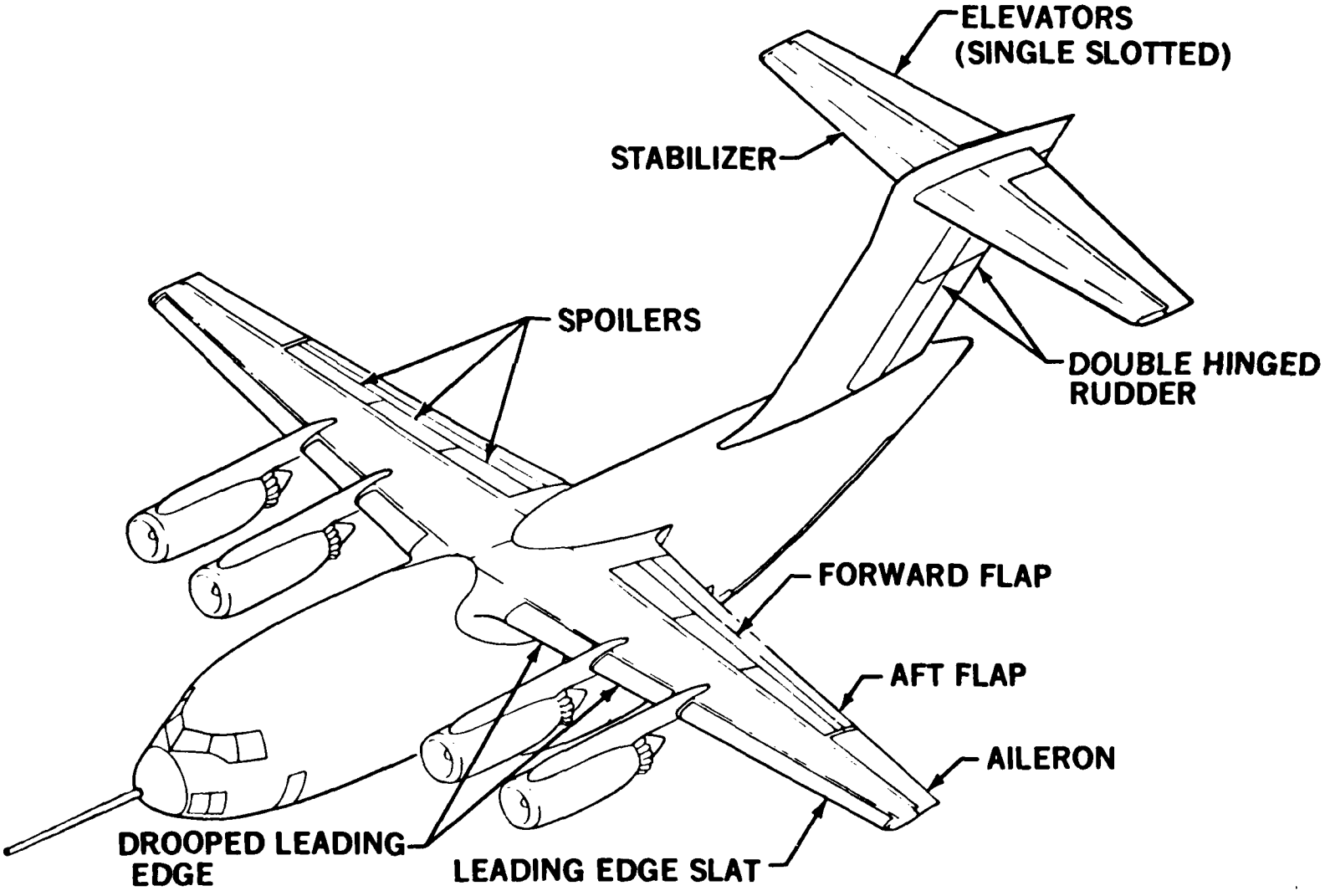

FIGURE 2 FLIGHT CONTROL SURFACES FOR YC-15

III. DATA ACQUISITION SYSTEM

The data acquisition system for the interior acoustic tests is diagrammed in Figure 3. Three basic transducer types were used to measure exterior acoustic loads, local fuselage vibrations, and interior noise levels. High intensity piezoelectric microphones were used for the acquisition of the exterior acoustic loads data. Fuselage vibration was measured with piezoelectric accelerometers with internal preamplifier and mating power supply. Interior noise equipment consisted of one-half inch diameter condenser microphone cartridges, microphone preamplifiers, power supplies, and signal conditioners.

The mounting system for the flush-mounted exterior microphones is shown in Figure 4. They were mounted so that the diaphragm of each exterior microphone was flush with the exterior skin of the aircraft.

The transducers were located as shown in Figure 5 (except for Microphone 9, the forward exterior flush-mounted microphone location) and listed in Table 1. The accelerometers were mounted one panel below the microphones where possible, in order to locate the accelerometers in the proximity of the flush-mounted microphones and reduce the effects of the microphone mounts.

More details on the data acquisition system can be found in the Appendix.

IV. DATA REDUCTION

Data processing was performed in two places: The Douglas Acoustics and Vibration Data Center at Long Beach, California; and later by the Flight Dynamics Laboratory, Structures and Dynamics Division at Wright-Patterson AFB, Ohio. More details are contained in the Appendix.

V. GROUND AND FLIGHT TEST CONDITIONS

Acoustic and vibration measurements were obtained during two testing periods. The first series consisted of simultaneously measuring the exterior fuselage noise levels, fuselage vibration, and interior noise levels. Both ground and flight tests were conducted in the first and second series measurements. These are shown in Table 2 and 3. The second series of test consisted of supplemental measurements made of the exterior fuselage noise levels.

Test No. G-1 was planned to provide a better understanding of the effects of flap and power settings on engine-and flap-generated noise. Tests G-2 and G-3 yield information regarding the contributory effects of the inboard and outboard engines to exterior fuselage and interior noise. The taxi test, G-4, provided information on forward speed effects.

Tests F-1 and F-3 provided takeoff and landing data and F-3 data (after liftoff), in comparison with G-4, permits evaluation of ground reflection effects. Tests F-2 and F-4, in conjunction with F-1 and F-3, provided additional data on the contributions of the inboard and outboard engines. Test F-5 provided data on the turbulent boundary layer and forward speed effects during cruise at 18,000 feet. Test F-6 provided data with high thrust and extended

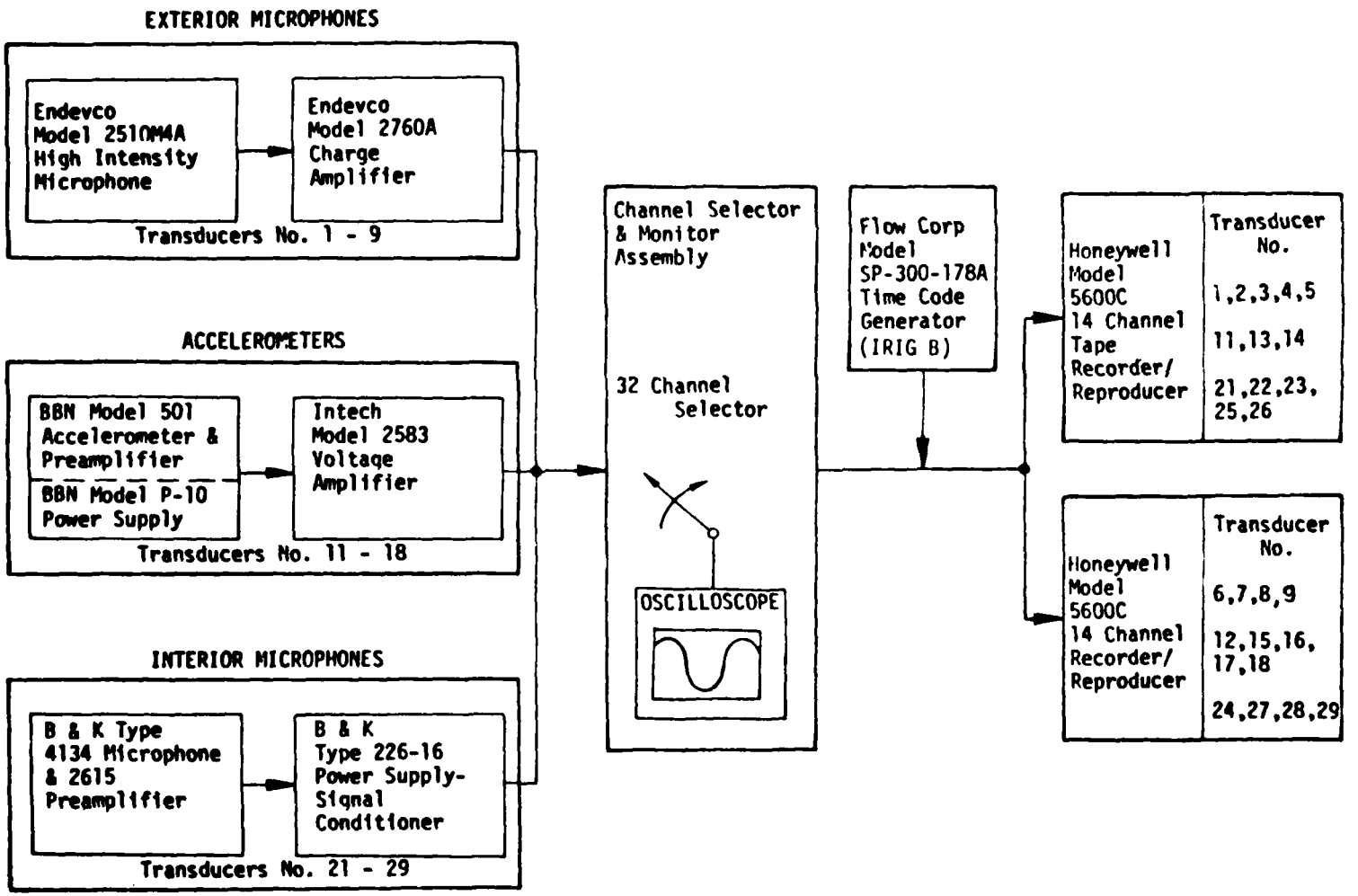

FIGURE 3 DATA ACQUISITION SYSTEM BLOCK DIAGRAM

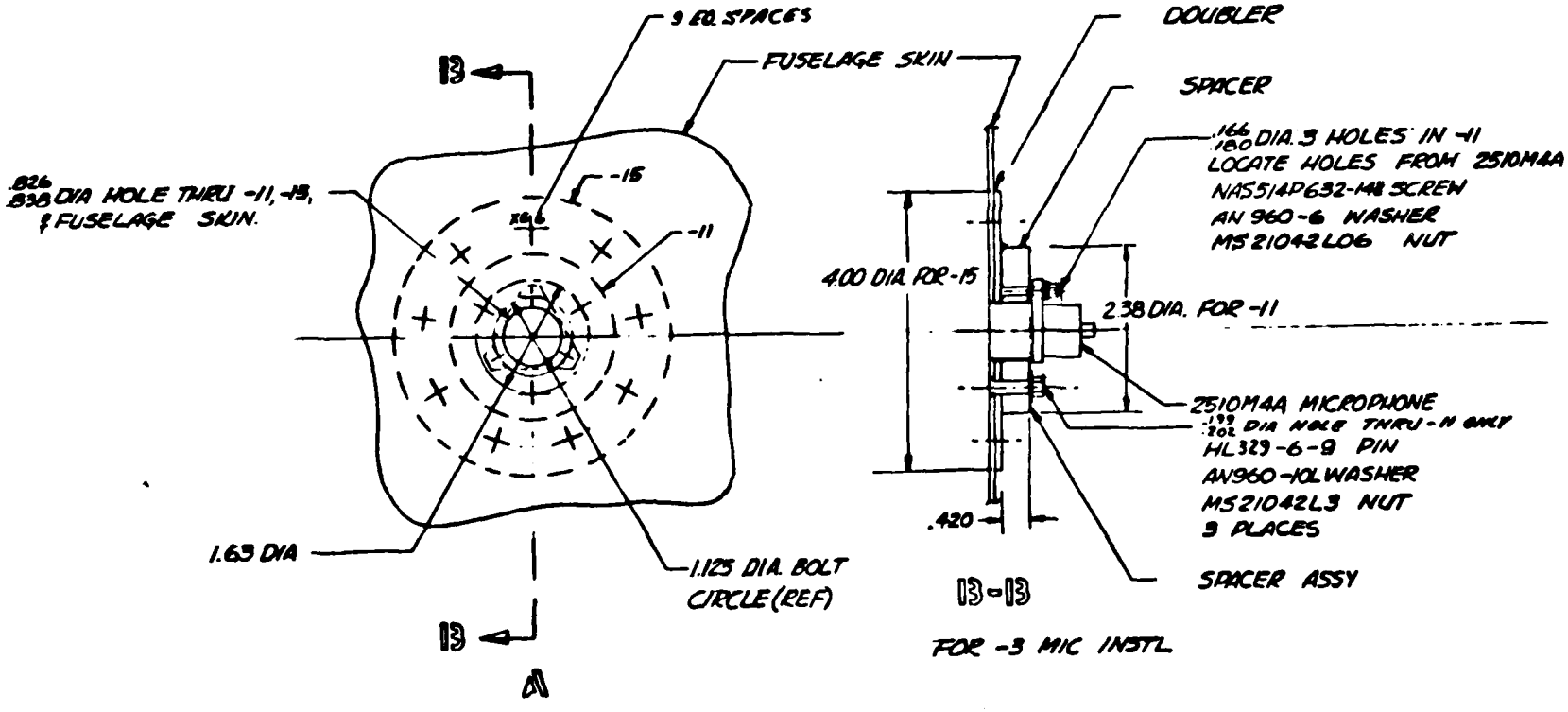

FIGURE 4 MOUNTING SYSTEM FOR FLUSH-MOUNTED EXTERIOR MICROPHONES

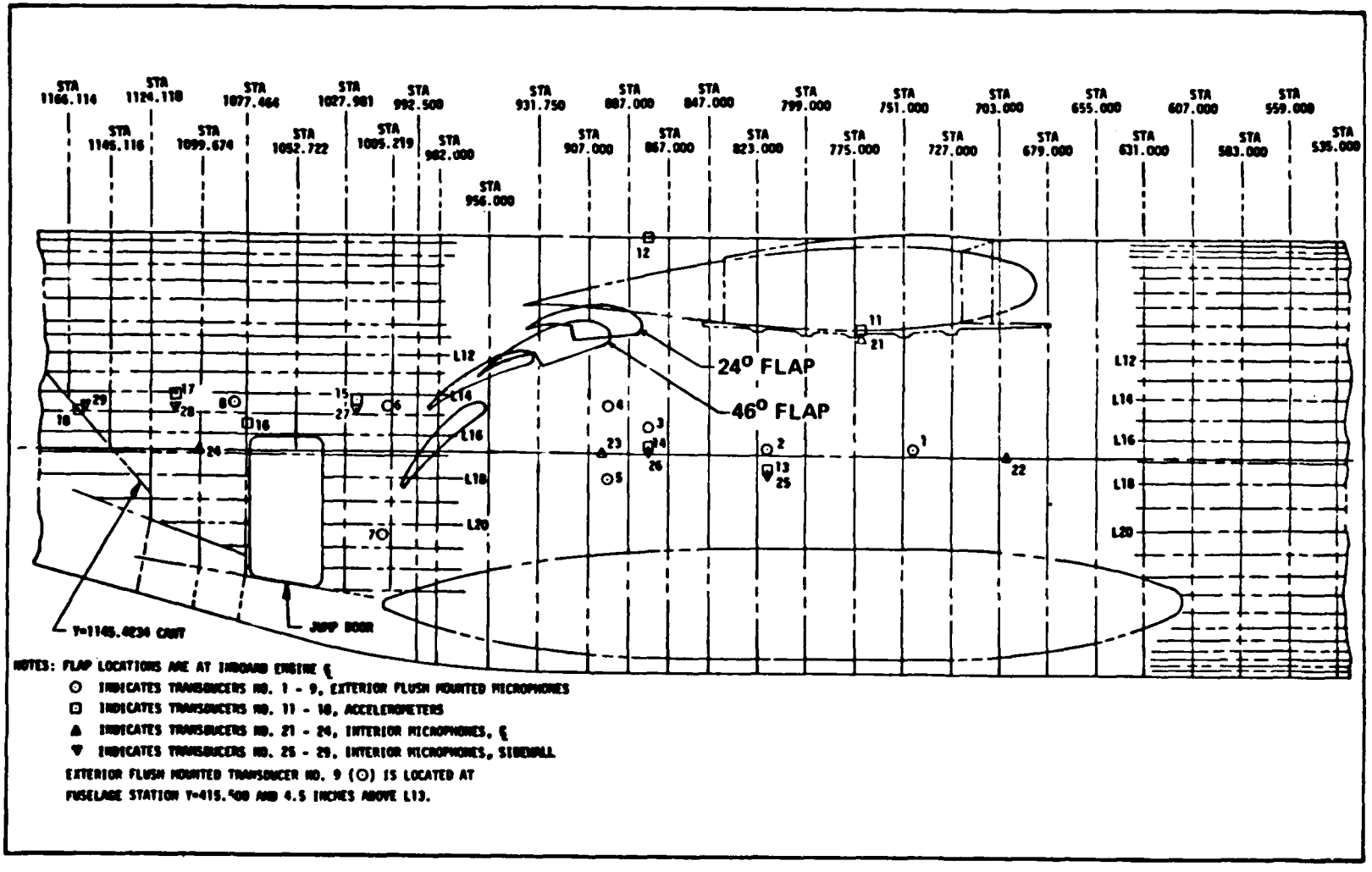

FIGURE 5 TRANSDUCER LOCATIONS

TABLE 1 TRANSDUCER LOCATIONS

TRANSDUCER NUMBER	TRANSDUCER TYPE	X*	Y*	Z*
1	Exterior Flush-Mounted Microphones	-108	745	3
2		-108	818	3
3		-107	877	13
4		-105	897	24
5		-108	897	-7
6		-105	1009	24
7		- 99	1014	-41
8		-103	1094	25
9		- 85	415	43
11	Accelerometers	- 45	773	55
12		- 45	877	97
13		-108	818	-7
14		-108	877	3
15		-106	1020	24
16		- 94	1077	13
17		-104	1104	14
18		- 86	1160	20
21	Interior Centerline Microphones	- 45	769	53
22		0	700	0
23		0	900	0
24		0	1100	0
25	Interior Sidewall Microphones	-104	818	-7
26		-104	877	3
27		-102	1020	24
28		-100	1104	14
29		- 86	1145	18

* Airplane coordinates
Note: All dimensions inches

TABLE 2 GROUND TESTS

TEST NO.	FLAP ANGLE	ENGINE NO. @ EPR[b]	THRUST[a] LBS (N)	
G.1-1	1°	1,2,3,4 @ 1.05	1,000 (4400)	First Series
G-1.2	1°	1,2,3,4 @ 1.59	9,100 (40,500)	
G-1.3	1°	1,2,3,4 @ 1.89	12,600 (56,000)	
G-1.4	1°	1,2,3,4 @ 2.21	16,200 (72,100)	
G-1.5	23°	1,2,3,4 @ 1.06	1,000 (4400)	
G-1.6	23°	1,2,3,4 @ 1.59	9,100 (40,500)	
G-1.7	23°	1,2,3,4 @ 1.90	12,800 (56,900)	
G-1.8	23°	1,2,3,4 @ 2.21	16,400 (73,000)	
G-1.9	46°	1,2,3,4 @ 1.06	1,000 (4400)	
G-1.10	47°	1,2,3,4 @ 1.39	6,400 (28,500)	
G-2.2	1°	1,4 @ 1.57	8,900 (39,600)	
G-2.3	1°	1,4 @ 1.89	12,600 (56,000)	
G-2.4	1°	1,4 @ 2.20	16,000 (71,200)	
G-2.6	23°	1,4 @ 1.59	9,100 (40,500)	
G-2.7	23°	1,4 @ 1.88	12,500 (55,600)	
G-2.8	22°	1,4 @ 2.19	15,900 (70,700)	
G-2.10	47°	1,4 @ 1.58	9,000 (40,000)	
G-3.1	23°	2,3 @ 1.90	12,800 (56,900)	
G-3.2	24°	2,3 @ 2.20	16,000 (71,200)	
G-3.4	1°	2,3 @ 2.19	15,900 (70,700)	
G-4	48°	1,2,3,4 @ 2.20		
G-1.1	0°	1,2,3,4 @ 1.05	1,000 (4400)	Second Series
G-1.2	0°	3,4 @ 1.55	8,500 (38,300)	
G-1.3	0°	3,4 @ 1.85	12,200 (54,300)	
G-1.4	0°	3,4 @ 2.21	16,100 (71,600)	
G-1.5	21°	1,2,3,4 @ 1.05	1,000 (4400)	
G-1.6	21°	3,4 @ 1.55	8,600 (38,300)	
G-1.7	21°	3,4 @ 1.85	12,200 (54,300)	
G-1.8	21°	3,4 @ 2.21	16,100 (71,600)	
G-1.9	47°	1,2,3,4 @ 1.05	1,000 (4400)	
G-1.10	45°	3,4 @ 1.55	8,600 (38,300)	
G-2.2	0°	1,4 @ 1.55	8,600 (38,300)	
G-2.3	0°	1,4 @ 1.85	12,200 (54,300)	
G-2.4	0°	1,4 @ 2.21	16,100 (71,600)	
G-2.6	22°	1,4 @ 1.55	8,600 (38,300)	
G-2.7	22°	1,4 @ 1.85	12,200 (54,300)	
G-2.8	22°	1,4 @ 2.21	16,100 (71,600)	
G-2.10	46°	1,4 @ 1.55	8,600 (38,300)	
	0°	2,3 @ 1.55	8,600 (38,300)	
	0°	2,3 @ 1.85	12,200 (54,300)	
	0°	2,3 @ 2.21	16,100 (71,600)	
	22°	2,3 @ 1.55	8,600 (38,300)	
G-3.1	22°	2,3 @ 1.85	12,200 (54,300)	
G-3.2	22°	2,3 @ 2.21	16,100 (71,600)	
	47°	2,3 @ 1.55	8,600 (38,300)	
G-4	46°	1,2,3,4 @ 1.60	9,200 (40,900)	

NOTES: (a) Installed thrust values are for each engine mentioned.
(b) Unmentioned engines were operated at idle; EPR is average for engines mentioned.

TABLE 3 FLIGHT TESTS

TEST NO.	ALTITUDE FT (m)	SPEED KEAS (m/sec)	FLAP ANGLE	ENGINE NO.[a] @ EPR	
F-1	Field	0	23°	1,2,3,4 @ 2.20	First Series
F-2	Field	0	24°	1,2,4 @ 2.20	
F-3	Approach	85 (44)	48°	1,2,3,4 @ 1.60	
F-4	Approach	85 (44)	41°	1,2,4 @ 2.10	
F-5.1	18,022 (5493)	195 (101)	1°	1,2,3,4 @ 1.42	
F-5.2	17,897 (5455)	239 (123)	1°	1,2,3,4 @ 1.53	
F-5.3	17,908 (5458)	280 (144)	2°	1,2,3,4 @ 1.66	
F-5.4	17,883 (5451)	331 (171)	1°	1,2,3,4 @ 1.89	
F-6	Go Around Approach	100 (51)	48°	1,2,3,4 @ 1.40	
F-7.1	29,813 (9087)	248 (128)	3°	1,2,3,4 @ 2.01	
F-7.2	29,813 (9087)	248 (128)	3°	1,2,3,4 @ 2.01	
F-7.3	29,813 (9087)	248 (128)	3°	1,2,3,4 @ 2.01	
F-7.4	29,813 (9087)	248 (128)	3°	1,2,3,4 @ 2.01	
F-8	29,813 (9087)	248 (128)	3°	1,2,3,4 @ flight idle	
F-1	Field	0	24°	1,2,3,4 @ 2.21	Second Series
F-2	Field	0	24°	1,2,4 @ 2.21	
F-3	Approach	85 (44)	48°	1,2,3,4 @ 1.40	
F-4	Approach	85 (44)	46°	1,2,4 @ 1.70	
F-5.1	18,072 (5508)	192 (99)	0°	1,2,3,4 @ 1.42	
F-5.2	18,065 (5506)	245 (126)	0°	1,2,3,4 @ 1.60	
F-5.3	17,998 (5486)	287 (148)	0°	1,2,3,4 @ 1.68	
F-5.4	18,035 (5497)	326 (168)	0°	1,2,3,4 @ 1.90	
F-6	Go Around Approach	100 (52)	24°	1,2,3,4 @ 2.10	
F-7.1	29,779 (9077)	238 (123)	0°	1,2,3,4 @ 2.01	

NOTES: (a) Unmentioned engines were operated at idle; EPR is average for engines mentioned.

flaps used in a "go-around approach". Test F-7 provided data during cruise at 30,000 feet. Data were obtained during a sequence of securing the air conditioning, the avionics cooling fans, and the fuel boost pumps. In an attempt to isolate the acoustic effects of on-board equipment, Test F-8 provided cruise data at 250 KEAS and 30,000 feet with all engines at idle to provide data on the effects of jet/engine noise and boundary layer noise on interior noise.

VI. RESULTS

6.1 General

An effort was reported in Reference 1, which made preliminary assessments of exterior fuselage and interior noise for the YC-15 EBF STOL airplane. Some of the trends observed from this effort are summarized in Figures 6 and 7. The highest noise levels on the exterior and in the cabin occur close to and aft of the engine exhaust exit plane where the exhaust flow appears to impinge and/or scrub on the fuselage (Figure 6). This suggests that the noise levels for the aft fuselage and cabin are controlled by the engine sources. The patterns of the exterior and interior noise are similar for the conditions shown in Figure 6. This suggests that the interior noise is directly related to the exterior noise. Peak overall sound pressure levels on the exterior varied from 152 dB at takeoff to 133 dB at low speed cruise. The sound pressure levels for these same two conditions in the center-aisle aft cabin were 127 and 107 dB, respectively.

The overall sound pressure level as a function of thrust for a single engine and different flap settings for a center-aisle aft cabin microphone is shown in Figure 7. The ground static and flight data indicate a relationship between overall levels and engine gross thrust to be $p^2 \propto (F/\delta)^{3.8}$, where F is the thrust and δ is the relative absolute pressure. This holds for all values of thrust except at idle. The idle values should be controlled by turbomachinery noise rather than aerodynamic noise, and are not expected to follow the same trend.

The various trends and results from Reference 7 are reviewed in the remainder of Section 6, with hopes of identifying new trends. Exterior fuselage noise is discussed in Section 6.2. Section 6.3 contains discussion on the fuselage wall vibration and how it is related to the noise environment. The interior cabin noise environment is discussed in Section 6.4, in which emphasis will be placed on the observation (from Figure 6) that interior levels are dependent on the exterior environment. Interior noise prediction technology is discussed in Section 6.5.

6.2 External Fuselage Noise Field

6.2.1 Ground Test Results

The position of the flaps and the engine power settings has an effect on the exterior fuselage exterior noise field. In Figure 8(a), the variation in overall level indicates the dependence on distance from the engine flow field with changes in position of the flow field (which is dependent upon flap position). The effect of the flap setting is shown in part (b) of Figure 8. The

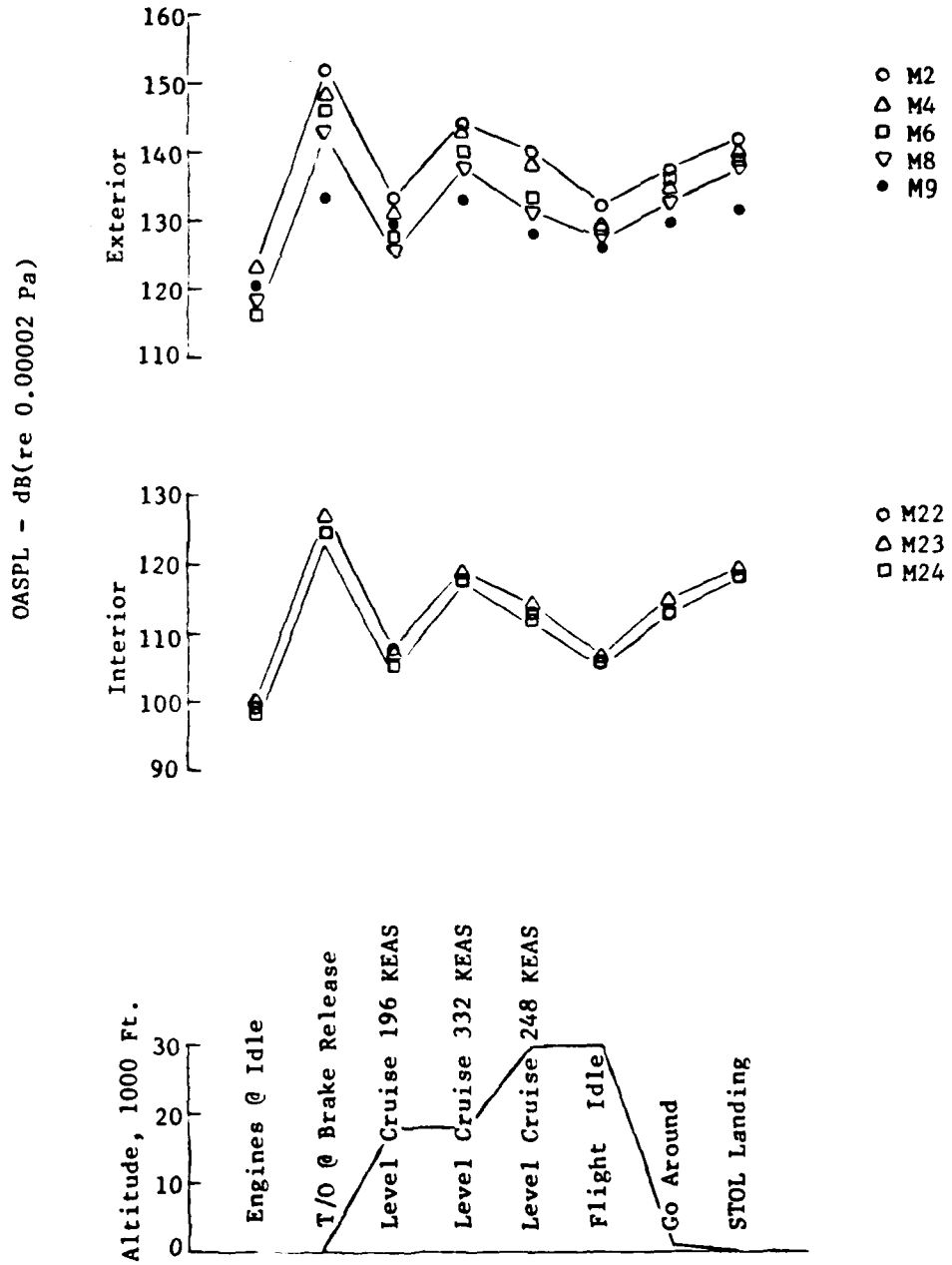

FIGURE 6 SUMMARY OF EXTERIOR AND INTERIOR NOISE LEVELS

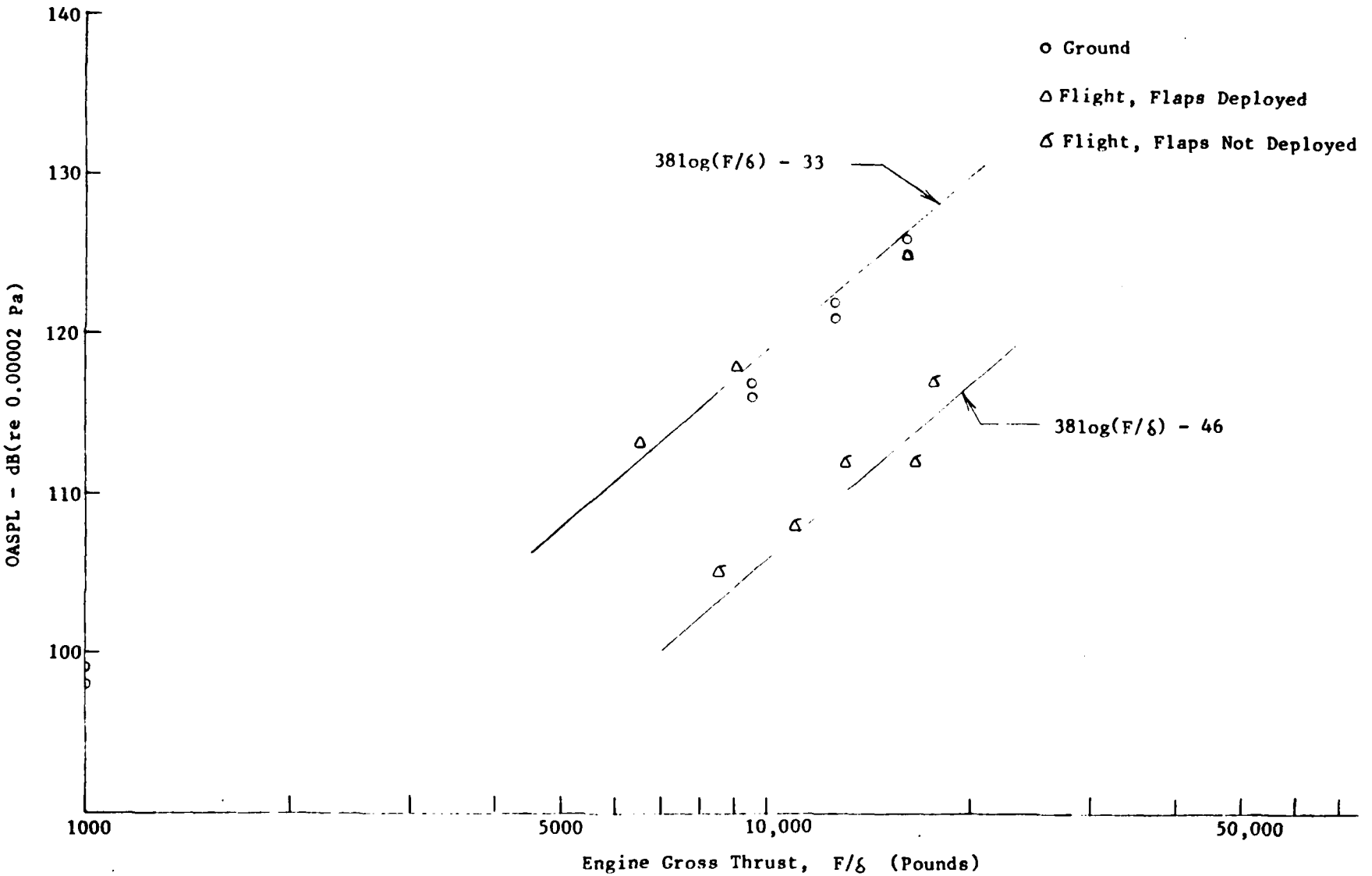

FIGURE 7 INTERIOR CABIN NOISE LEVELS WITH ALL ENGINES AT SAME THRUST - MICROPHONE 24

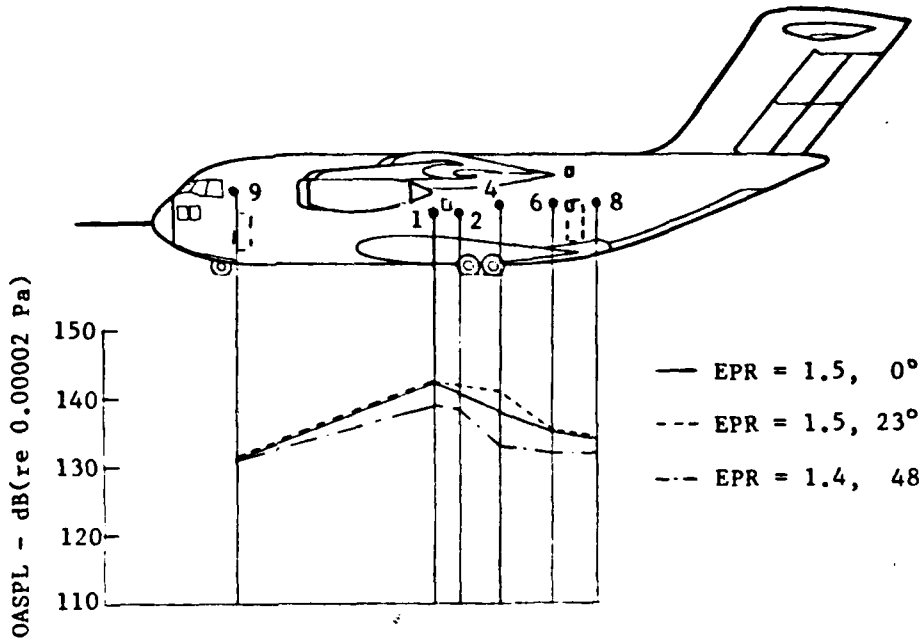

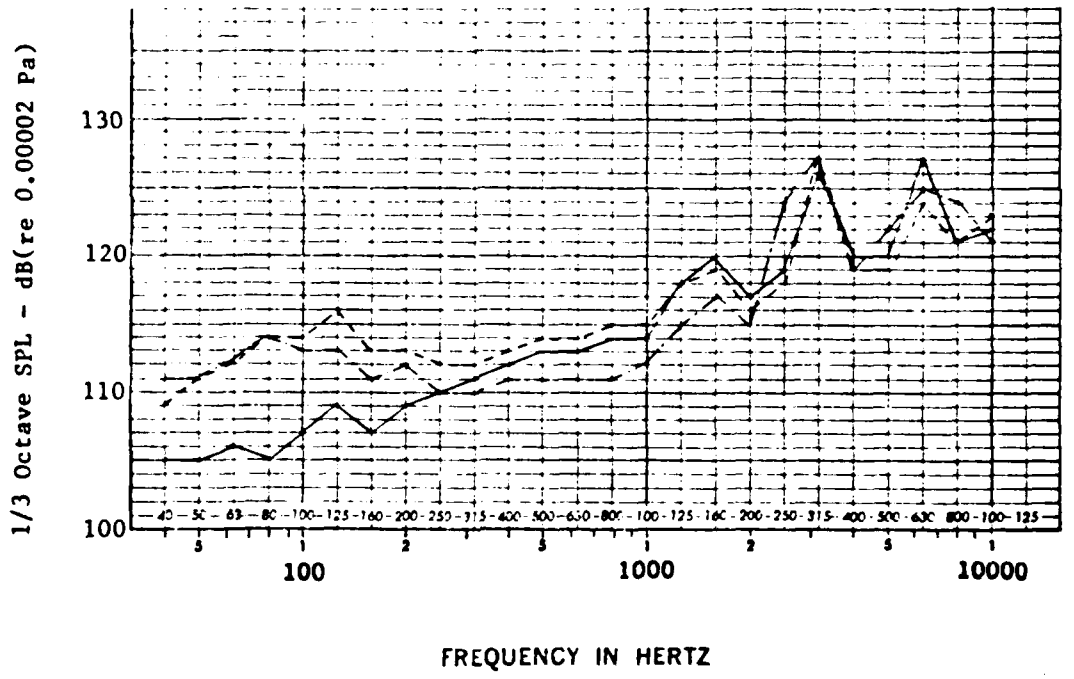

FIGURE 8 EFFECT OF FLAP SETTING ON EXTERIOR NOISE DURING GROUND STATIC

spectra exhibit distinctive low frequency content below 250 Hz, when the flaps are deployed. Further evidence of the flap setting on noise is shown in Figure 9. Even at this low power setting, the deployment of flaps increases the noise spectra, however at a much lower frequency band than for the previous figure, which is for a higher power setting.

Increasing the engine pressure ratio (EPR) is accompanied by an increase in thrust. EPR is used in this report only as a reference for engine thrust setting. The EPR varied from 1.0 at idle to 2.2 at full throttle (take-off thrust). Increasing thrust has already been shown to raise overall sound pressure levels. The effect of increasing thrust is reflected in the noise spectra (Figure 10). The levels are increased across the frequency region above 20 Hz. These same increases are reflected in the overalls. The effect of flaps is again evident when comparing plots in Figure 10. Increasing flap angle increases the overall levels, with this increase generally attributed to the low frequency region. The increases in the levels at the higher frequencies (>250 Hz) correlate with 38 log of thrust.

The contributory effects of the inboard and outboard engines to exterior fuselage noise for the ground static tests is shown in Figures 11 and 12. AT Microphone Location 8, the inboard environment is significantly greater (4-9 dB) than the outboard, but only in the frequencies below 250 Hz. This is true for both 1° and 23° flaps. For an exterior location closer to the jet exhausts (Microphone 7), this increase in acoustic environment of 4-9 dB is apparent all across the spectra. Not unexpectedly, the inboard acoustic environment on the fuselage is greater than the outboard. A comparison between inboard engines and all engines is also shown in Figures 11 and 12. All the engines' data for Microphone 4 are approximately 0-1 dB greater than the inboard data. This comparison suggests that the exterior fuselage noise is dominated by the inboard engines.

The characteristics of noise sources are determined based on static values. Aircraft motion does influence the noise generation and propagation of sources. The amount of influence depends on the noise source mechanism and the location of the source. The effect of aircraft motion on acoustic energy for propulsive lift systems is due to two sources: jet noise and lift augmentation noise (Figure 13). Jet noise is generated from the turbulent flow developed by the mixing of the jet exhaust with the ambient air. The noise source mechanisms of an EBF propulsive lift system are due to impingement, trailing edge, and trailing-edge wake. Impingement arises when a rigid surface is introduced into the flow. Jet flow leaving a trailing edge mixes with ambient air and generates high turbulence. The effect of forward speed on the fuselage noise for several microphone locations is shown in Figure 14. The effect of motion is greatest at the low and high frequencies, the largest difference being as much as 10 dB. Little motion effect is seen between 500 and 2000 Hz. The results from a generalized empirical relation in Reference 9, which gives the change in dB due to forward speed are also plotted on Figure 14. The incremental SPL is given by $dB = 50 \log (1 - V_a/V_j)$ where V_a and V_j are the aircraft and jet velocities, respectively. This correction term results in excellent agreement for the ground static and taxi curves between 250 and 2000 Hz. However, good agreement is lacking in the frequencies less than 125 Hz and greater than 2000 Hz.

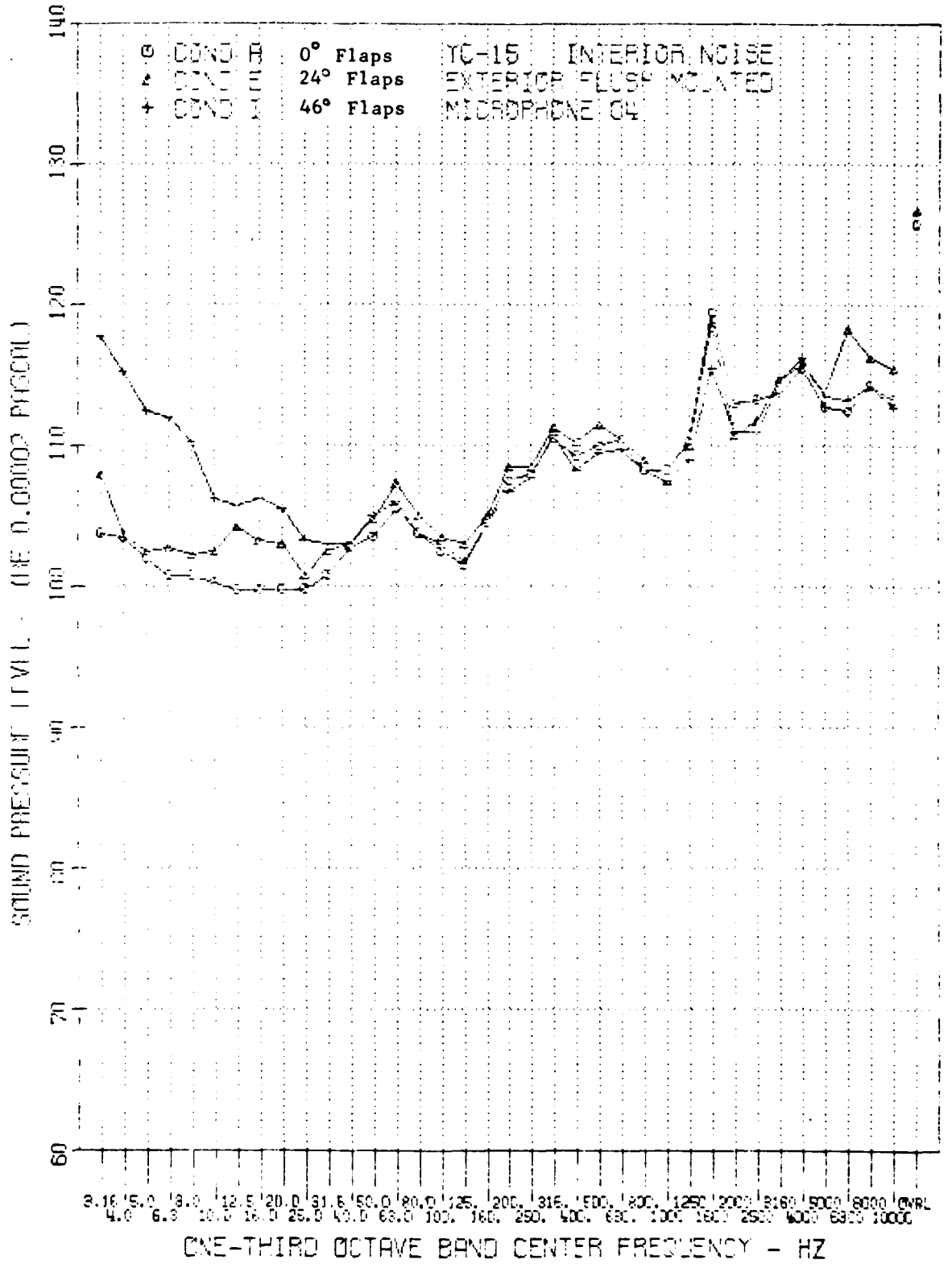

FIGURE 9 EFFECT OF FLAP SETTING ON EXTERIOR NOISE DURING GROUND STATIC WITH ALL ENGINES AT IDLE - MICROPHONE 4

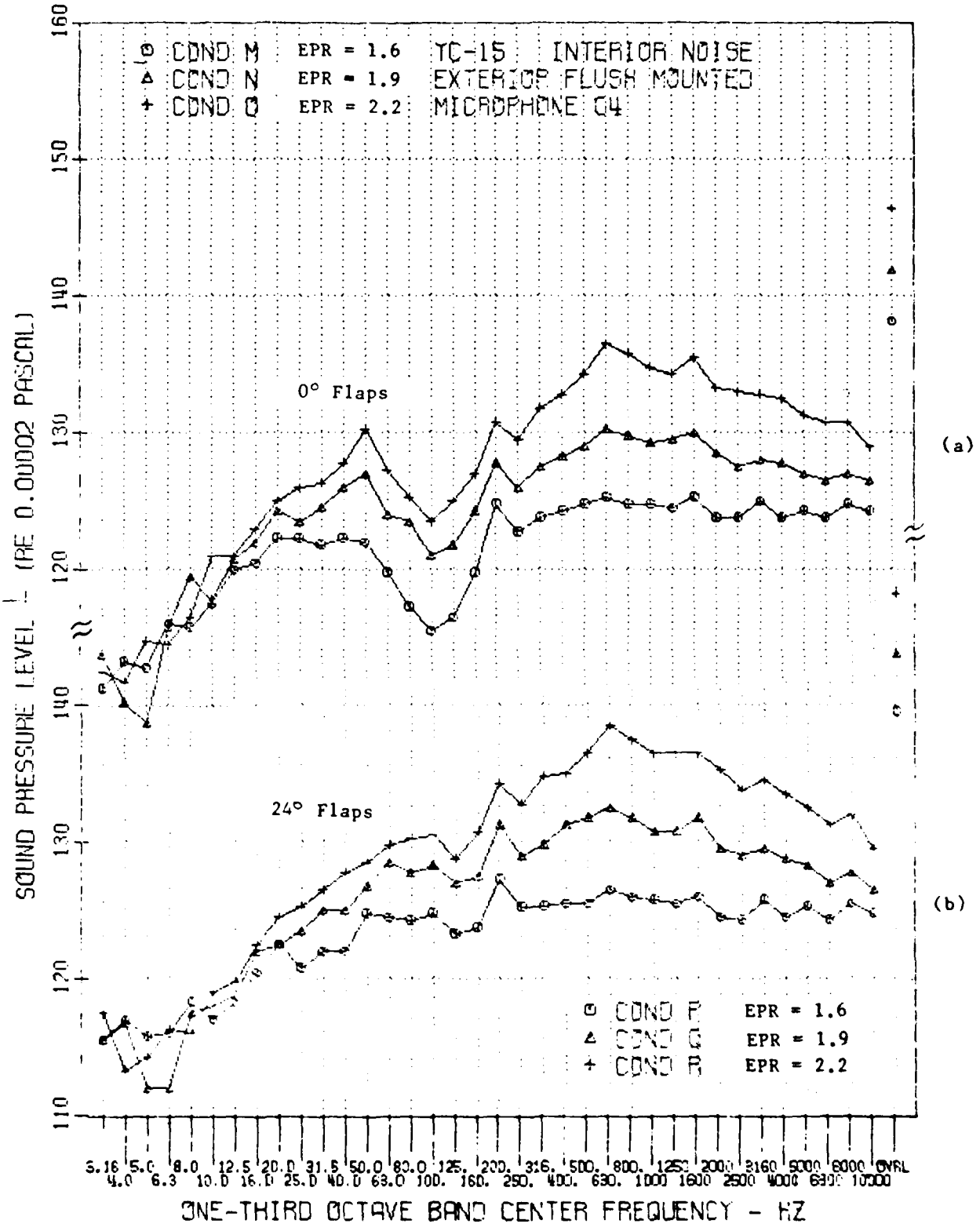

FIGURE 10 EFFECT OF INCREASING POWER SETTING ON EXTERIOR NOISE - MICROPHONE 4

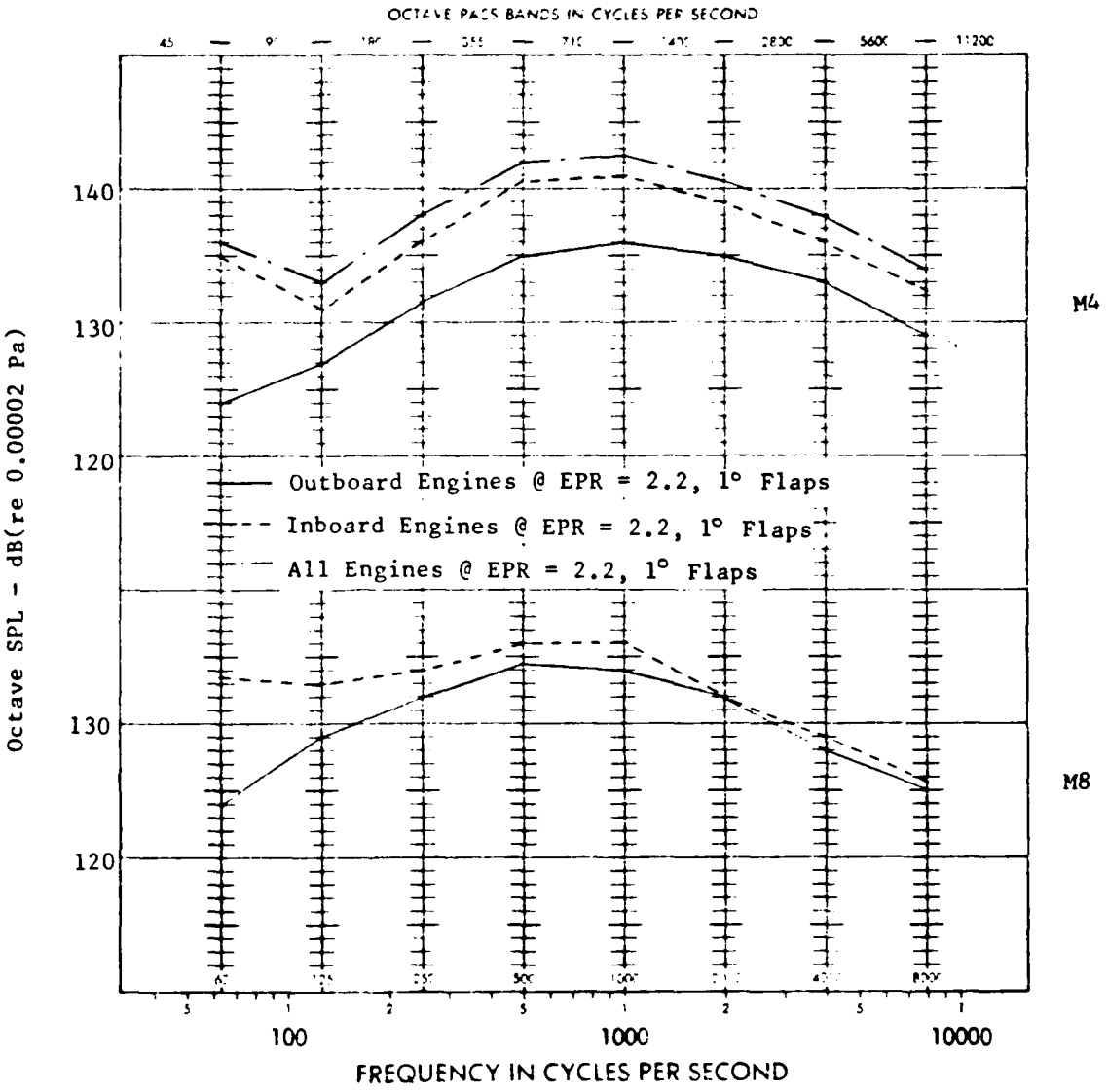

FIGURE 11 EFFECTS OF INBOARD AND OUTBOARD ENGINES ON EXTERIOR NOISE AT GROUND STATIC

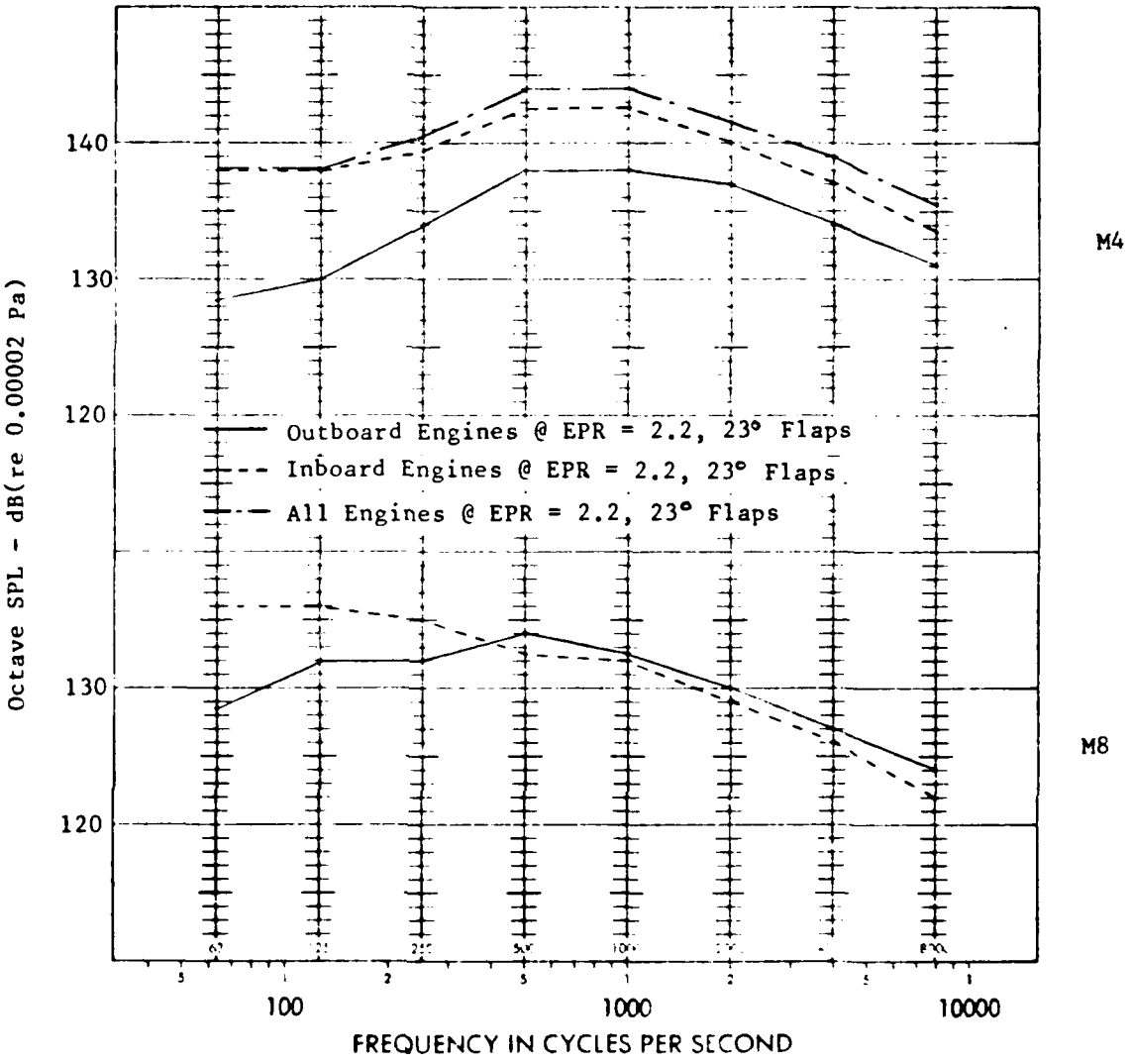

FIGURE 12 EFFECTS OF INBOARD AND OUTBOARD ENGINES ON EXTERIOR NOISE AT GROUND STATIC

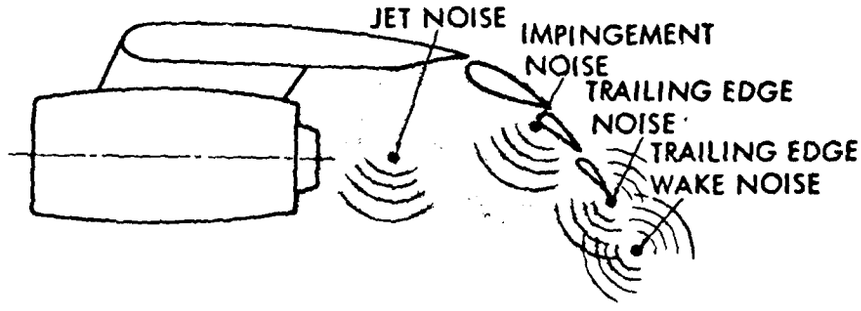

FIGURE 13 NOISE SOURCES OF EXTERNALLY-BLOWN FLAP SYSTEM

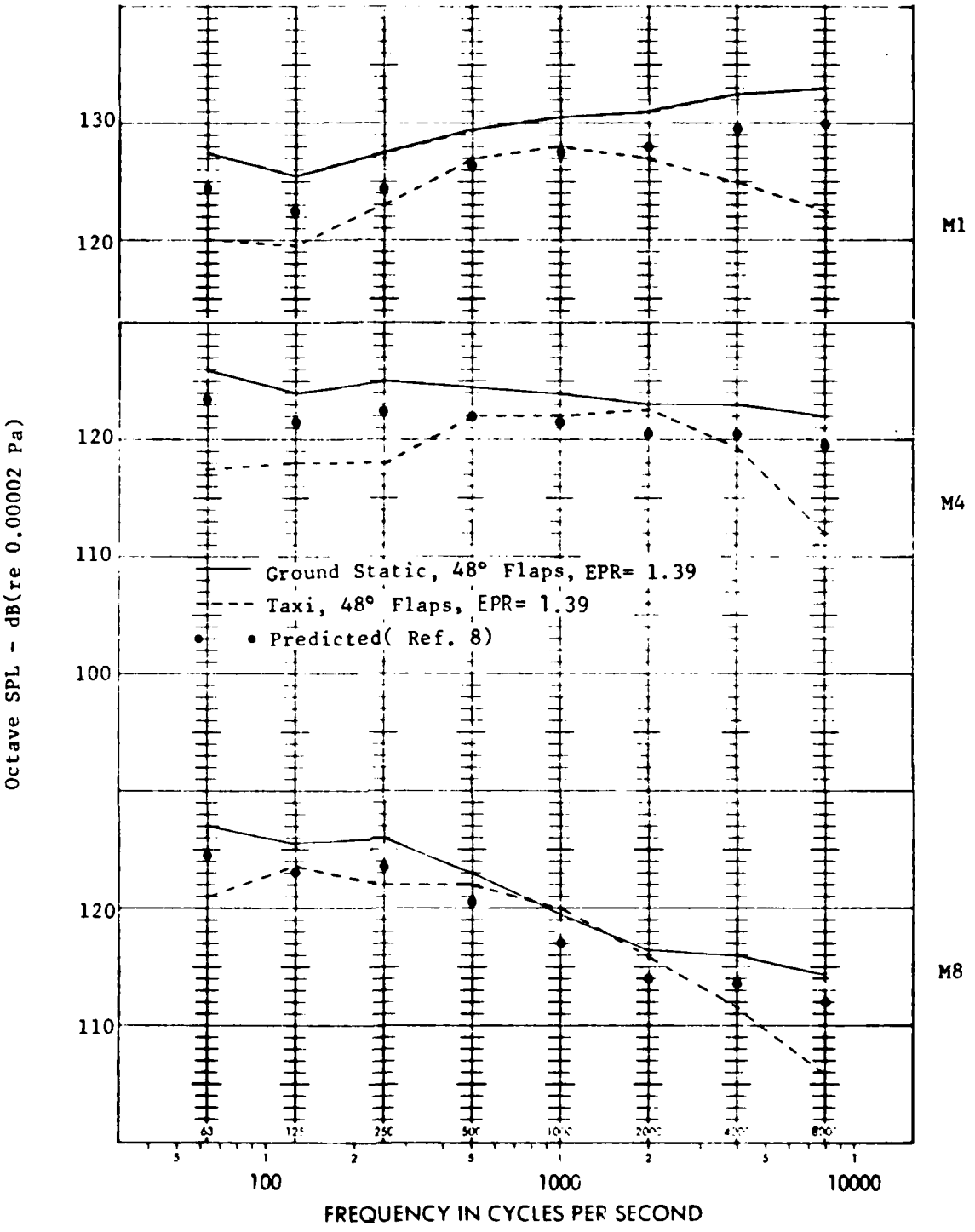

FIGURE 14 EFFECT OF FORWARD SPEED ON EXTERIOR FUSELAGE NOISE

Acoustic measurements taken in the vicinity of the ground are distorted as compared with free-field measurements. These effects consist of a series of cancellations and reinforcements in the measured spectra. These effects are functions of the acoustic impedance of the reflecting surface (the ground in this case), the location of the observer with respect to the source and reflecting surface, the size of the source, and the frequency. Comparing low level flight data with ground taxi data permits evaluation of ground reflection effects. This comparison is shown in Figure 15. The flight data which are plotted for an altitude 300 feet above the ground, have been corrected for forward speed effects in the manner discussed above. Cancellation is most prominent in the low and high frequencies, resulting in lower SPL's at microphone locations 2 and 4. Microphone 8 does not follow this, possibly due to the shielding effect of the flaps. The flaps were in the 48° position. Cancellation occurs in the lower frequencies for this microphone location.

6.2.2 Flight Test Results

Takeoff, STOL landing approach, and cruise are three representative flight conditions for the YC-15. These three conditions are shown for Microphone 8 in Figure 16(a). For frequencies less than 1000 Hz, the magnitude differences among the three curves is less than or equal to 11 dB. The landing curve shows higher values of low frequency noise with respect to the rest of its spectrum than for the other two curves. This is attributable to the low frequency noise generated by the blown flaps.

The relative contribution of inboard and outboard engines on typical takeoff noise is shown in Figure 16(b). The effect of one inboard engine at idle power is quite dramatic. The acoustic environment on the fuselage is reduced 6 to 12 dB at this location. These large differences occur across the entire spectrum and are typical for other measurement locations on the fuselage. The resulting interior noise field could be expected to be lowered by this same amount.

Increasing aircraft speed has an increase in SPL associated with it. Figure 17 shows this effect for cruise conditions at 18,000 feet altitude. Increasing velocity affects the entire spectrum as well as the overall. The incremental differences between the spectra can be approximated by 50 times the logarithm of the change in velocity (50 $\log \Delta V$) where $\Delta V = 1 - V_a/V_j$. This observation is consistent with other data comparisons made in the literature.

Figure 18 provides data with high thrust and extended flaps used in a go-around approach condition. The flaps are in the fully extended position (48°). Microphones ahead of the flaps (2,4,5) have a relatively flat spectrum shape. However, behind the flaps (Microphones 6 and 8), higher values of low frequency noise are exhibited in relation to the rest of its spectrum. This is due to the low frequency radiated noise generated by the blown flaps.

Additional cruise data were obtained at 30,000 feet, constant speed (248 KEAS), and 3° flaps. The effect of operating at a powered condition and flight idle is depicted in Figure 19. At normal cruise thrust, the engines dominate in all frequency bands. Idling the engines results in a much lower spectrum above 100 Hz. Since the flaps are not extended, no difference is seen in the lower frequencies. The flight idle curve is typical of turbulent

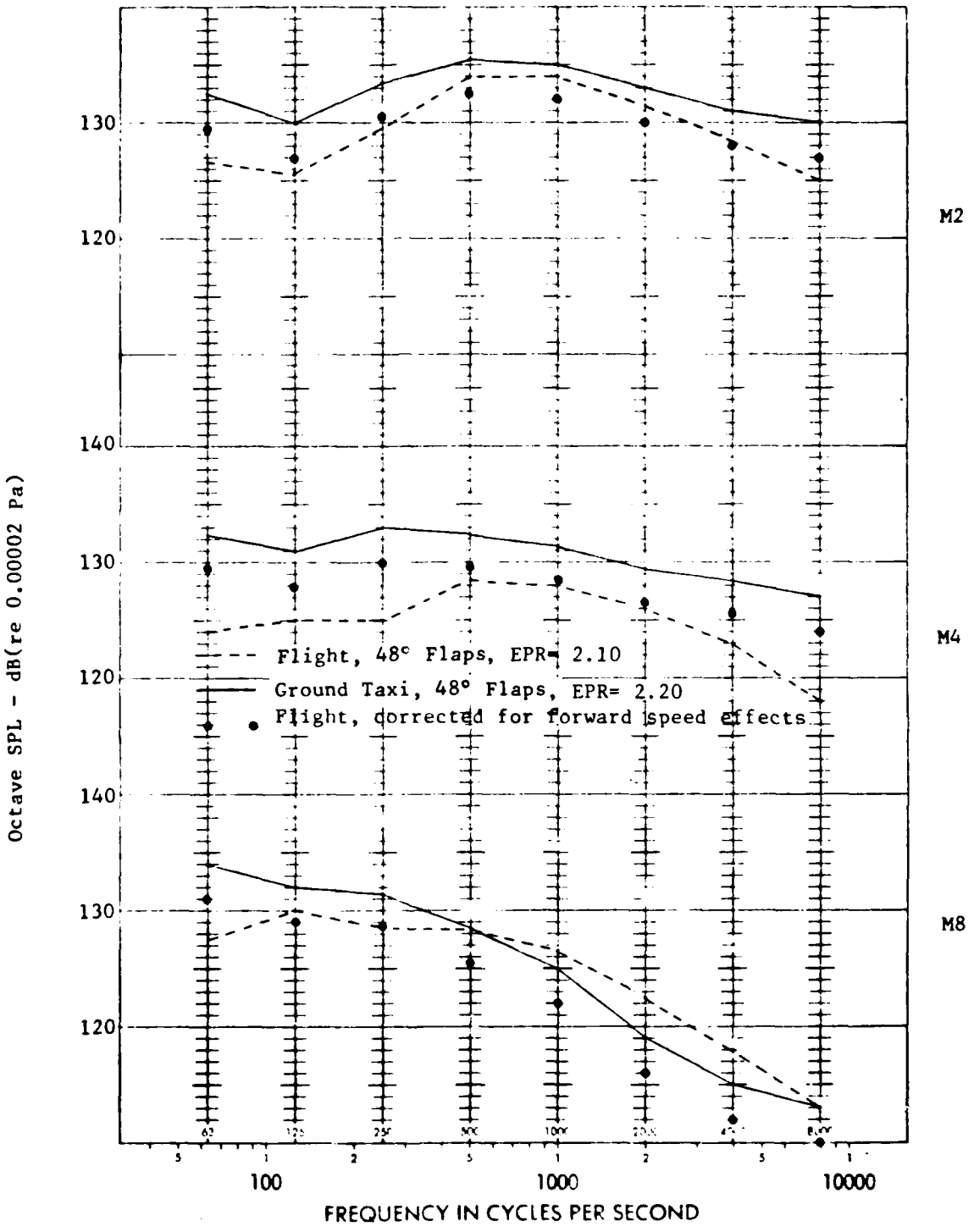

FIGURE 15 EFFECTS OF GROUND REFLECTION ON EXTERIOR FUSELAGE NOISE

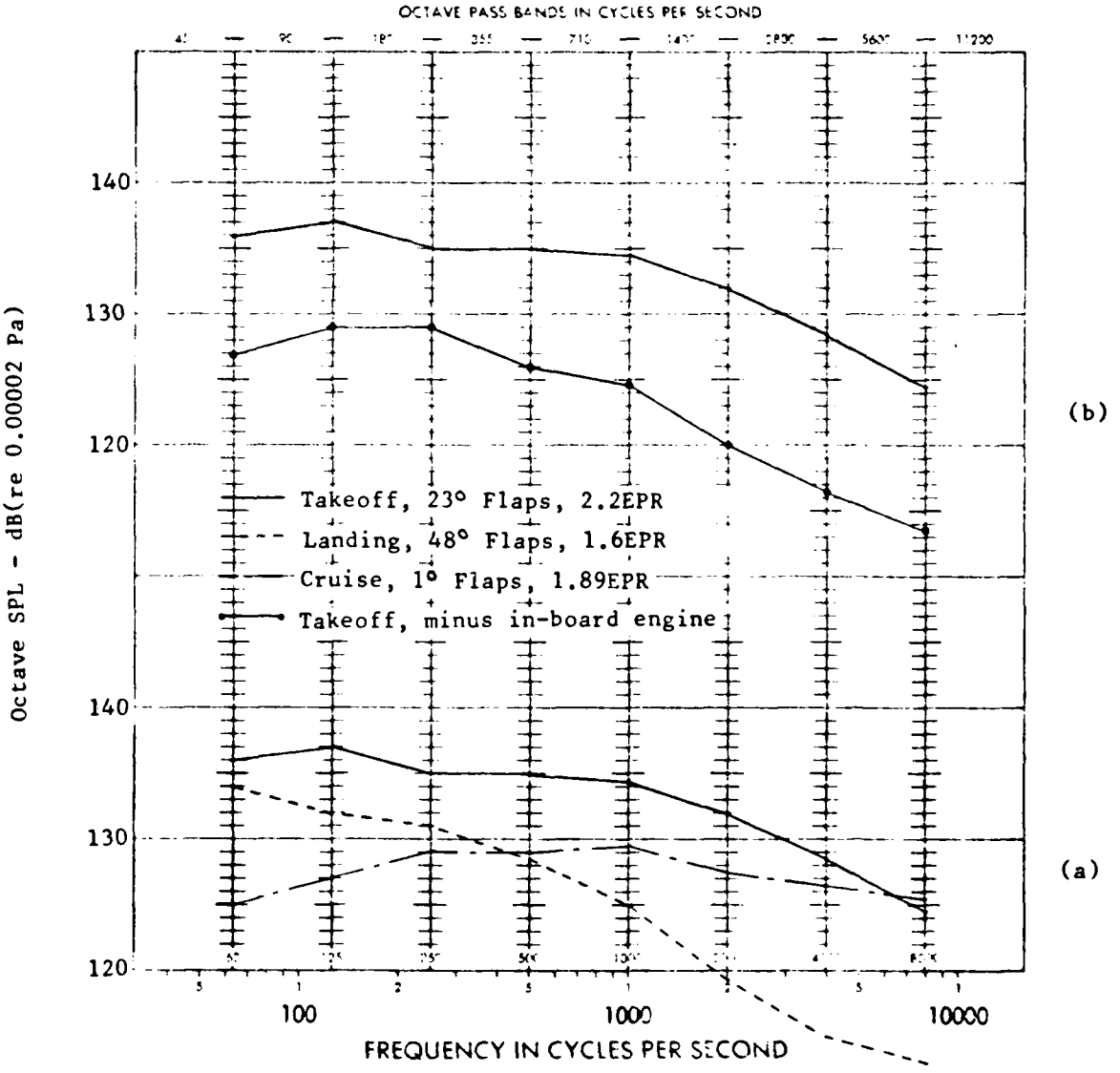

FIGURE 16 EXTERIOR FUSELAGE NOISE DURING DIFFERENT FLIGHT CONDITIONS - MICROPHONE 8

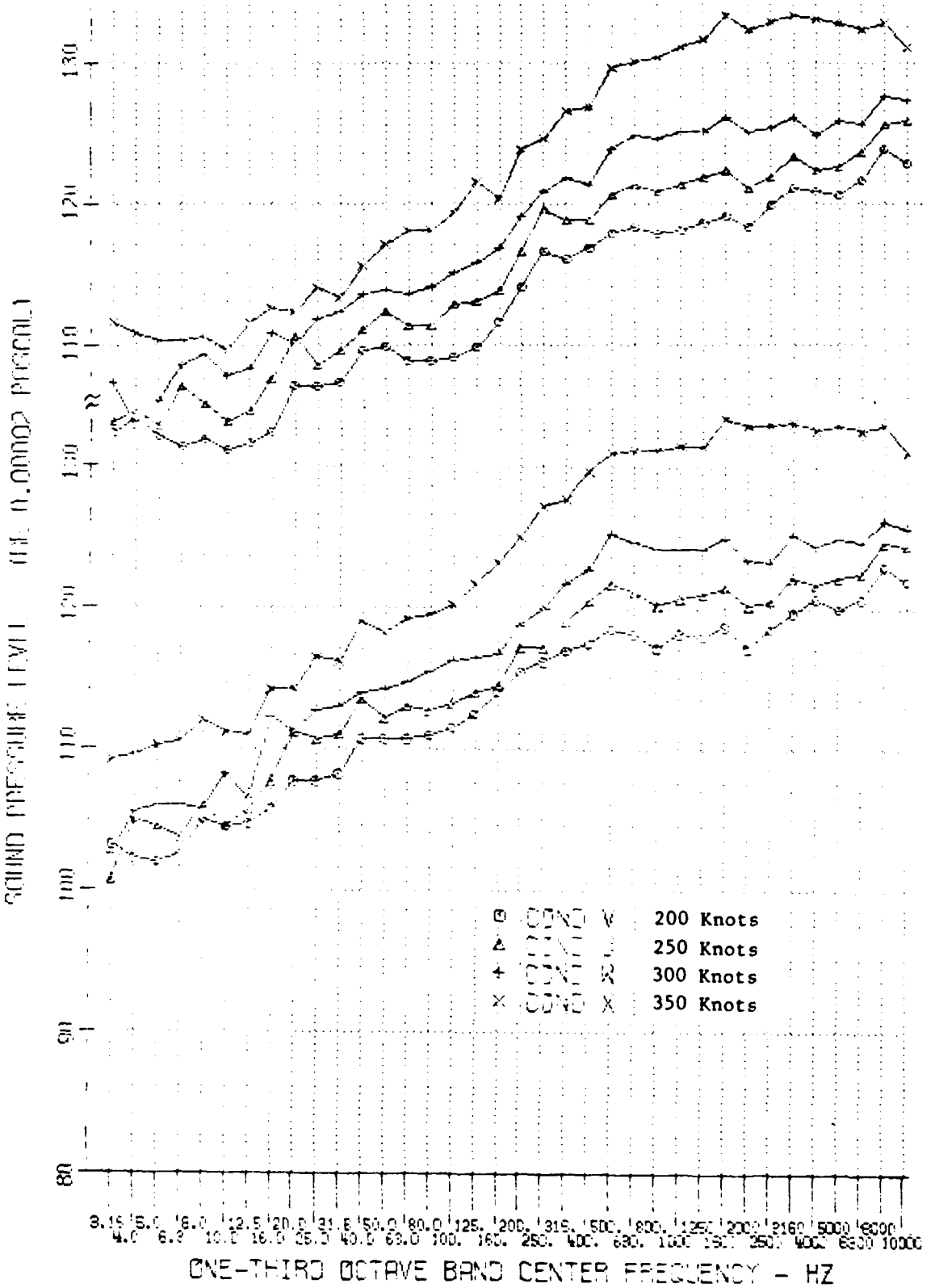

FIGURE 17 EFFECT OF FORWARD SPEED DURING CRUISE AT 18,000 FEET AND 1° FLAPS

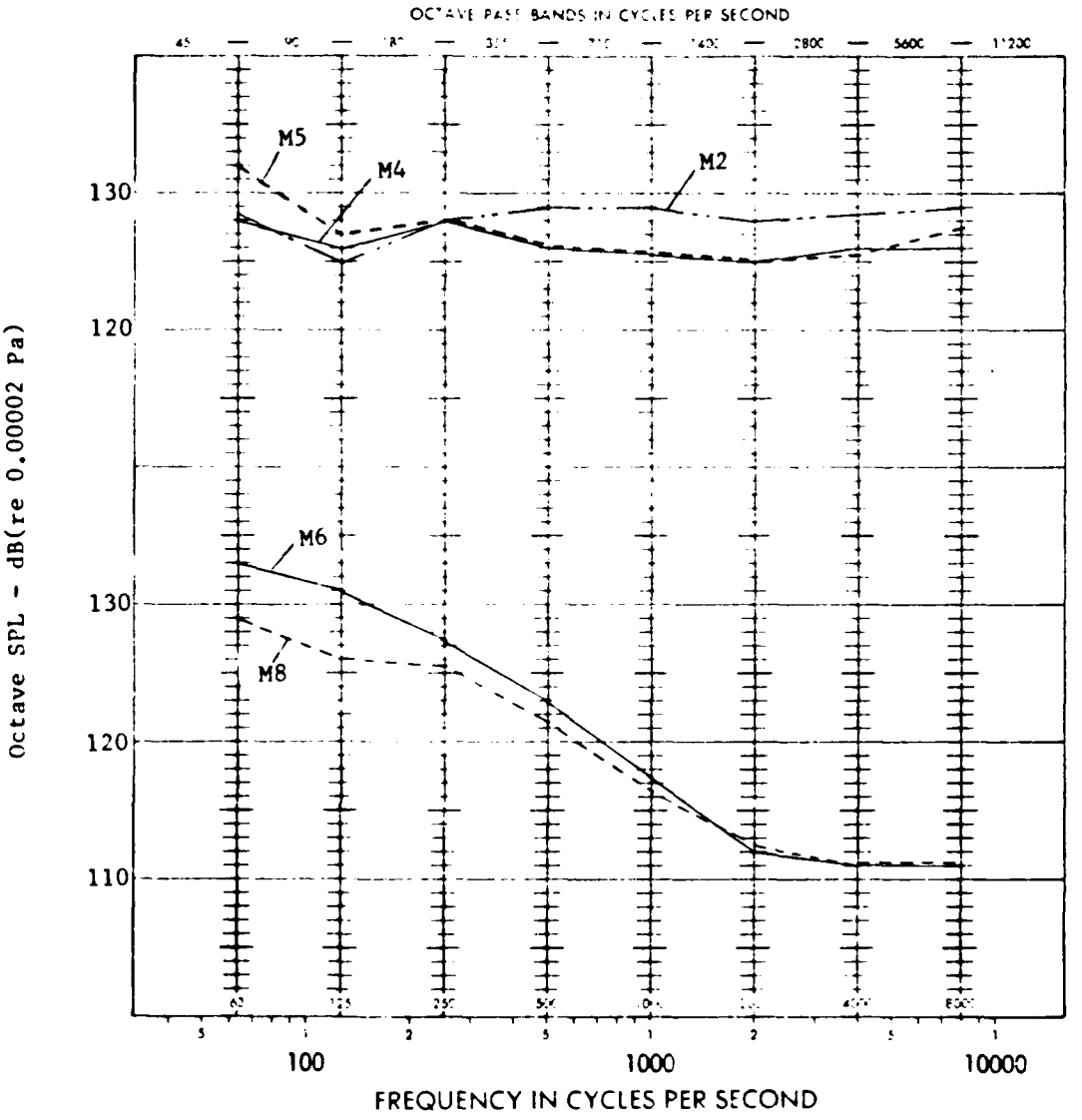

FIGURE 18 EXTERIOR FUSELAGE NOISE FOR GO-AROUND APPROACH - 48° FLAPS, 100KEAS, EPR= 1.40

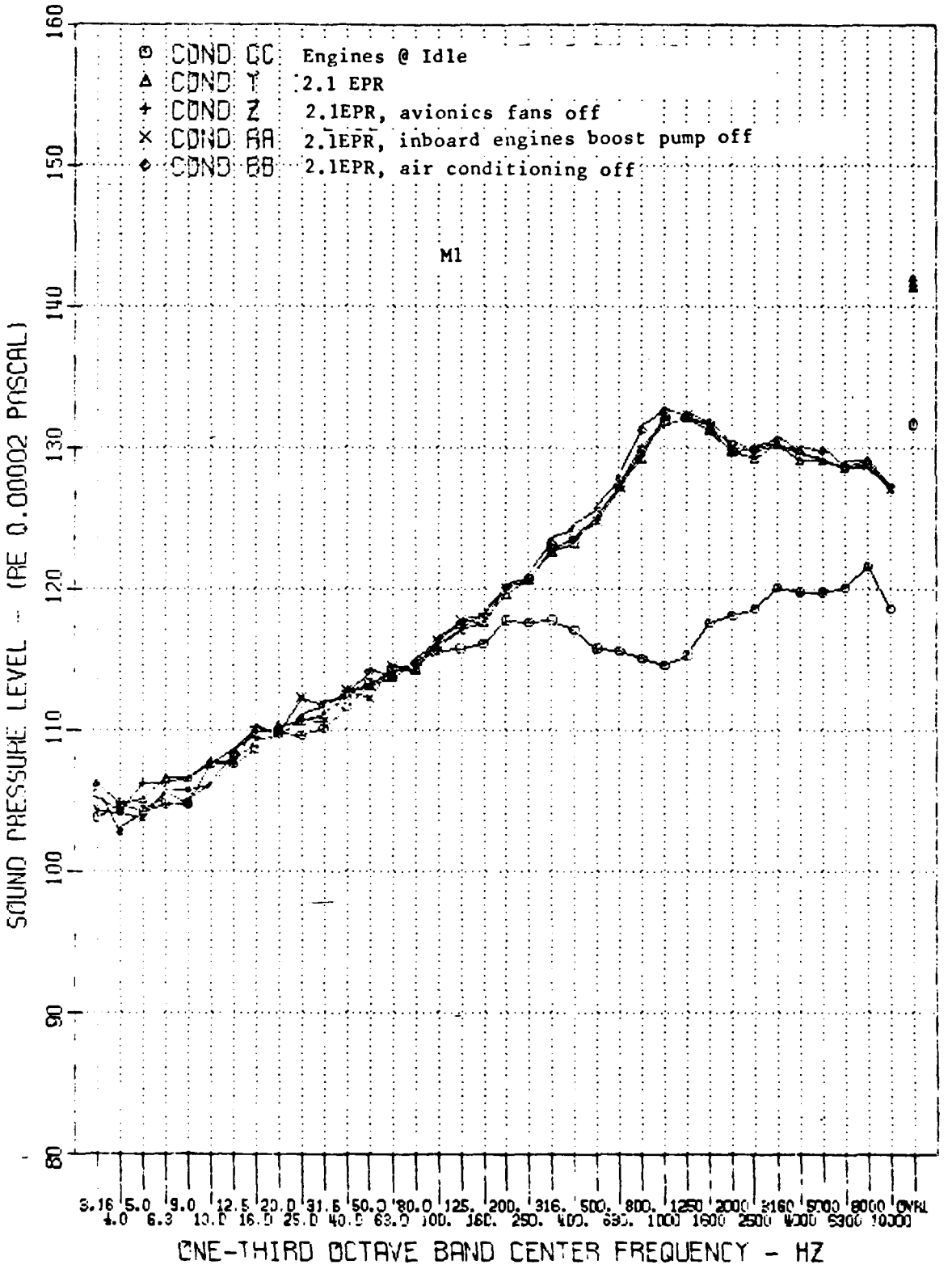

FIGURE 19 EXTERIOR NOISE FIELD DURING CRUISE AT 30,000 FEET, 3° FLAPS, 250 KEAS

boundary layer noise, which was anticipated to be the dominant contributor. The turbulent boundary layer which forms along the skin of an aircraft moving in the atmosphere is a source of skin vibration. This type of aerodynamic excitation is referred to as aerodynamic boundary layer noise.

The basic mechanism underlying the production of pressure fluctuations within a turbulent boundary layer is associated with the eddies at the edge of the laminar sublayer and the eddies in the outer portions of the boundary layer. At subsonic speeds, the wall layer is the most effective source of fluctuating pressures. Experimental and theoretical information on the overall pressure fluctuation levels in attached turbulent boundary layers has been shown to have reasonably good correlation with p_{rms}/q as a parameter (Ref. 9 and 10), where P_{rms} is the root mean square pressure fluctuation, and q is the dynamic head. The accuracy of this prediction has been shown by several investigators at subsonic speeds. This suggests that, since the YC-15 is a subsonic aircraft, the measured data should collapse to this parameter. An empirical curve suggested by Lowson (Ref. 10) for the fluctuating pressure intensity beneath an attached turbulent boundary layer is shown in Figure 20. Also shown on this figure are data from microphones 2 through 5 measured at 30,000 feet, 3° flaps, EPR= 1.00. This is a flight idle condition. Figure 20 shows that there is reasonable agreement between the prediction and the measured data, with the curve being a fairly good, slightly conservative fit to the available data. The frequency spectra of attached turbulent boundary layer pressure fluctuations are found to scale on a Strouhal basis. The frequency is a nondimensional quantity which relies on a typical length and velocity. An empirical prediction curve which is a fair representation of subsonic data is shown in Figure 21. The measured data is from Microphone 5 at the same conditions as those in Figure 20. For this particular Microphone (which was at the high end of the p_{rms}/q ratio range shown in Figure 20) the data and prediction follow the same shape with the data consistently higher above 400 hertz.

6.3 Fuselage Sidewall Vibration

6.3.1 Ground Test Results

The amount of available vibration data are substantially less than the amount of exterior noise data. What is available indicates that on an overall basis, the wall vibration tracks linearly with the exterior noise level (see Figure 22). The fuselage vibration, therefore, is expected to show the same dependence on thrust as did the exterior fuselage noise. This is borne out in Figure 23. These observations apply to the aft cabin area.

Figure 24 shows the effect of the inboard and outboard engines on the fuselage vibration response during takeoff conditions (23° flaps, EPR = 2.20). The in-board engines appear to control the vibration responses at locations under the wing (Accelerometer 14) and on the aft cabin (Accelerometer 16). The vibration measured on the aft cabin is less sensitive to the change in the inboard or outboard engines than the under-the-wing area.

The octave band levels for Accelerometers 11, 12, and 14, are shown in Figure 25 with all engines at takeoff thrust and for 24° flaps. The wing box response (Accelerometer 11) is substantially lower than the fuselage response (Accelerometers 12 and 14). The vibration levels for the side and top of the fuselage are similar below 1000 Hz. The same relative response between these accelerometers was evident at a lower power setting (Ref. 1). This indicates that the wing box is not a good radiator of acoustic energy, and that the sound

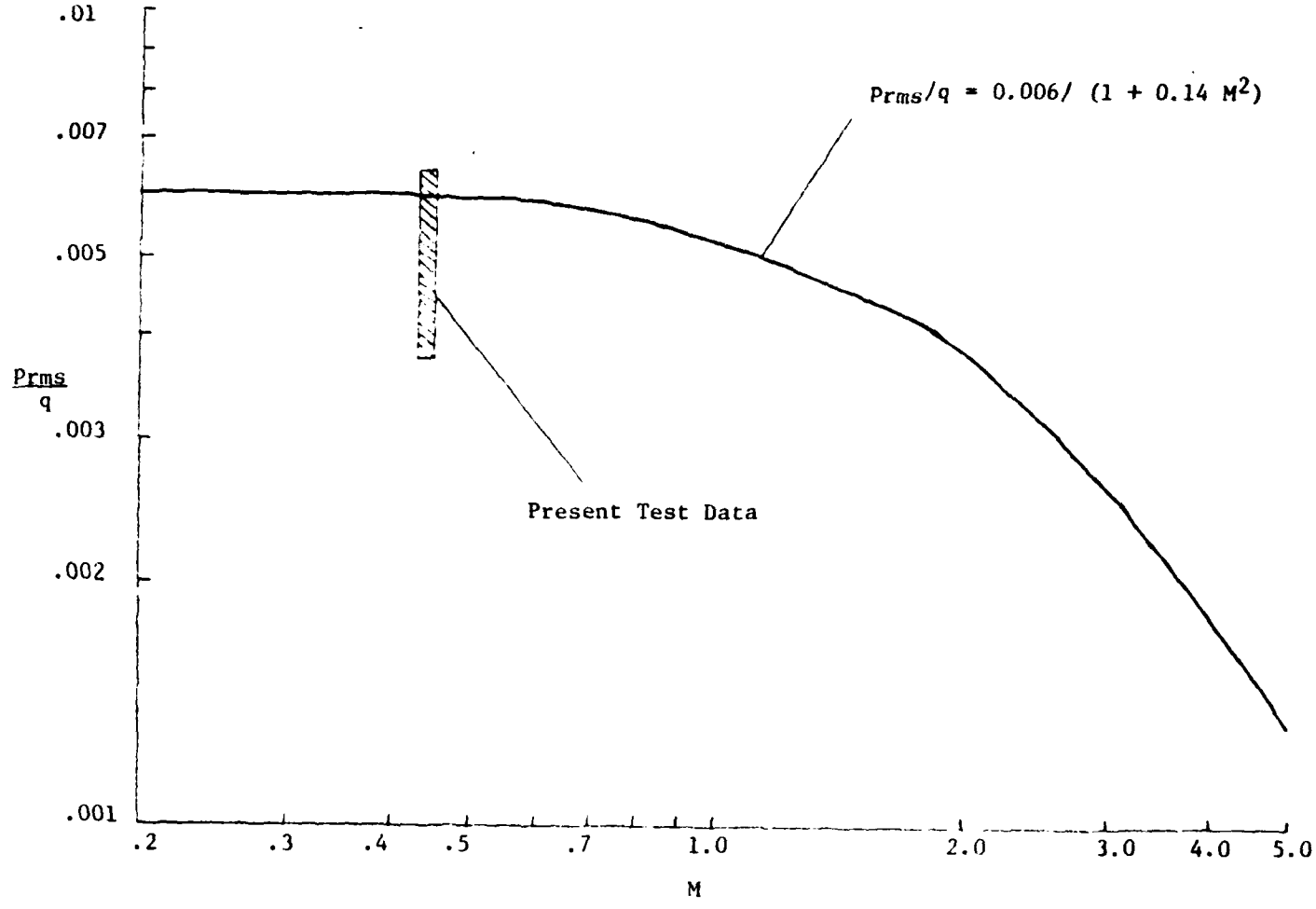

Figure 20 - Fluctuating Pressure Nondimensionalized by Dynamic Head vs. Mach Number at 30,000 Feet, Flight Idle, 3° Flaps, EPR = 1.00

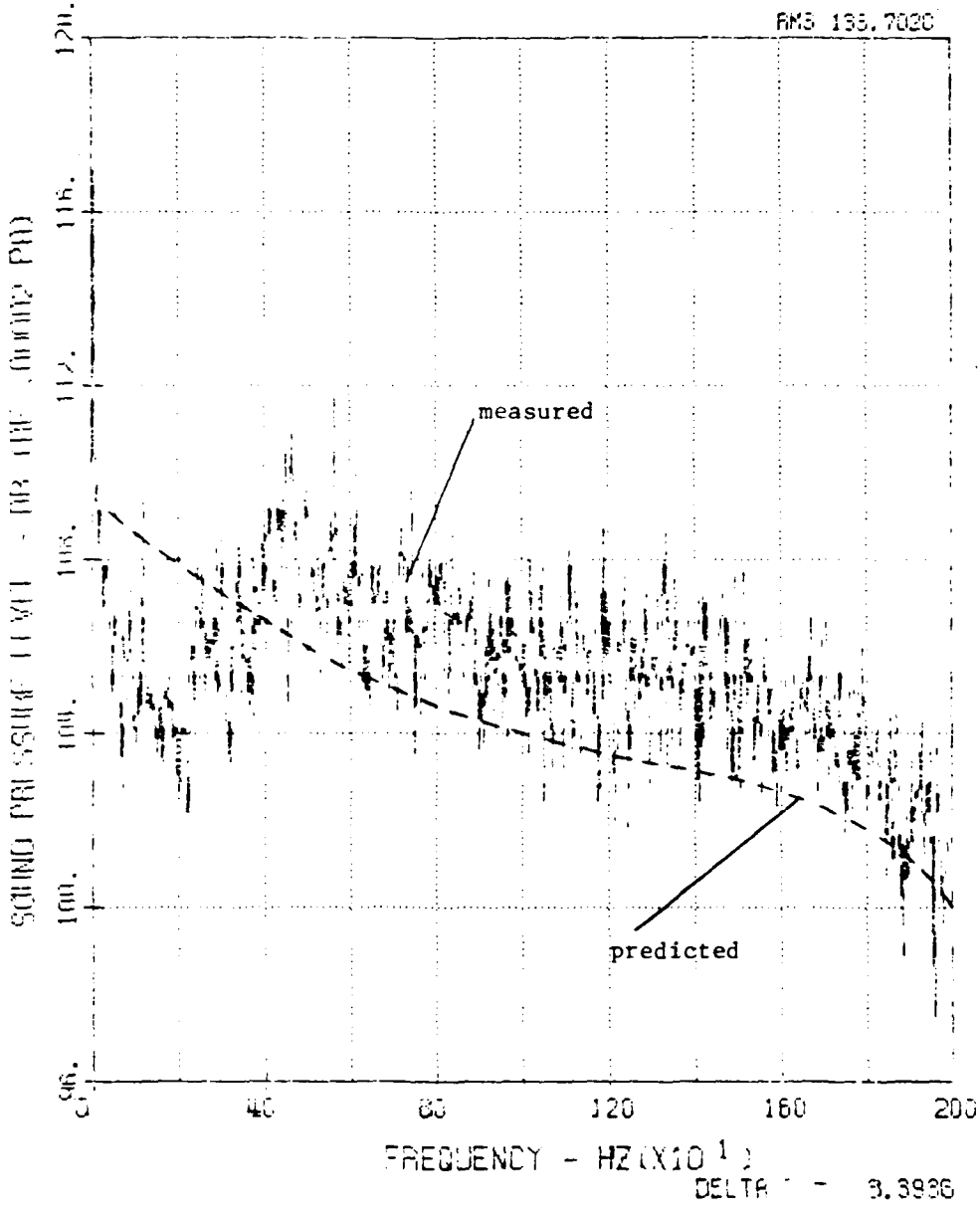

Figure 21 - Comparison of Predicted and Measured Turbulent Boundary Layer Noise at 30,000 Feet, Flight Idle, 3° Flaps, EPR= 1.00

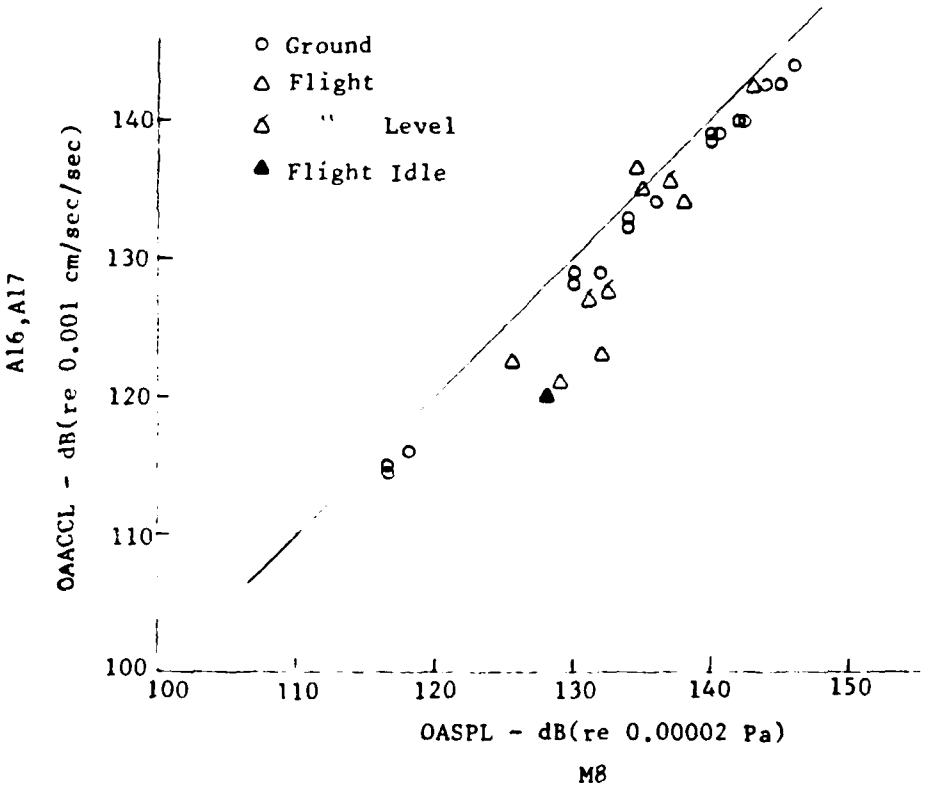

FIGURE 22 CORRELATION OF OVERALL FUSELAGE VIBRATION WITH OVERALL EXTERIOR FUSELAGE NOISE

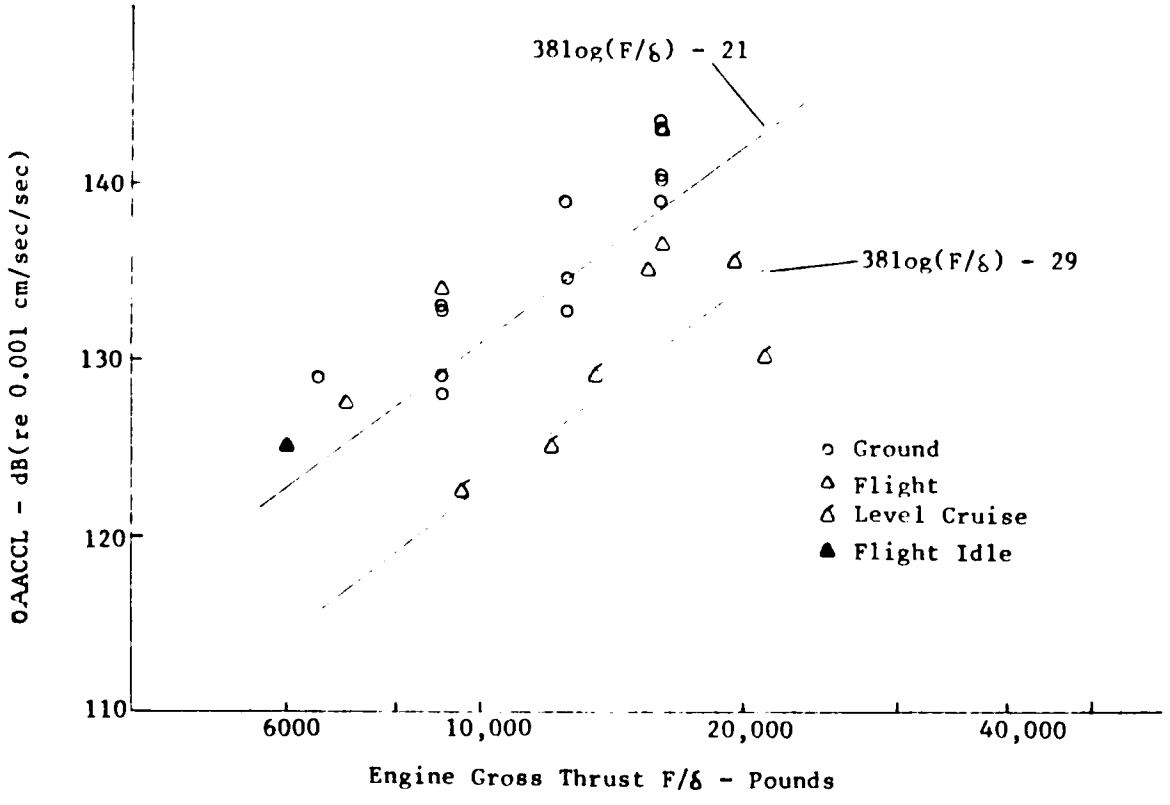

FIGURE 23 FUSELAGE VIBRATION LEVELS WITH ALL ENGINES AT SAME THRUST - ACCELEROMETER 16

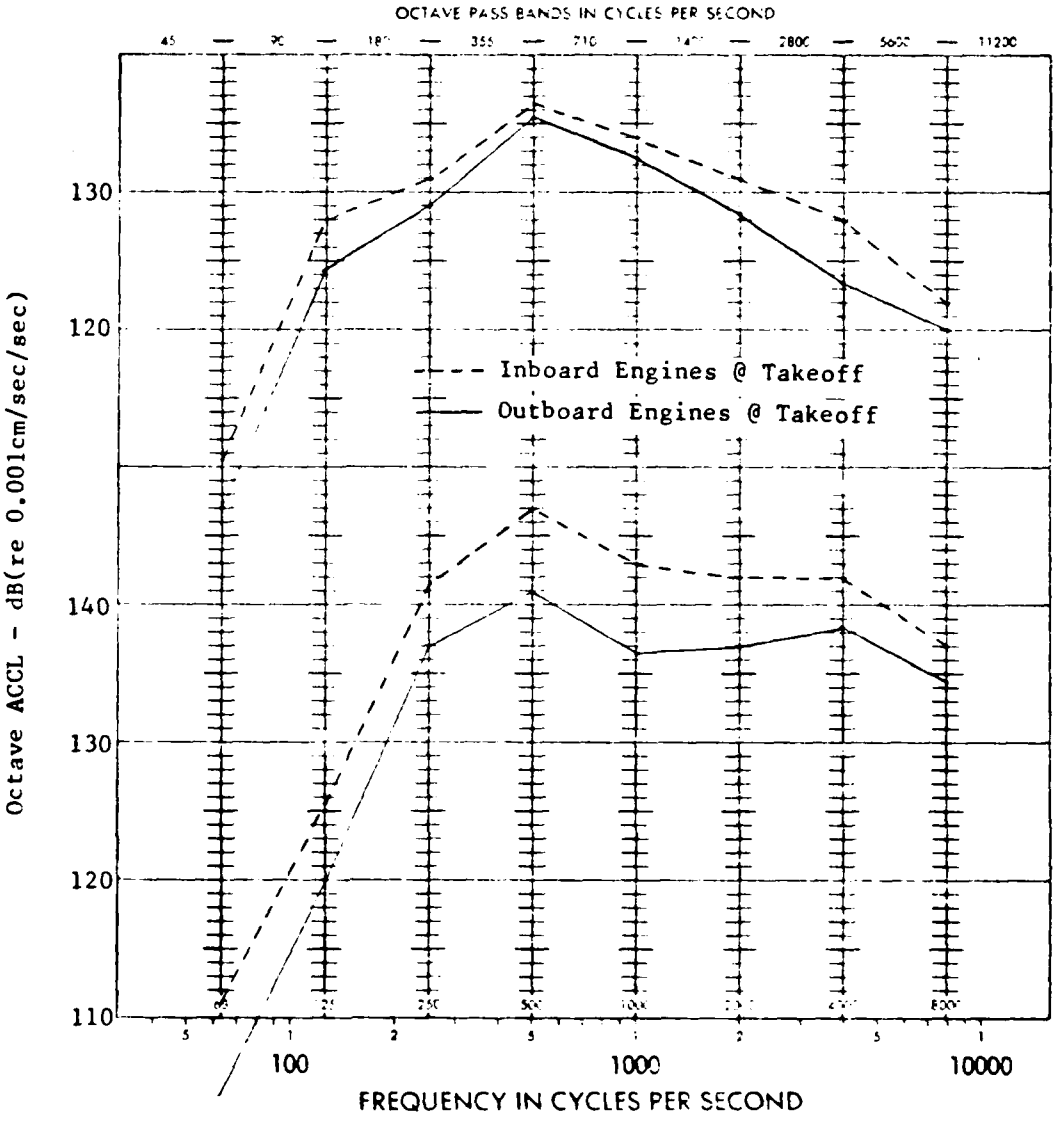

FIGURE 24 EFFECT OF IN-BOARD AND OUT-BOARD ENGINES ON FUSELAGE VIBRATION RESPONSE

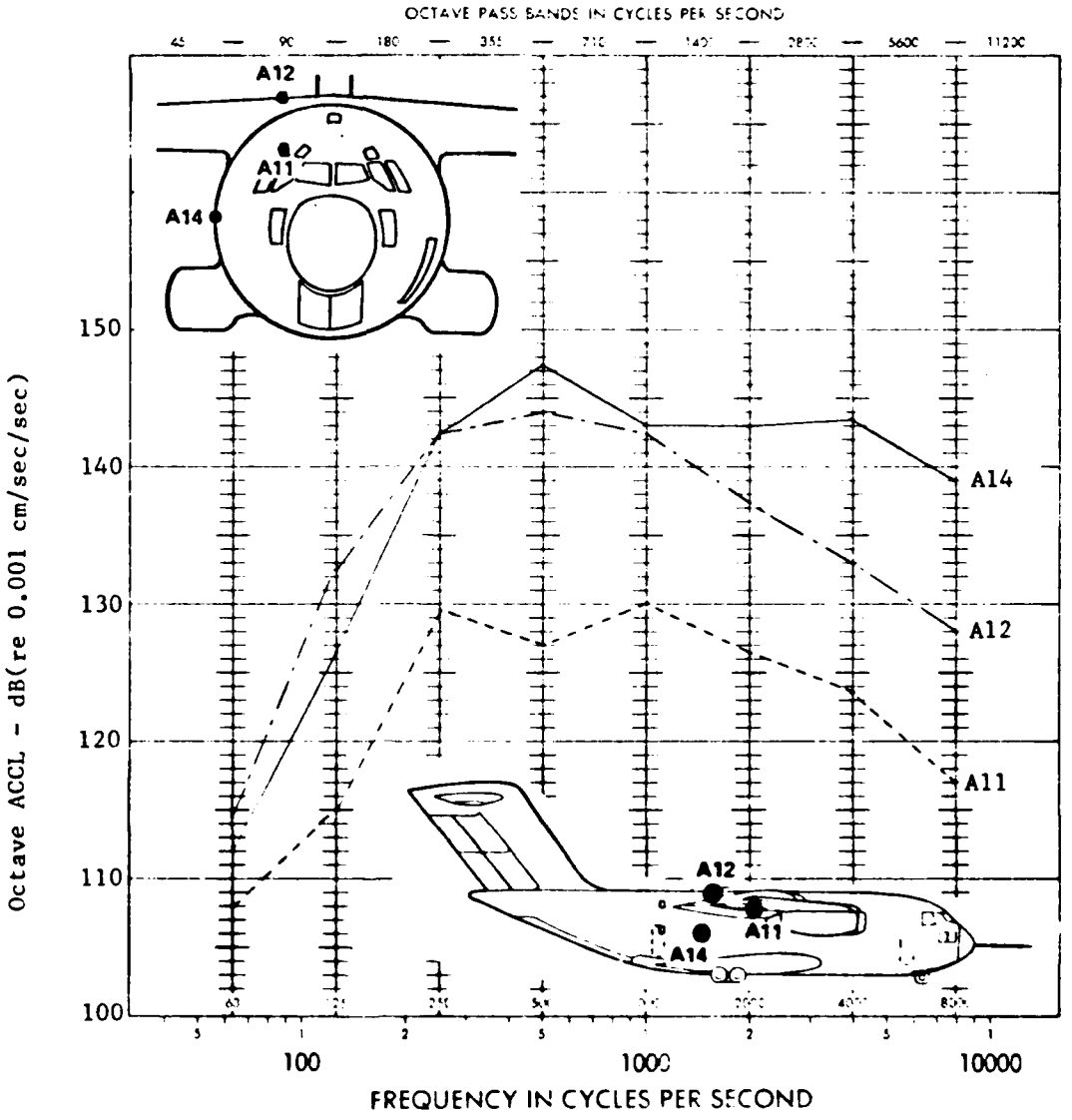

FIGURE 25 VIBRATION LEVELS DURING GROUND STATIC TAKEOFF THRUST AND 24° FLAPS, EPR= 2.2

which enters the cabin is controlled by that which comes through the fuselage sidewall.

The relationships between the octave band behavior of the exterior fuselage noise and fuselage wall vibration for the aft cabin region, are illustrated in Figure 26. The general shape of the vibration curves is similar to the noise curves in the mid- and higher frequencies, but differ in the low frequencies. The aft cabin vibration does not seem to respond to the exterior noise excitation in the low frequencies.

6.3.2 Flight Test Results

Fuselage wall vibration levels during takeoff are highest in the flap area (Accelerometer 14 and 15). During landing, the highest levels are under the wing (see Figure 27a). Two representative curves are shown in Figure 27b, which compare the octave band level differences for the maximum levels measured in the flap area (Accelerometer 14) and under the wing (Accelerometer 13). The spectra are almost the same below 250 Hz. Above 250 Hz, significantly more energy is present in the takeoff spectra, which accounts for the 5 dB difference in the peak overall levels between Accelerometers 13 and 14.

The acceleration levels for the aft cabin cruise at 18,000 feet and 1° flaps are presented in Figure 28. The levels increase with an increase in airspeed. This is the same trend observed for the exterior noise levels.

It was shown earlier that wall vibration is controlled by the noise excitation on the exterior fuselage on an overall basis. This suggests that a method described in the literature (Ref 11) for predicting the one-third octave band behavior of acoustically induced vibration for transport aircraft could be used with good success. The prediction method of Reference 11 presents charts which correlate randomly fluctuating noise and vibration levels at various confidence levels, for the frequency range of 50 to 2500 Hertz. The prediction charts are based on modern transport aircraft measured data for shell-type and box-type structure. It is assumed that shell structure is conventional skin-frame-stringer structure and that no discrete frequency appears in the acoustic signal. A comparison between predicted and measured values is shown in Figure 29. The one-third octave band sound pressure levels measured at Microphone 8, were used to make vibration predictions for Accelerometer 16. The agreement is excellent for the cruise condition in which the YC-15 resembles a conventional transport aircraft, i.e., no flaps deployed. However, for the takeoff condition with flaps deployed 23°, the agreement is not good below 250 Hz. This poor agreement is not unexpected since the prediction method was developed for non-STOL configured aircraft. Reference 11 provides a good vibration prediction method except for low frequency spectra with flaps deployed.

6.4 Cabin Noise

6.4.1 Ground Test Results

Figure 30 presents the overall sound pressure levels measured by Microphone 24 as a function of the vibration of the sidewall, as measured by

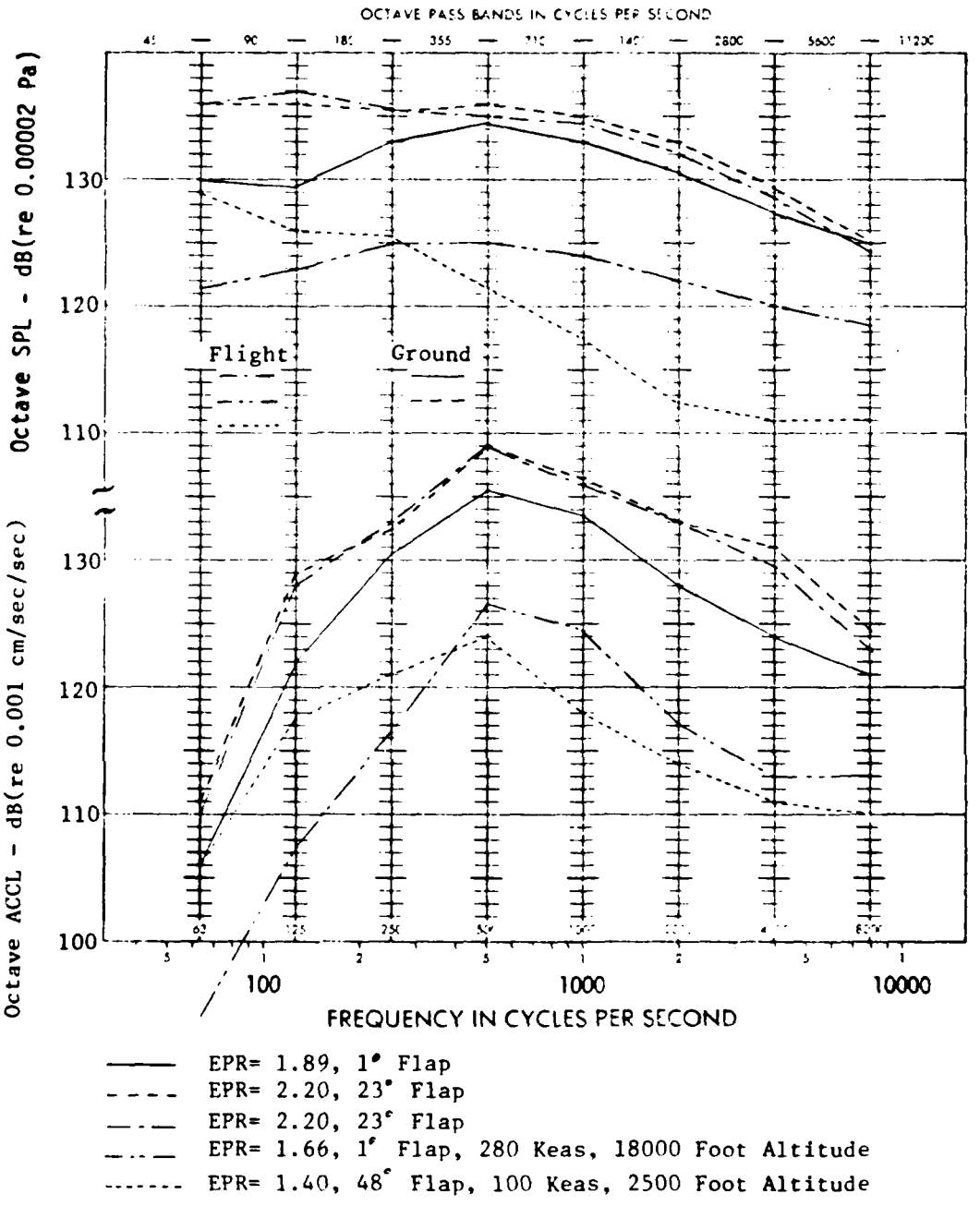

M8

A16

FIGURE 26 COMPARISON OF WALL VIBRATION AND EXTERIOR FUSELAGE NOISE ON AFT CABIN

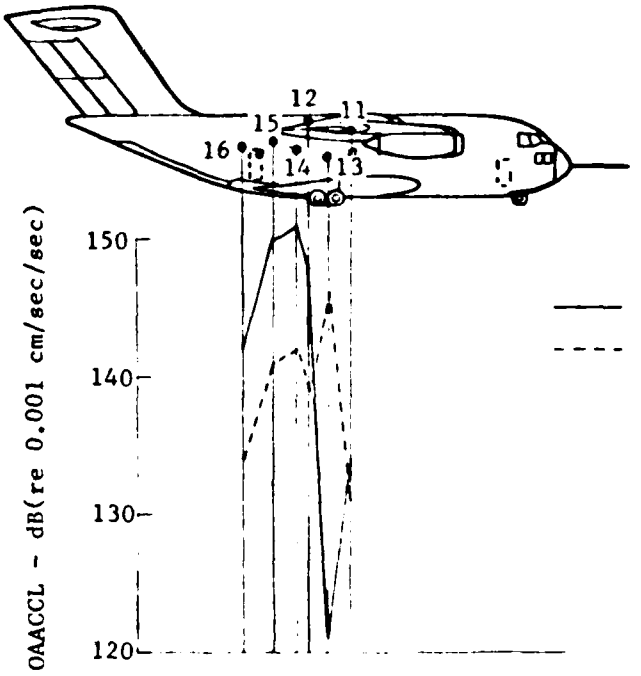

(a)

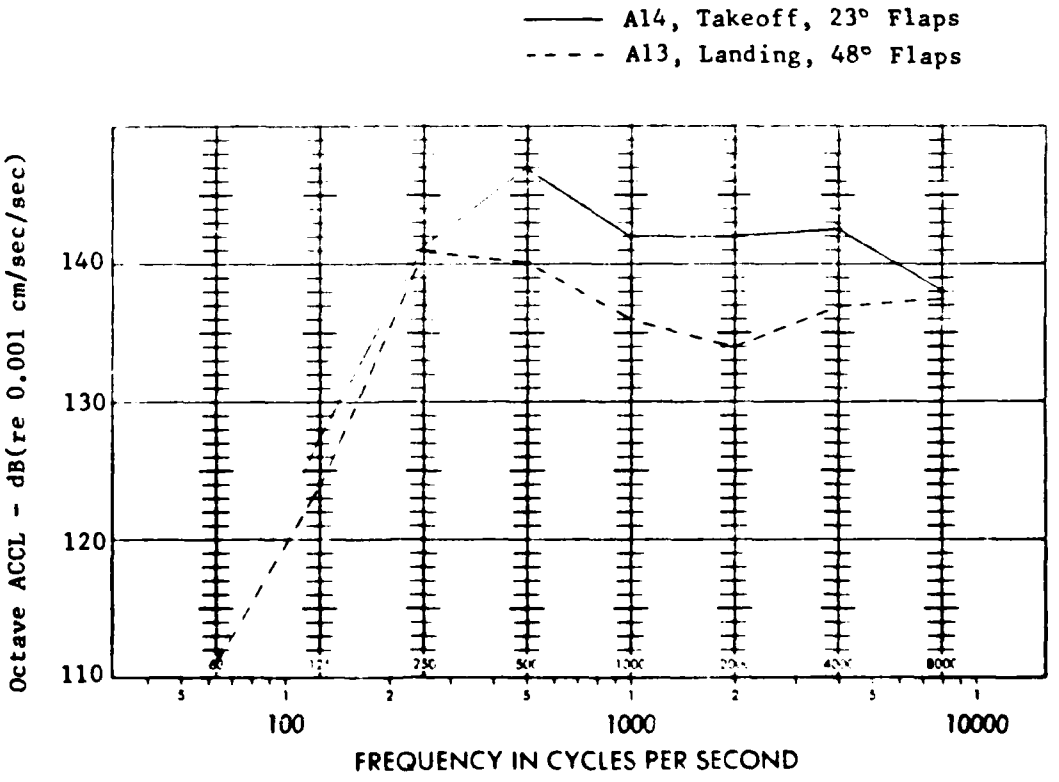

(b)

FIGURE 27 FUSELAGE WALL VIBRATION DURING TAKEOFF AND LANDING

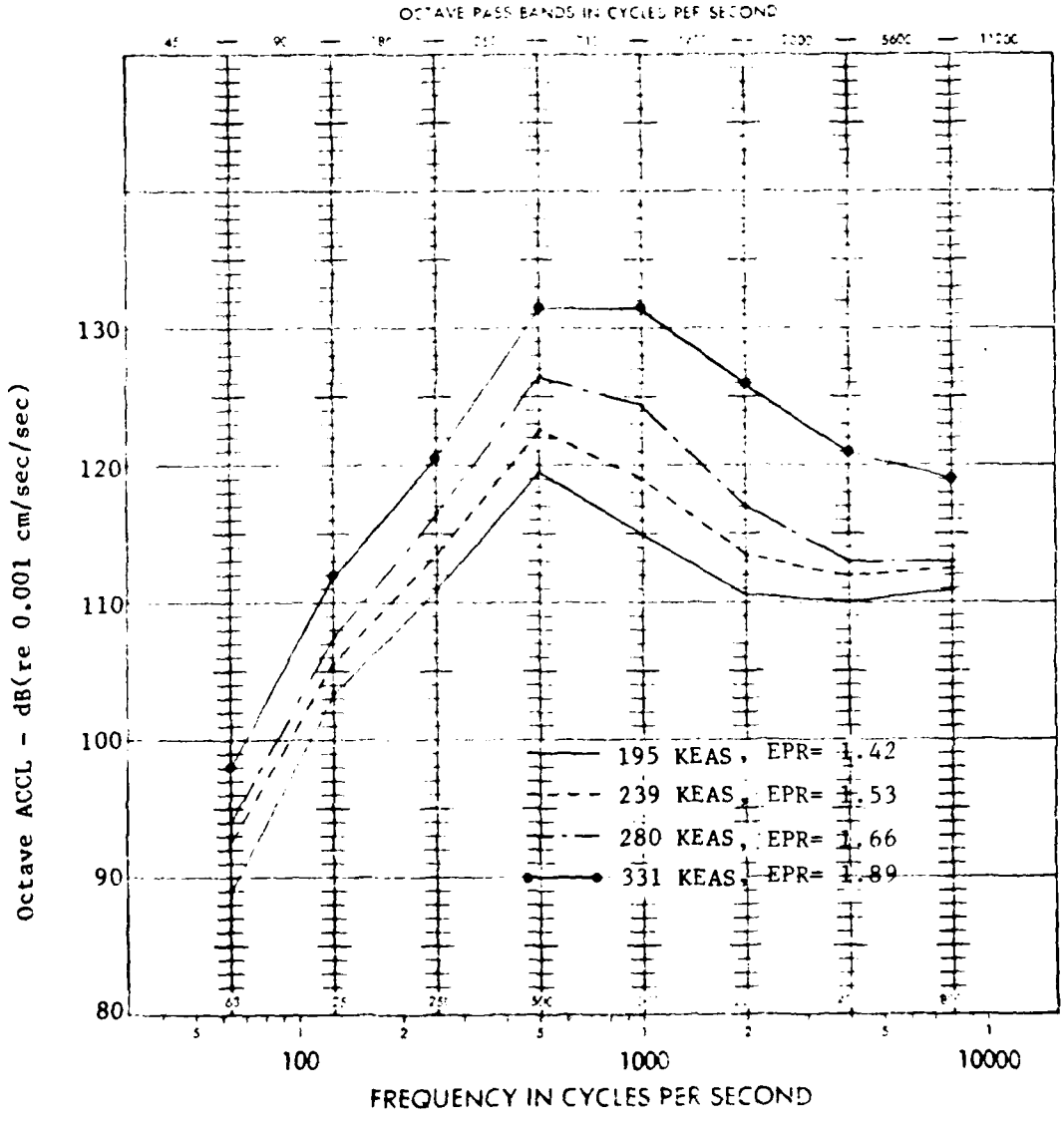

FIGURE 28 EFFECT OF INCREASING AIRSPEED ON AFT CABIN VIBRATION LEVELS FOR ACCELEROMETER 16, 18,000 FEET, 1° FLAPS

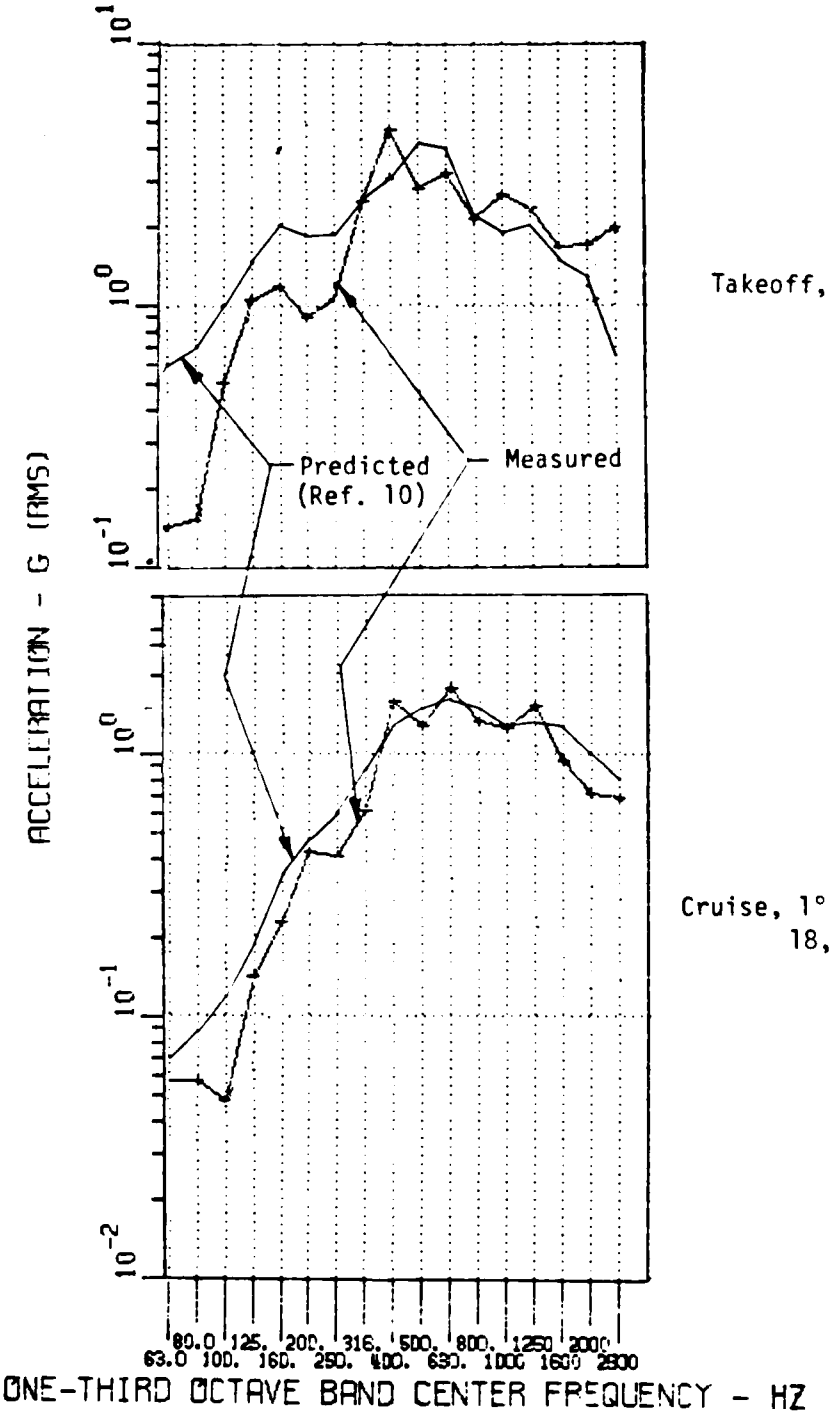

FIGURE 29 COMPARISON OF MEASURED AND PREDICTED SPECTRA FOR ACCELEROMETER 16

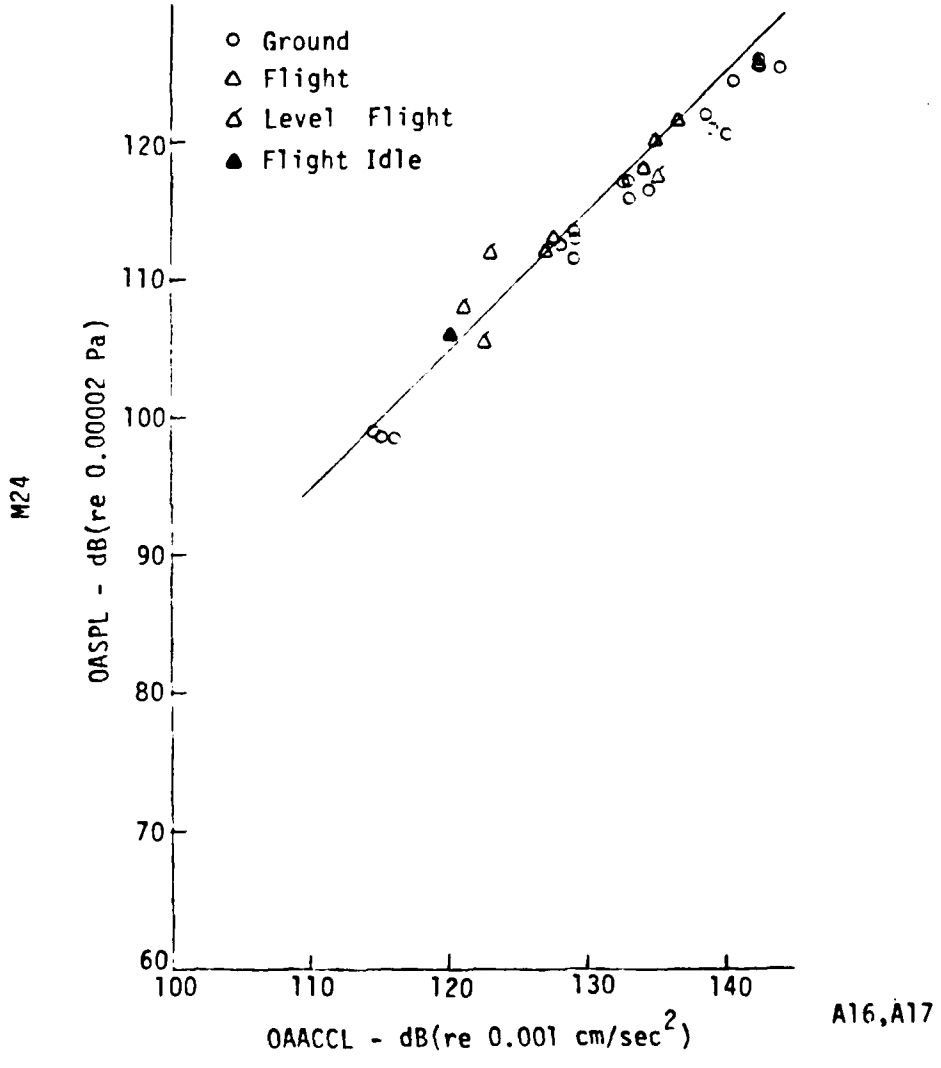

FIGURE 30 CORRELATION OF OVERALL FUSELAGE VIBRATION WITH OVERALL INTERIOR CABIN NOISE

Accelerometers 16 and 17. The noise inside the main cabin appears to track with the fuselage vibration.

The overall interior acoustic levels along the centerline is shown in Figure 31(a). These locations indicate that the interior is highly reverberant with the levels being nearly the same except for the area of the flaps (Microphone 21). A sampling of the octave band spectra for these same microphones is shown in Figure 31(b). These data indicate the similarity of the interior noise field above 250 Hz. Any differences which occur in the overall are a result of the low frequency (less than 500 Hz) data. SPL for Microphone 21 are several dB greater than the other centerline locations.

The effect of the inboard and outboard engines on interior noise is shown in Figure 32. The data at both microphone locations indicate that the inboard engines control the interior noise environment. The inboard engines add 3-5 dB to the frequencies below 500 Hz at both locations. However, at the aft microphone (Location 24), the effect of the outboard engines is seen above 500 Hz. The noise levels are nearly the same for both inboard and outboard engine data.

The interior noise data shown in the previous figures are from the center aisle area. Figure 33 provides data from locations close to the sidewall, as well as from the center aisle. This figure indicates that the sidewall noise levels are several decibels higher than the centerline levels, which indicates that energy is being transmitted through the fuselage walls into the interior. The noise appears to be quite different between sidewall and centerline in the lower frequencies. The differences could be caused by interior room mode resonances.

Figure 34 presents the octave band spectra for the interior sidewall microphones during takeoff conditions at ground static, 23° flaps, EPR=2.20. Part (a) shows that small differences exist below 1000 Hertz for microphones 25 through 28. Microphones behind the flaps (27 and 28) exhibit lower SPL above 1000 Hertz as compared to locations ahead of the flaps (mics 25 and 26). Part (b) of Figure 34 presents a comparison between two aft cabin sidewall microphones, one of which is located beside a deep frame (Microphone 29). Microphone 29 does not indicate that the aft deep frame is a major acoustic energy radiator. The SPL's for Microphone 29 are, in fact, 3-4 dB less between 250 and 500 Hz.

It was noted earlier that increasing the flap angle increased the exterior noise levels in the low frequencies. The same effect is noted in Figure 35 for the aft interior noise environment. The greatest increase occurs between flaps not deployed (0°flaps) and takeoff condition (23° flaps). These data are compared in this same figure with the noise level criteria in MIL-S-008806B for personnel using standard-issue crew member head gear. The noise data fall within the curve for a cumulative mission exposure limit of 15 minutes with the exception of the SPL at 500 Hz. The data only exceed the criteria by 2 dB maximum at this frequency. It should be noted that crew members in the aft cabin should be exposed to much less than 15 minutes of static takeoff power. Utilizing MIL-S-008806B criteria, planned flights should pose no hearing damage to personnel assigned to the aft cabin.

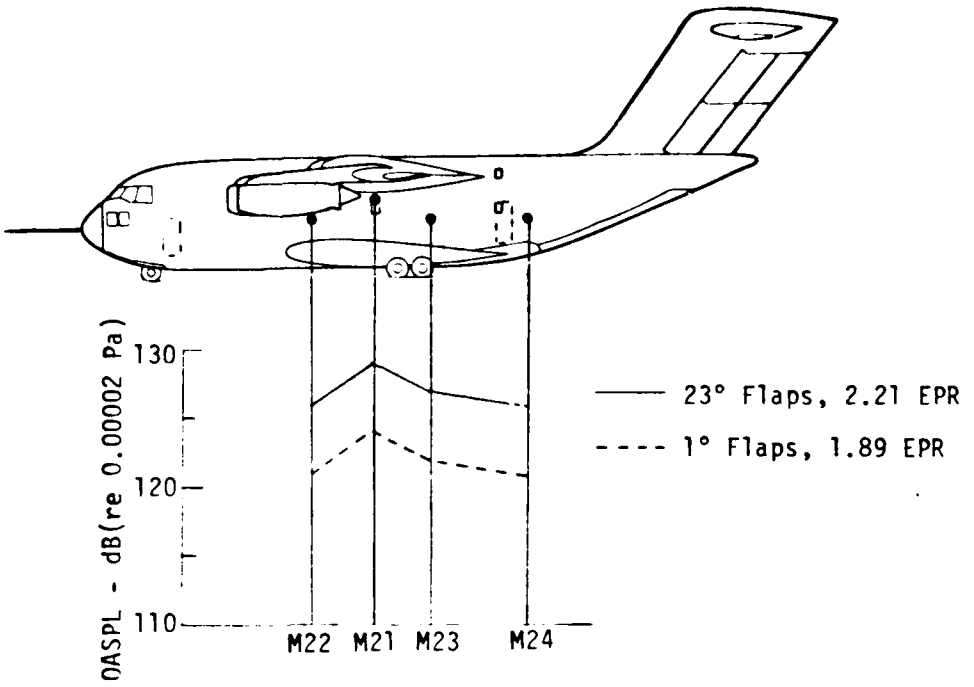

(a)

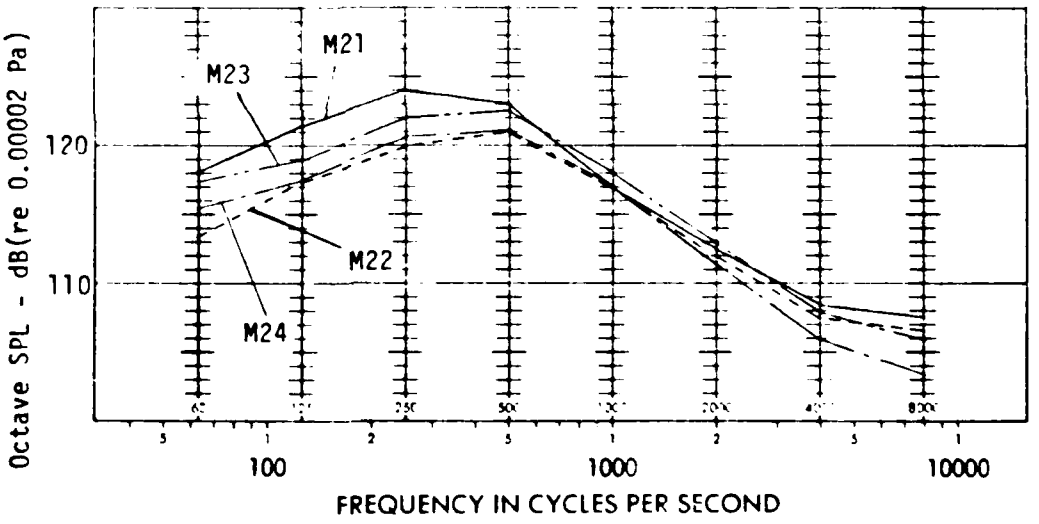

(b) 23° Flaps, 2.21 EPR

FIGURE 31 INTERIOR CABIN ACOUSTIC LEVELS DURING STATIC CONDITIONS

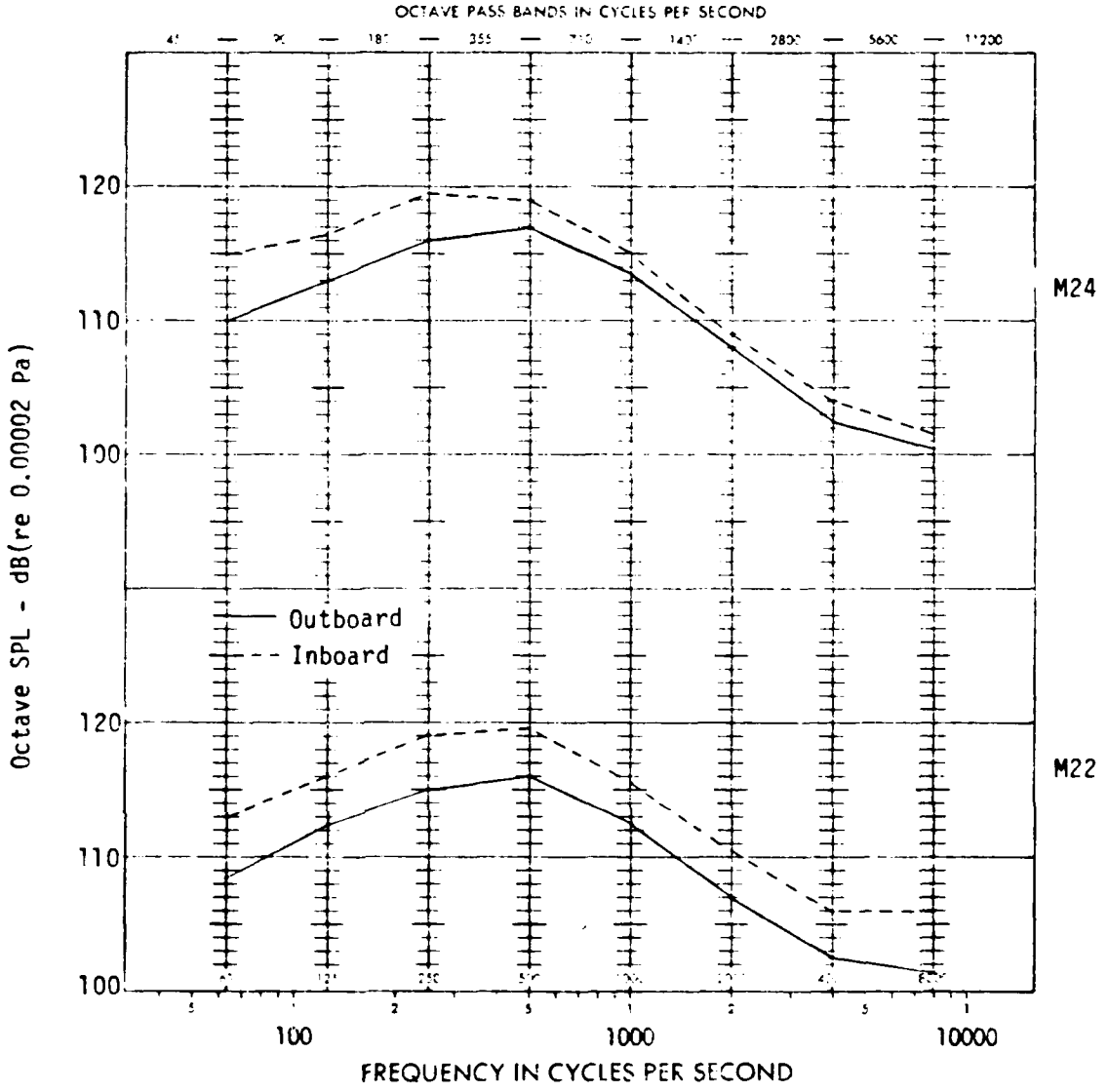

FIGURE 32 EFFECT OF INBOARD AND OUTBOARD ENGINES ON INTERIOR NOISE AT 23° FLAPS, 2.2 EPR

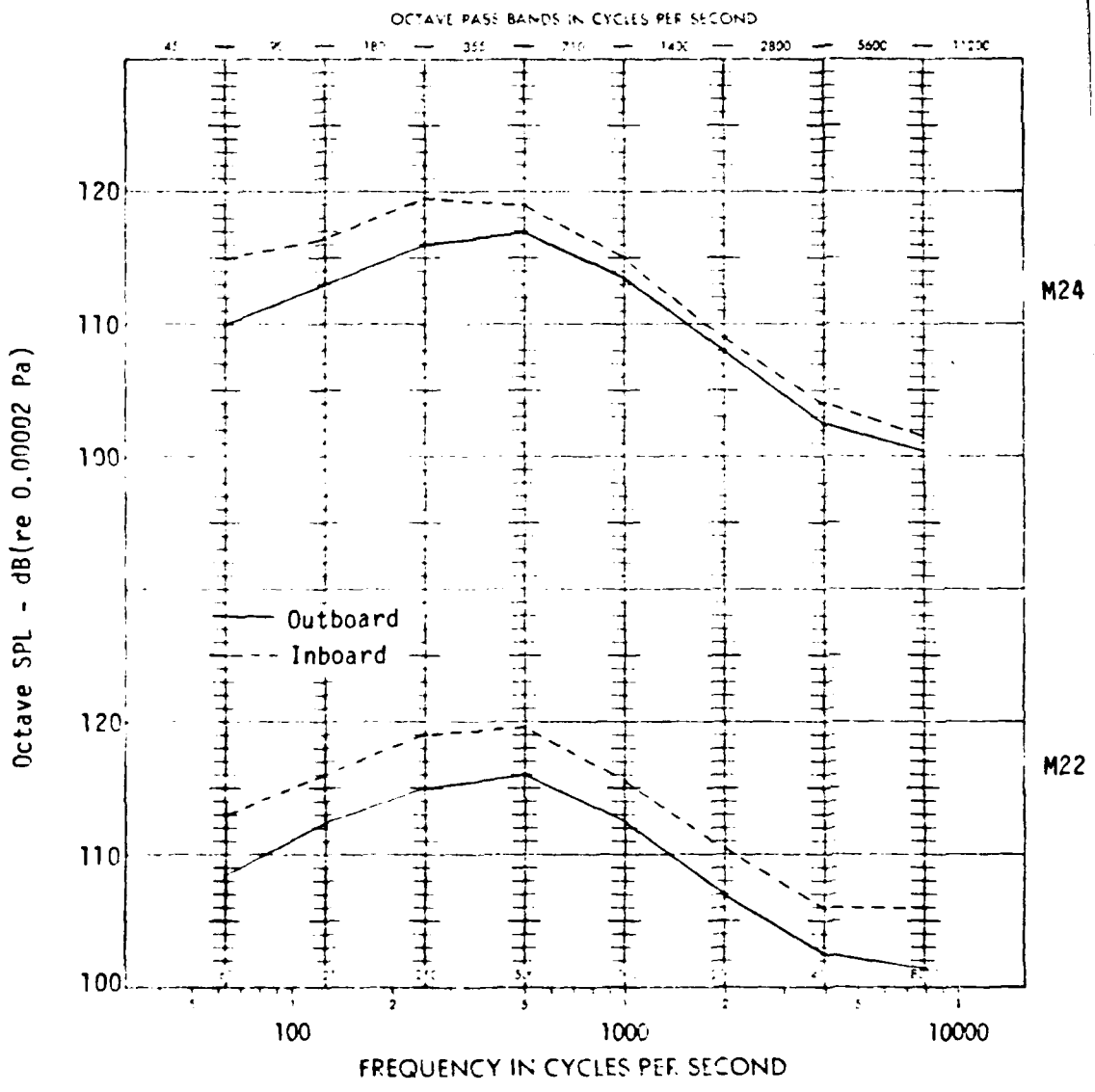

FIGURE 32 EFFECT OF INBOARD AND OUTBOARD ENGINES ON INTERIOR NOISE AT 23° FLAPS, 2.2 EPR

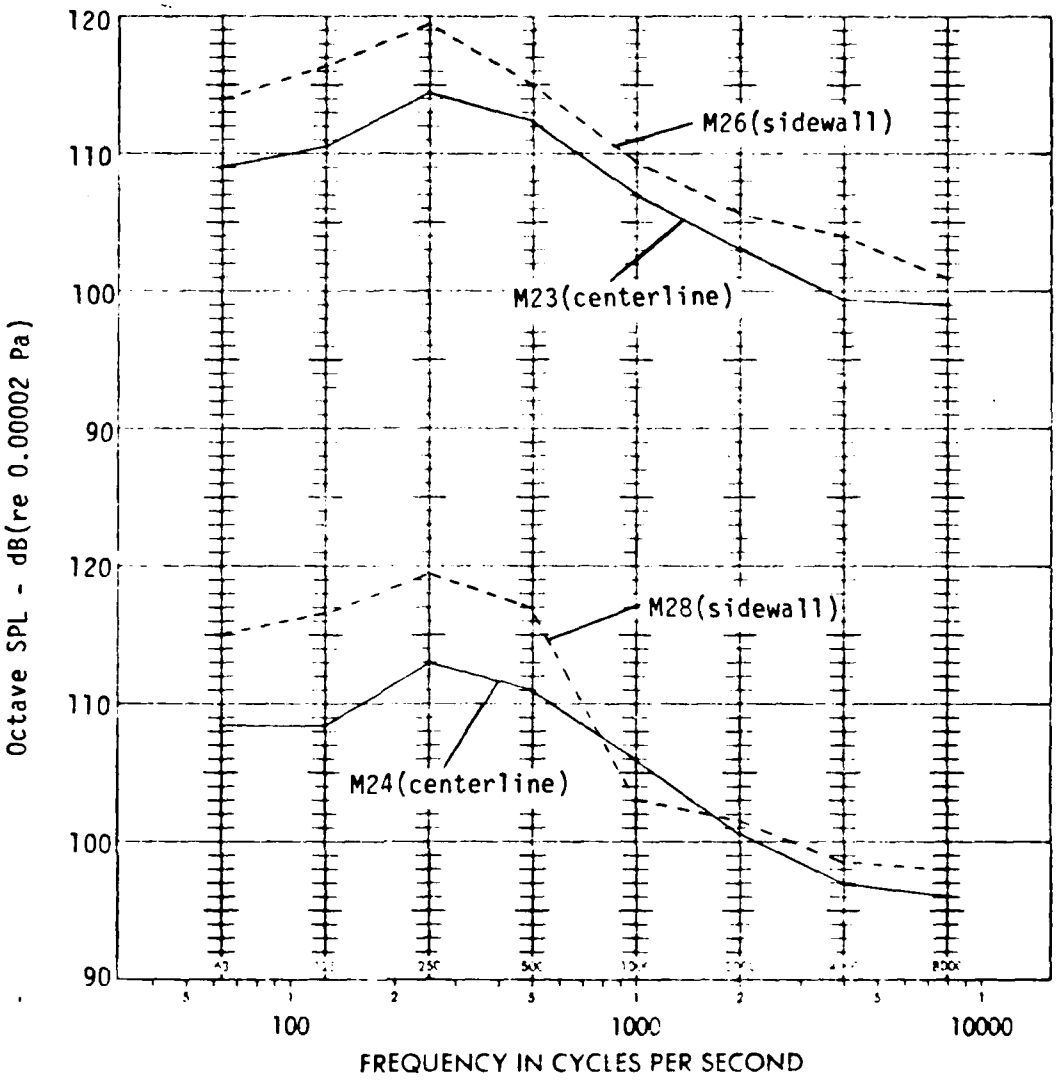

FIGURE 33 COMPARISON OF SIDEWALL AND CENTERLINE CABIN NOISE AT GROUND STATIC, 23° FLAPS, 1.60 EPR

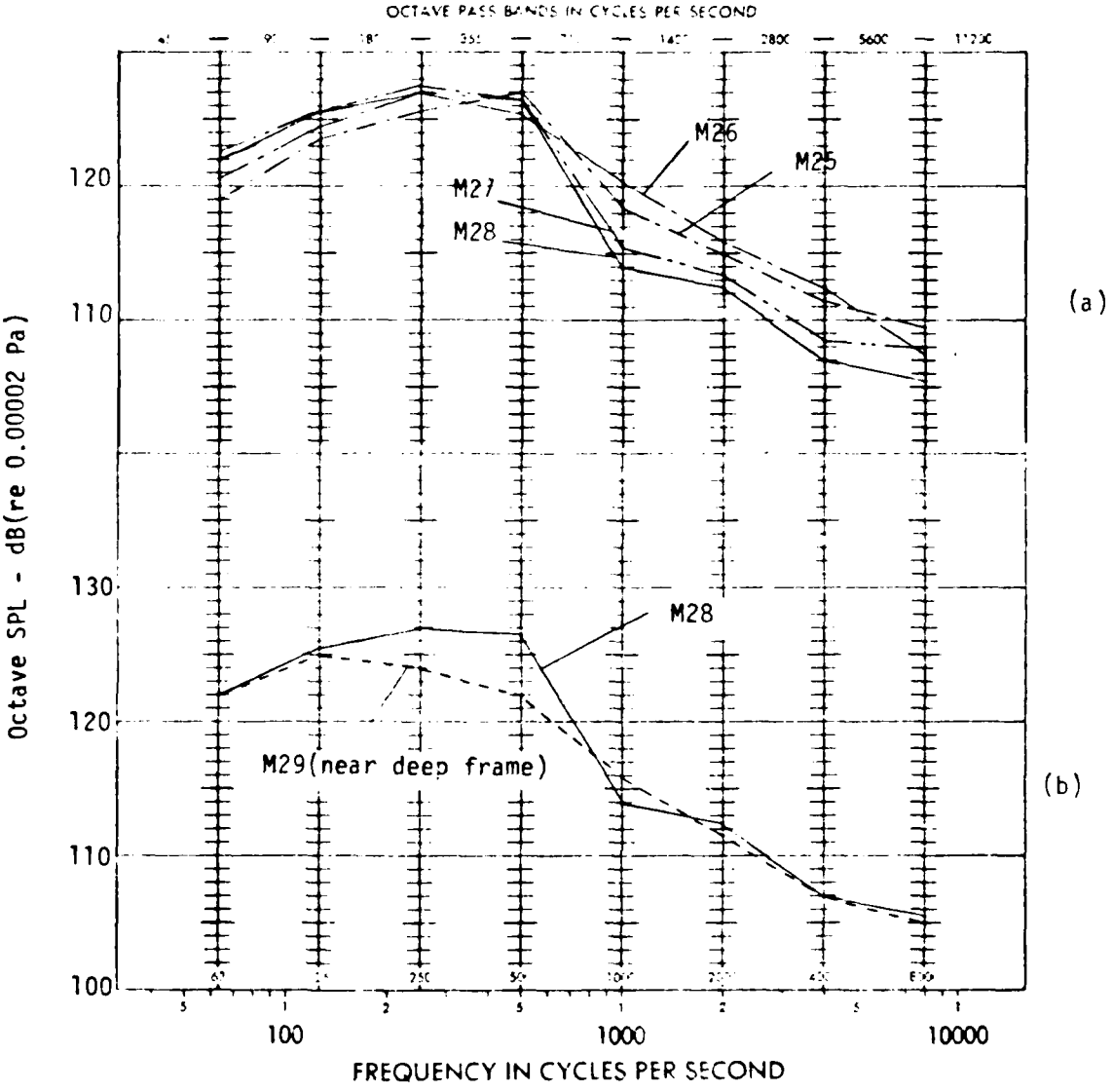

FIGURE 34 SIDEWALL CABIN NOISE AT TAKEOFF POWER, GROUND STATIC, 23° FLAPS, 2.20 EPR

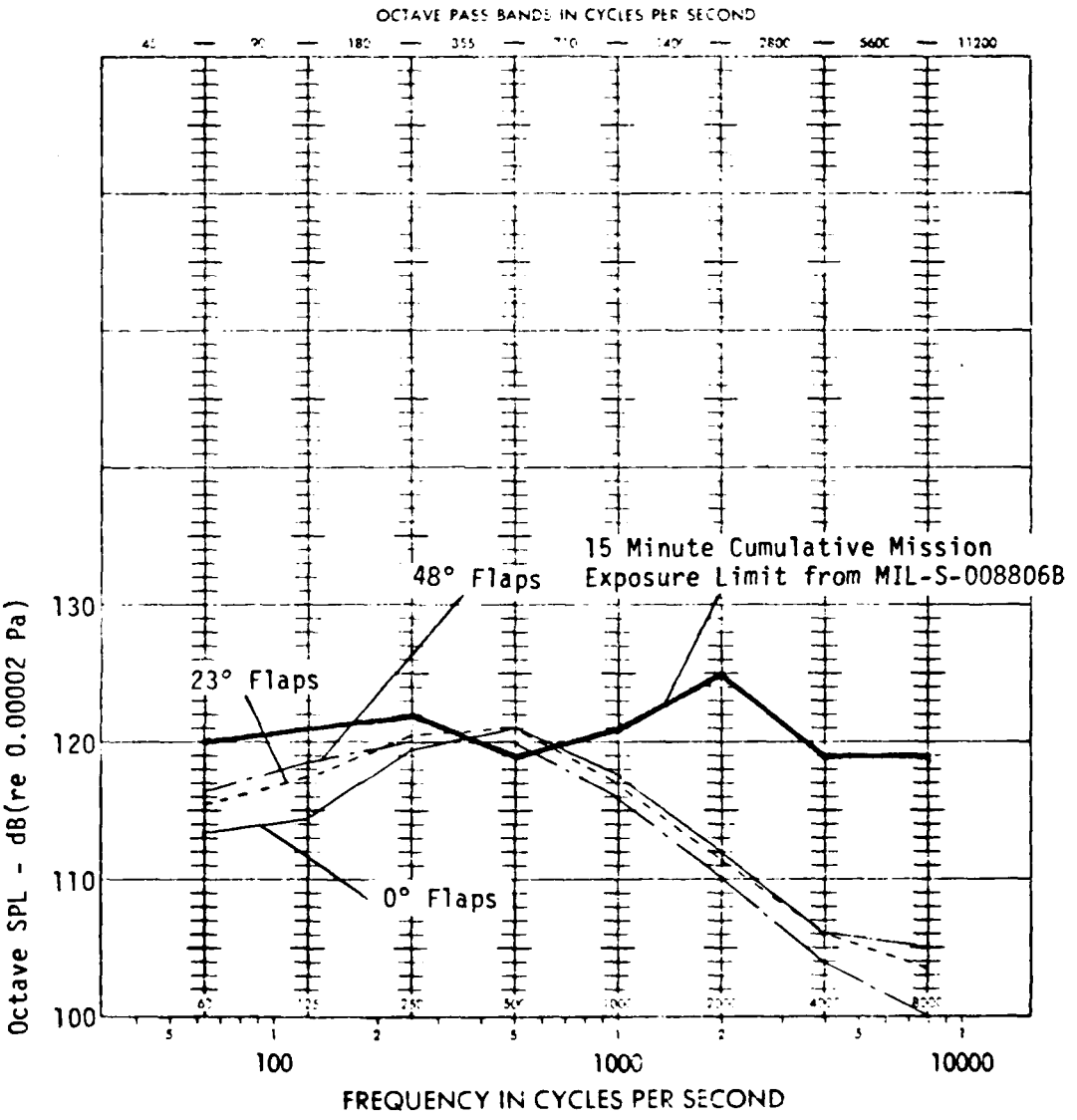

FIGURE 35 EFFECT OF FLAP SETTING ON INTERIOR NOISE AT TAKEOFF POWER - MICROPHONE 24

The cabin is known to be highly reverberant based on data presented earlier with SPL being constant throughout. The relationship between the overall noise in the main cabin (Microphone 23) and the cockpit does not show this one-for-one comparison (Figure 36). The cockpit data were measured during preliminary testing and were unpublished. Even though the data track linearly, about 13 dB difference between cockpit and cabin noise is observed.

6.4.2 Flight Test Results

Figure 37 summarizes overall cabin noise levels (Microphone 24) experiences during the program. Similarity is seen between the condition-to-condition variation of interior noise and the indicated flight condition. This same trend was noted earlier with the exterior noise levels. This suggests that interior noise is predominantly controlled by the exterior noise field. Note that the overall noise levels for ground and flight idle are within 4 dB of each other. Levels at these two conditions could be controlled by interior noise sources such as hydraulic systems, air conditioning system, etc. Also plotted on this figure, is the relationship of the condition-to-condition noise levels with jet velocity (V_j), aircraft velocity (V_a), and relative velocity (V_j-V_a) Of the three velocity patterns, the correlation between noise and relative jet exhaust velocity is reasonably good.

Noise levels within the aft cabin increase with flap extension. Figure 38 shows that this increase is quite modest and amounts to about 0.025 dB per degree of flap extension. This increase is noted at three different engine pressure ratios.

Figure 39 and 40 present sidewall and centerline one-third octave spectra that were measured inside the YC-15 during takeoff, cruise at 18,000 feet, and landing approach. In the case of the centerline microphones, the sound pressure levels are fairly uniform throughout the interior. The levels increase in the vicinity of the flaps (Microphones 22, 23, 25, 26), for all flight conditions shown. The peak in the spectra shifts downward in frequency as the flap angle is increased. In the case of landing approach, the peak is quite broad, ranging from approximately 50 to 400 Hz in width.

Increasing aircraft speed led to an increase in exterior noise and fuselage vibration for cruise conditions at 18,000 feet altitude. The same trend is noted for the aircraft interior (Figure 41). The peak in the spectra shifts upward with increasing velocity as expected.

Data were acquired during cruise at 30,000 feet in an attempt to determine the acoustic effects of noise generated by on-board equipment on interior levels. Such things as the avionics cooling fans, inboard engine fuel pumps, and the air conditioning packs were cycled on and off, and the resultant sound pressure levels were subsequently measured. Figure 42 shows the results for Microphone 23 with engines at 2.1 EPR. Also plotted are similar cruise conditions, but with all engines at idle, and with engines at idle and all on-board equipment operating. This figure indicates that the equipment does not have an effect on the interior levels. Decreasing all engine power to idle does have an effect. This, too, shows that the cabin compartment noise levels are controlled by the exterior noise. It was thought the equipment noise would be discernible during flight conditions. Since it is not, it leads to the conclusion that the aircraft sidewall (which contains no acoustic or thermal

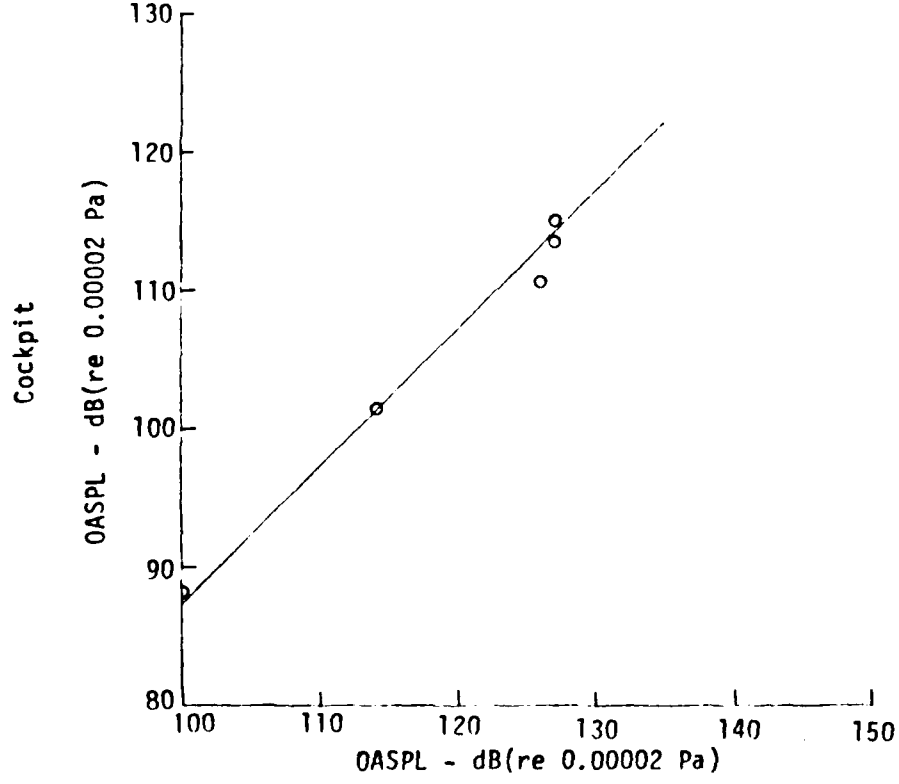

FIGURE 36 COMPARISON BETWEEN COCKPIT AND AFT CABIN ISLE OVERALL SOUND PRESSURE LEVELS

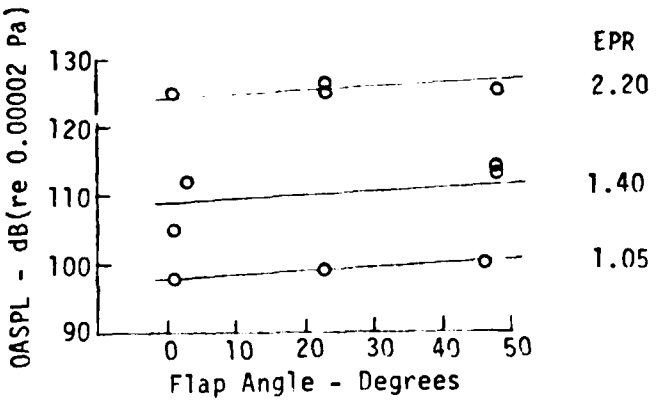

FIGURE 38 AFT TROOP OVERALL SPL AS FUNCTION OF FLAP ANGLE - MICROPHONE 24

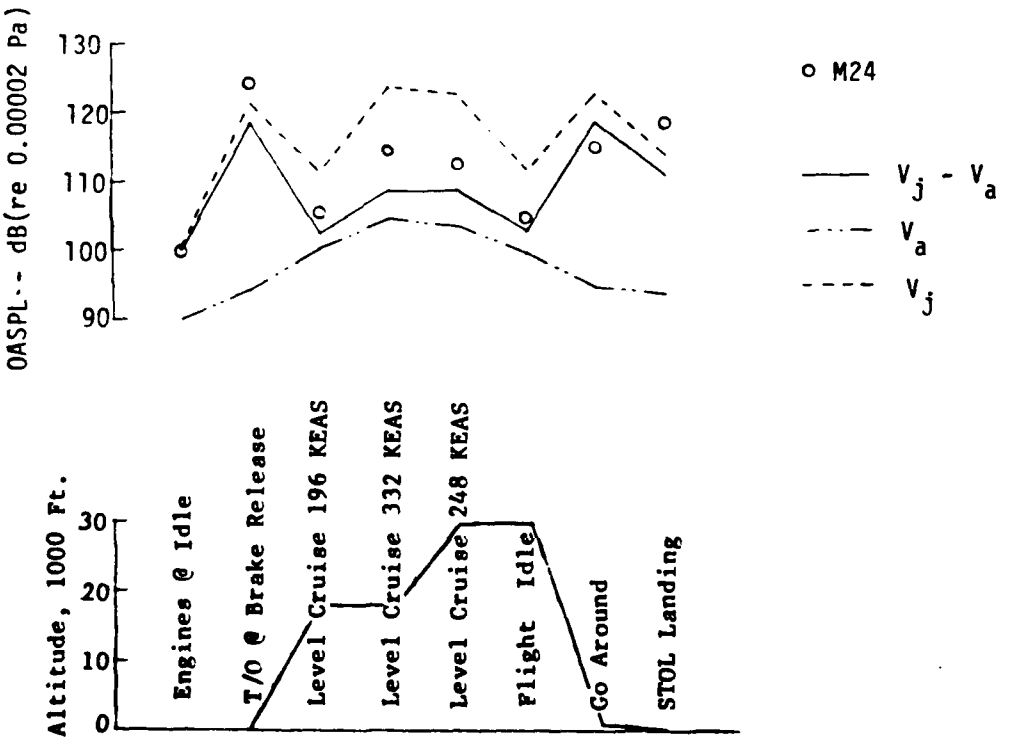

FIGURE 37 RELATIONSHIP BETWEEN AIRCRAFT PARAMETERS AND AFT INTERIOR NOISE

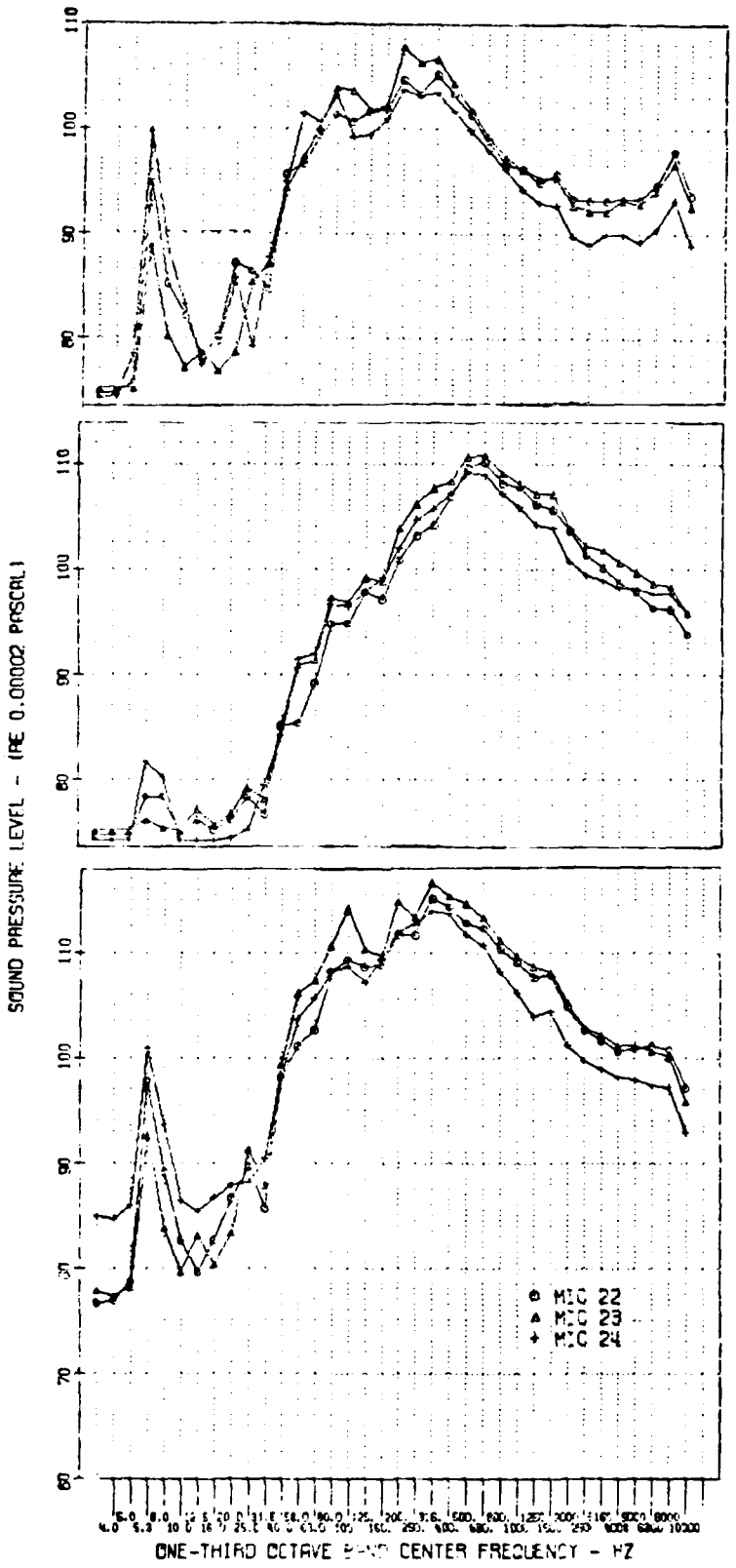

Landing Approach,
48° Flaps

EPR= 1.60

Cruise, 18,000 Feet,
1° Flaps, 1.89EPR,350 KEAS

Takeoff, 24° Flaps

EPR= 2.20

FIGURE 39 INTERIOR NOISE LEVELS MEASURED ALONG CENTERLINE DURING TAKEOFF, CRUISE, AND LANDING APPROACH

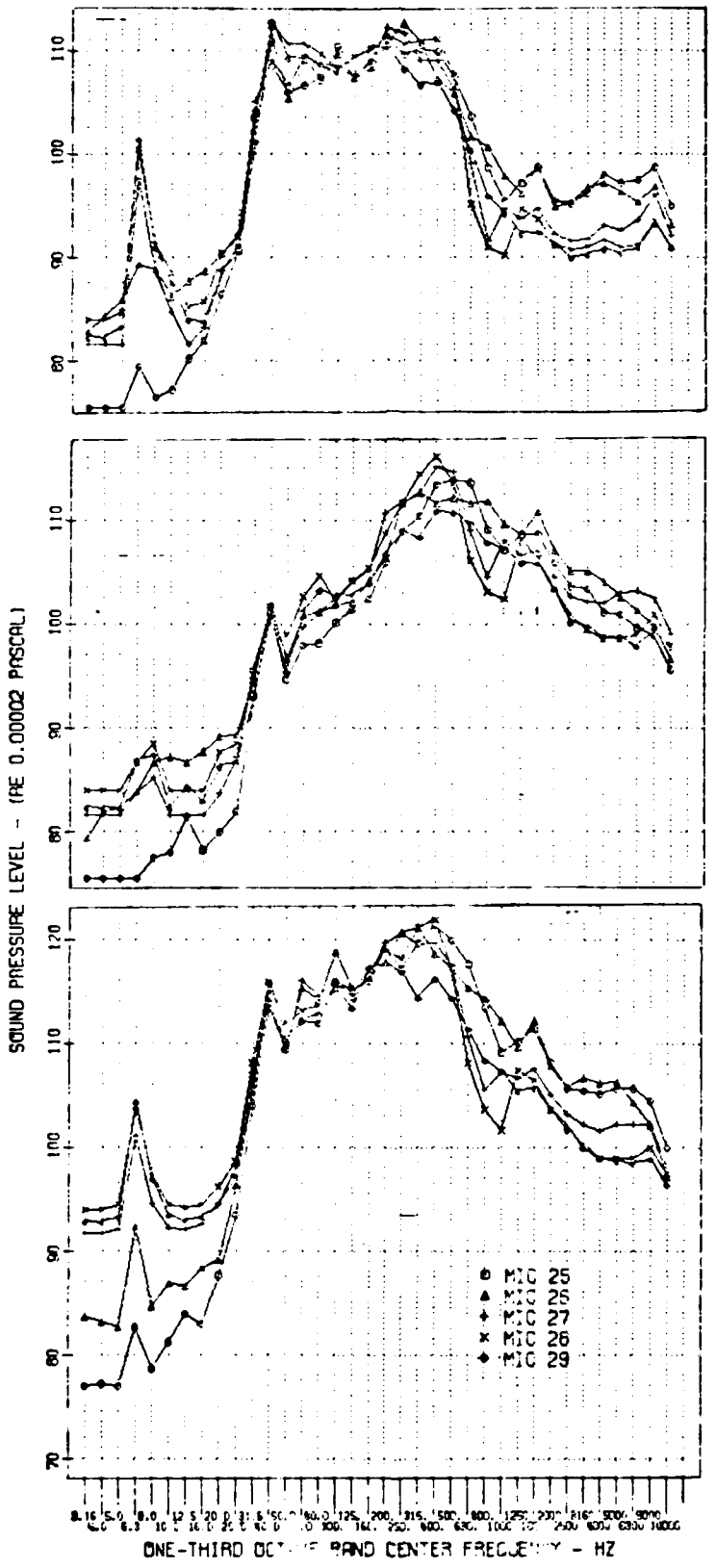

Landing Approach, 48° Flaps
EPR= 1.60

Cruise, 18,000 Feet,
350 KEAS, 1° Flaps, 1.89EPR

Takeoff, 24° Flaps
EPR= 2.20

FIGURE 40 INTERIOR NOISE LEVELS MEASURED ALONG FUSELAGE SIDEWALL DURING TAKEOFF, CRUISE, AND LANDING APPROACH

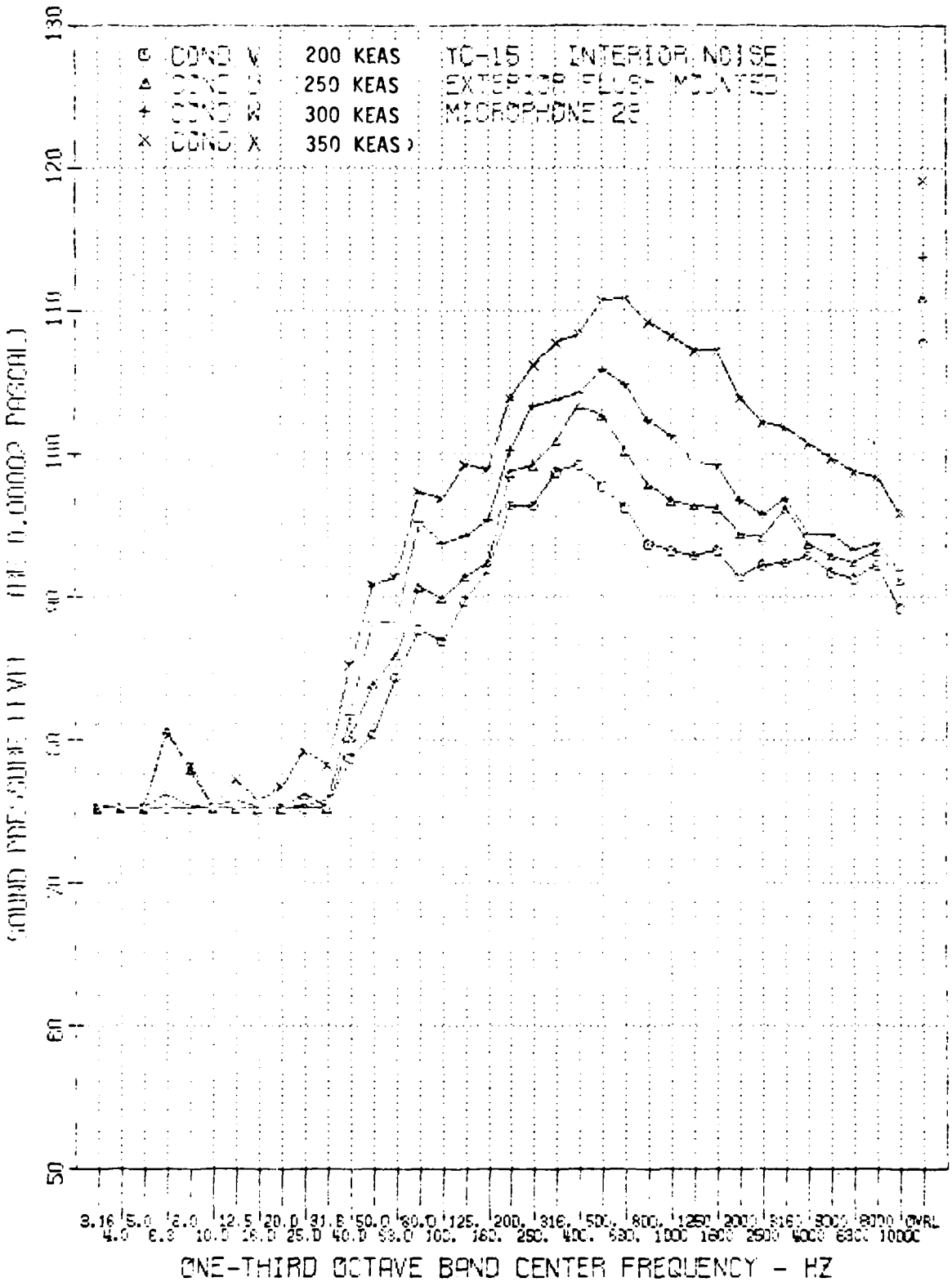

FIGURE 41 EFFECT OF FORWARD SPEED ON INTERIOR CENTERLINE NOISE DURING CRUISE AT 18,000 FEET, 1° FLAPS

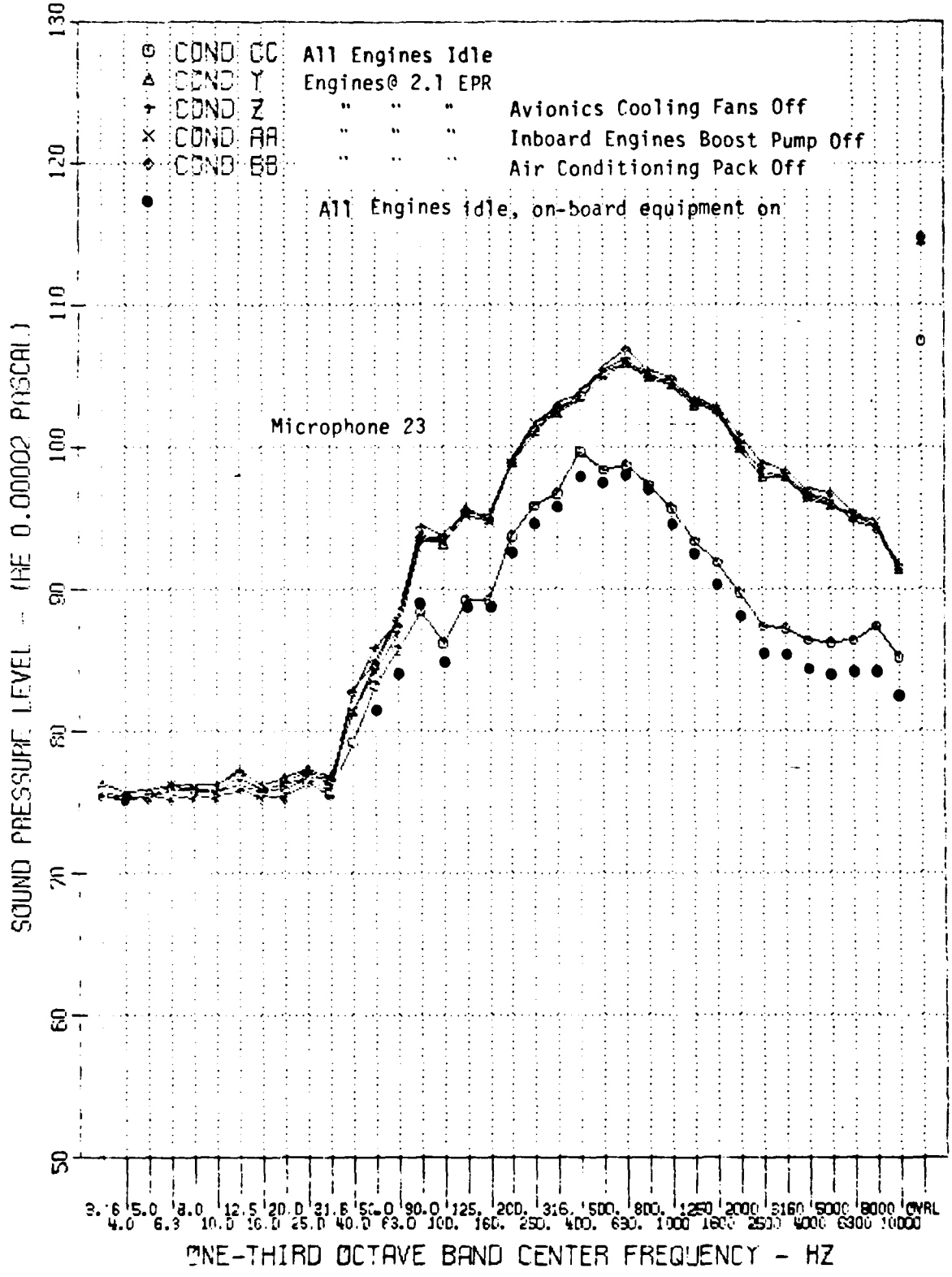

FIGURE 42 EFFECTS OF ONBOARD EQUIPMENT ON CENTER AISLE INTERIOR NOISE AT 30,000 FEET, 250 KEAS, 3° FLAPS, 2.01 EPR

insulation) does not provide sufficient noise reduction to measure the effects of on-board equipment noise.

Data provided in Figure 43 presents spectra for ground idle and takeoff at cabin aisle positions (Microphones 22, 23, 24). For the takeoff condition, the interior noise spectra are relatively smooth, whereas, for the ground idle condition, the spectra contain distinct peaks. These peaks could be characteristic of equipment noise (cooling fans, hydraulics, air conditioning). These peaks are also present in all sidewall spectra.

Octave band spectra for cruise conditions at 18,000 and 30,000 feet at a mid-cabin location are plotted in Figure 44. These data are compared to the noise criteria in MIL-S-008806B for personnel using standard-issue crew member head gear. The noise data at 30,000 feet fall below the 30 minute cumulative mission exposure limit. The 18,000 feet data also do with the exception of the SPL at 500 Hz. This could pose a hearing problem since a minimum of 2 hours of cruise is expected. It should be pointed out that these data were obtained with an aircraft which had no acoustic and/or thermal insulation on the fuselage sidewalls. An interior with insulation or septum would provide a better noise attenuation performance above 250 Hz and reduce cabin noise levels. This would allow the 120 minute cumulative exposure limit to apply.

6.5 Relationship Between Exterior and Cabin Noise

One of the objectives of the study is to determine the reduction in acoustic energy during transmission from the exterior to the interior. This reduction in traditional terms is referred to as the noise reduction (NR) of the fuselage sidewall. The noise reduction is the net effect of the transmission loss (TL) of the sidewall and the absorptivity of the cabin. If the sound source in the exterior produces an acoustic pressure level SPL_{ex}, corresponding to which these results a pressure level SPL_{in} in the cabin, then the noise reduction of the sidewall is:

$$NR = SPL_{ex} - SPL_{in} = 10 \log p_{ex}^2/p_{in}^2 \qquad (1)$$

The noise reduction afforded by the sidewall depends not only on the sidewall, but also the absorptive properties of the cabin. Equation (1) defines NR as the sound pressure level difference between a source and the cabin, with the sidewall in between.

The flow of power is one way to express the sound transmission through a structure. The difference between the transmitted acoustic power into the cabin (W_t) to the acoustic power incident on the sidewall (W_i) is called transmission loss (TL), i.e.:

$$TL = 10 \log \frac{W_t}{W_i} = 10 \log \frac{1}{\tau} \qquad (2)$$

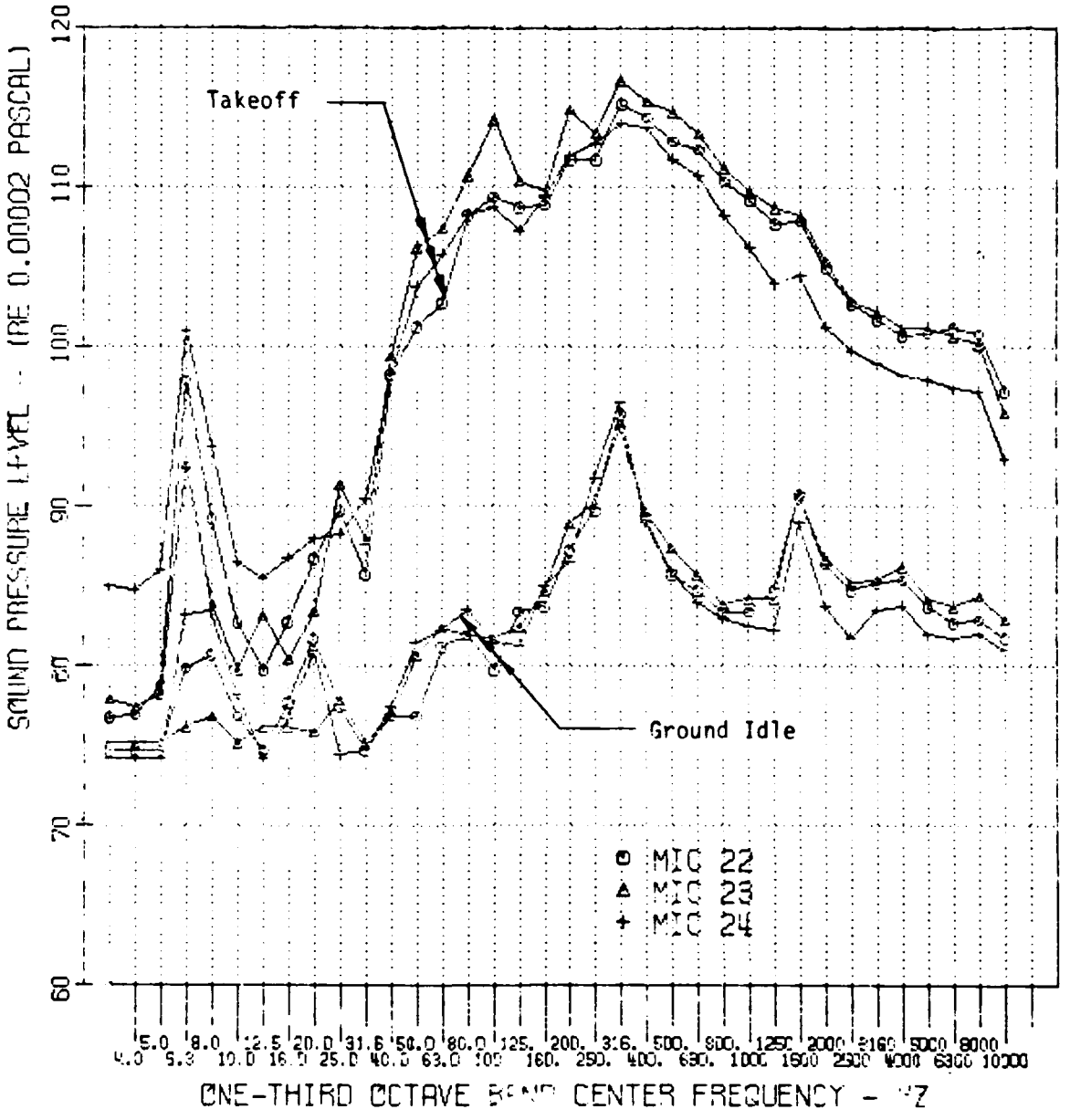

FIGURE 43 COMPARISON OF NOISE AT TAKEOFF AND GROUND IDLE CENTERLINE SPECTRA

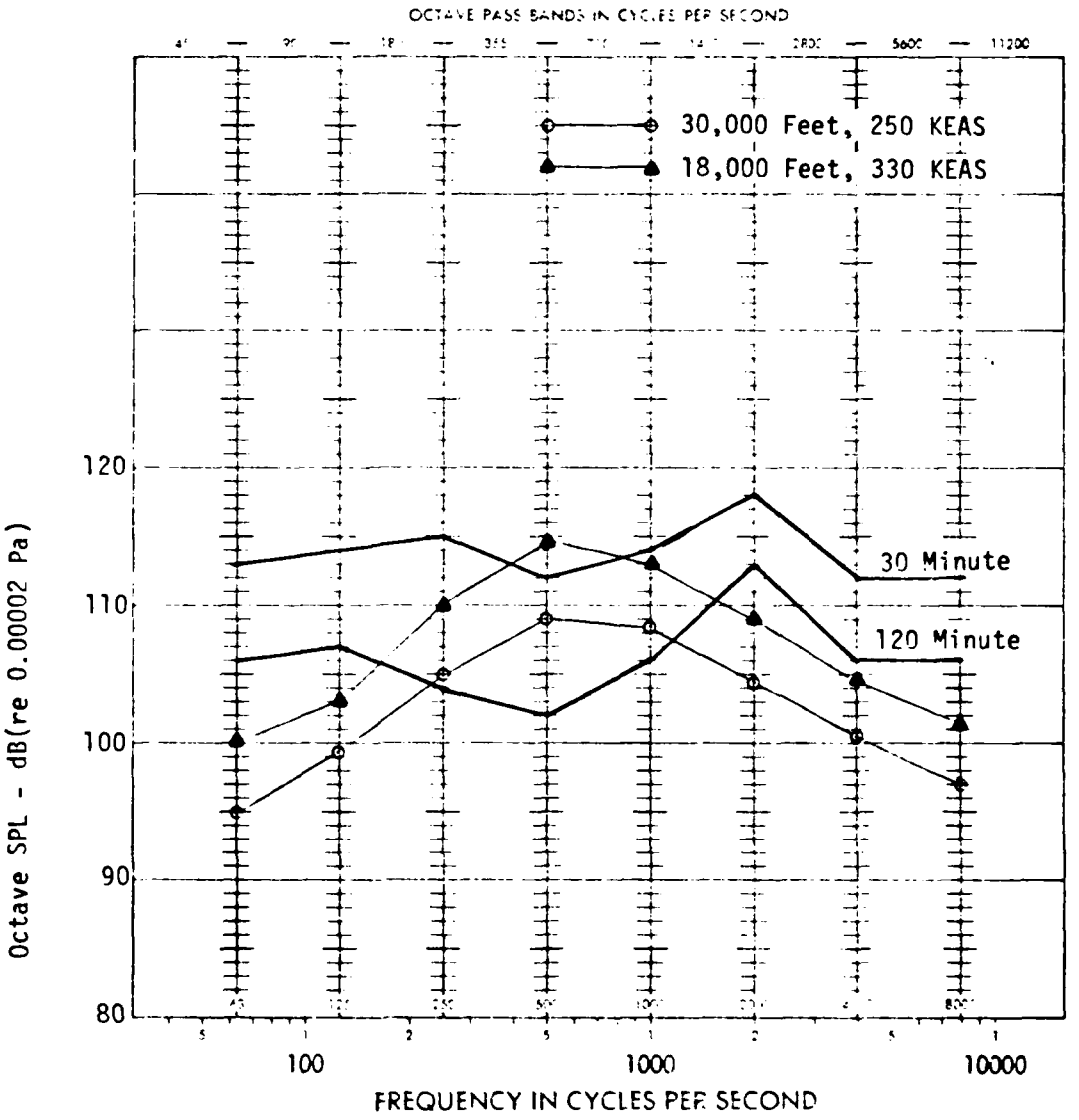

FIGURE 44 SOUND PRESSURE LEVELS AT MID-CABIN(M23) LOCATION AND CUMULATIVE MISSION EXPOSURE LIMIT FOR STANDARD ISSUE CREW MEMBER HEADGEAR

If the acoustic field on the exterior of the fuselage is reverberant, then W_i is related to the mean square pressure p_{ex} as:

$$W_i = A\ P_{ex}^2/4\rho c \qquad (3)$$

where A is the radiating surface area of the fuselage, and ρc is the characteristic impedance of the air surrounding the fuselage.

If a portion of the transmitted acoustic power into the cabin is absorbed by the sidewall, then the power supplied to the reverberant acoustic field in the cabin is $W_t\ (1-\bar{\alpha})$ where $\bar{\alpha}$ is the average absorption coefficient of the cabin. This input power must equal the power loss, which equals times the power incident on the cabin walls. Therefore, the transmitted power for the cabin is:

$$W_t(1 - \bar{\alpha}) = \bar{\alpha}\ S\ P_{in}^2/4\rho c \qquad (4)$$

where S is the cabin surface area. If Equations (1) through (4) are combined, then:

$$TL = NR + 10 \log A/R \qquad (5)$$

where R is the room constant of the cabin which accounts for acoustic properties of the interior and is equal to:

$$R = \bar{\alpha}\ S/\ (1 - \bar{\alpha}) \qquad (6a)$$

and

$$\bar{\alpha} = \frac{1}{S}\ \Sigma \alpha_i S_i \qquad (6b)$$

The last term in equation (5) is the room effect which is the increase in cabin noise due to incomplete wall absorption. The absorption coefficient is usually a slowly varying function of frequency. Since the YC-15 contained no acoustical insulation blankets or other acoustical treatment in the cabin, the acoustical absorption is low and the acoustic field in the cabin is diffuse. The acoustic absorption coefficients were determined inside the cabin by the Douglas Aircraft Company from reverberation times measured using a sound decay rate method (Ref. 3).

The character of transmission loss of sound through a fuselage sidewall can be described by architectural acoustics. It is shown graphically in Figure 45 as a function of the sound frequency incident on the sidewall. Several distinct regions can be shown. The first region is below the natural frequency of the structure where the transmission loss tends to be stiffness controlled except where cylinder or acoustic resonances may be present. The resonant region is next where the attenuation is low. The third region is above the sidewall resonance where mass of the sidewall is the controlling factor on the attenuation. The last region is where the sound wavelength in the atmosphere coincides with the bending wavelength on the sidewall. Only the stiffness of the structure (shell, frames, stringers) is important in the first

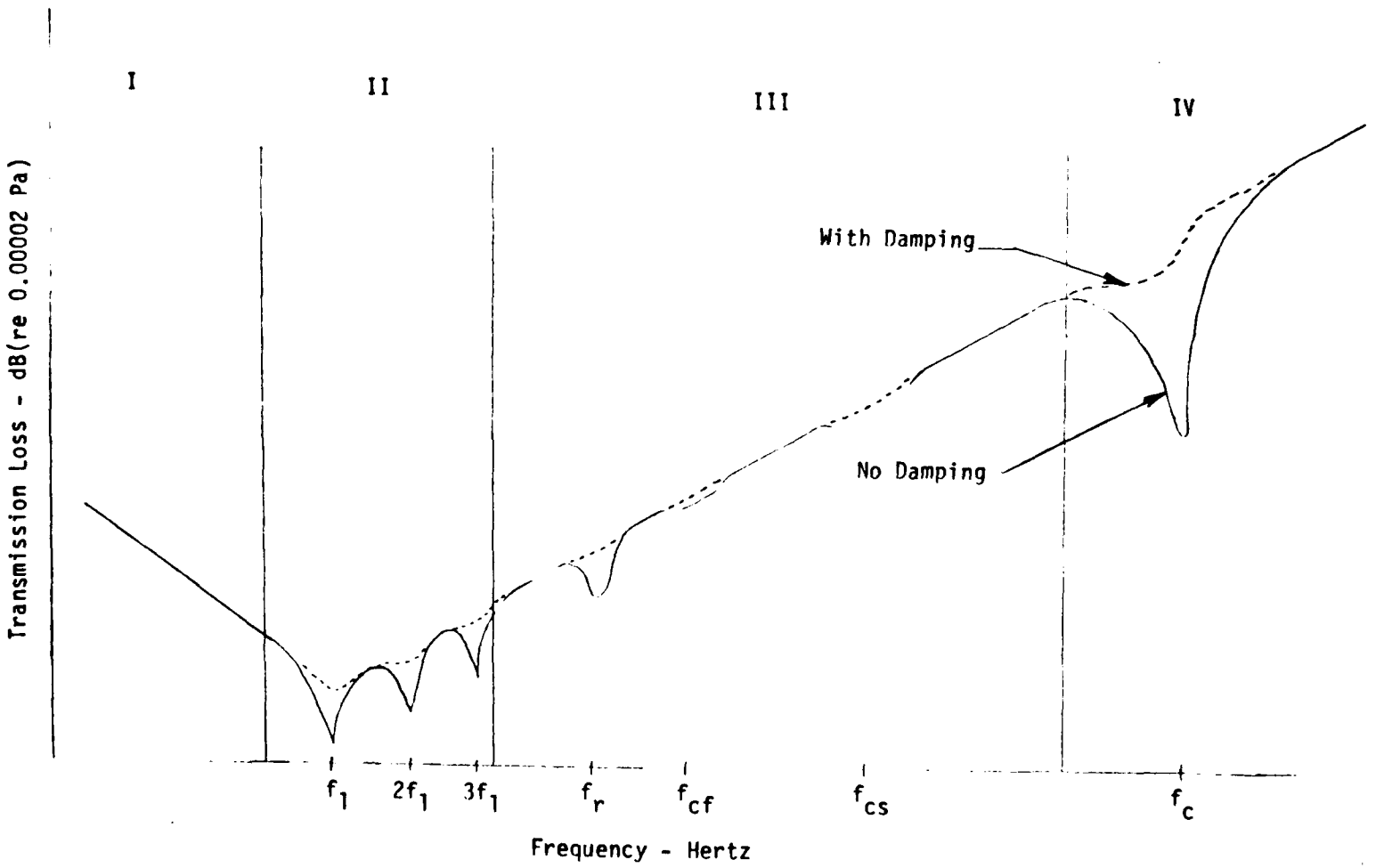

FIGURE 45 TRANSMISSION LOSS OF ACOUSTIC ENERGY THROUGH AIRCRAFT SIDEWALL

region. For most panels in a structure, the boundaries will be between simply supported and clamped. For this study, the diameter of the aircraft is so large (18 feet) that the fuselage panels can be assumed to be flat. The resonant frequency for a flat, simply-supported panel is given by (Ref 12):

$$fmn = \frac{\pi}{2}\left[\frac{Eh^3}{12M(1-\mu^2)}\right]^{0.5}\left(\frac{m^2}{L_x^2} + \frac{n^2}{L_y^2}\right) \qquad (7a)$$

where fmn = frequency of vibration of $(m,n)^{th}$ mode, Hertz

M = mass surface density of fuselage shell material, lb_m/in^2

ρ = mass density of fuselage shell material, lb_m/in^3

$= \frac{M}{h}$

m,n = positive integers, 1,2,3,...

E = Young's modulus of fuselage shell material, lb_f/in^2

μ = Poisson's ratio

h = skin thickness of fuselage shell, inches

L_x = panel short dimension, inches

L_y = panel long dimension, inches

From equation (7a) it can be seen that, for an aluminum panel of a given size, the fundamental mode response frequency is

$$f_{11} = 0.454\left[\frac{Eh^3}{M}\right]^{0.5}\left(\frac{1}{L_x^2} + \frac{1}{L_y^2}\right) \qquad (7b)$$

$$= 0.454\, h\, C_L\left[\frac{1}{L_x^2} + \frac{1}{L_y^2}\right] \qquad (7c)$$

where C_L = wave speed for longitudinal waves in fuselage shell material, in/sec

$$= \left[\frac{E}{\rho(1-\mu^2)}\right]^{0.5}$$

The frequency for a clamped panel is approximately twice that for a simply supported one.

In the second region, the damping of the shell can increase the attenuation, but the mass and stiffness have negligible effect. This region extends to about 3 to 4 times the panel fundamental frequency. Transmission loss in the third and fourth regions is controlled by mass law effects. However, major deviations in the transmission loss occur in the third region and at the intersection of the third and fourth regions. These frequencies cause a "dip" and are called coincidence (critical) frequencies. Coincidence is a condition at which flexural (structural) and acoustic wave speeds are equal. This is caused by the stiffness and the moment of inertia which is not constant in all directions. The fuselage skin as well as the frames and stringers are the structural elements that are capable of being excited under coincidence conditions. Another "dip" in the transmission loss curve which occurs in the third region is due to the curvature of the skin. This frequency, called the ring frequency, corresponds to the breathing mode, in which the fuselage undergoes uniform contraction and expansion without flexural deformation. It is this frequency at which the longitudinal wave in the shell equals the fuselage circumference. The frequencies which can cause these "dips" are given by (Ref 13):

$$f_r = \frac{C_L}{\pi D} \tag{8}$$

$$f_{cf} = f_r \left(\frac{c}{C_L}\right)^2 \frac{D\sqrt{12(1-\mu^2)}}{2h_f} \tag{9}$$

$$f_{cs} = f_r \frac{c}{C_L} \frac{D\sqrt{12(1-\mu^2)}}{2h_s} \tag{10}$$

$$f_c = \frac{\sqrt{3}}{\pi h} \frac{C^2}{C_L} \tag{11}$$

where f_r = ring frequency, Hertz

f_{cf} = coincidence frequency for flexural waves across the frames, Hertz

C = speed of sound of air, feet/second

D = fuselage diameter, feet

h_f = equivalent shell thickness in axial direction, inches

$$= h \left[1 + 12 (1 - \mu^2) \frac{I_f}{L_y h^3} \right]^{1/3}$$

f_{cs} = coincidence frequency for flexural waves across the stringer, Hertz

h_s = equivalent shell thickness in circumferential direction, inches

$$= h \left[1 + 12 (1 - \mu^2) \frac{I_s}{L_x h^3} \right]^{1/3}$$

I_f = area moment of inertia of frame cross-section, in^4

I_s = area moment of inertia of stringer cross-section, in^4

f_c = skin coincidence frequency, Hertz

Near the coincidence "dips", the transmission loss can be affected by decreasing the panel thickness so as to make the coincidence frequencies greater than the incident sound. Increasing the damping can affect the "dip" and make them not as predominant. The coincidence frequency for the frames is normally low frequency, and its behavior can be influenced by the pressure differential across the sidewall. This frequency is not always discernible in transmission loss plots (Ref 14).

The arithmetic differences in sound pressure level for three exterior positions (Microphones 2, 5, 8) and the corresponding interior centerline SPL (Microphones 25, 23, 24) are plotted in Figure 46. The resulting noise reduction shown is for ground static operation for two different flap settings. Displayed along with the data are the calculated values for natural frequency, ring frequency, and coincidence frequencies. Note that the calculated frequencies agree with the "dips" in the experimental data within one 1/3 octave band. The shape of the curves resemble that of Figure 45. Comparing the curves of Figure 46 reveals very little difference between them. The power setting apparently has little or no effect on the noise reduction of the fuselage. The only significant difference is comparison between the 1° and 23° flap setting for the Microphone pair 24 and 8. Above the ring frequency, deploying the flaps results in the noise reduction being lowered 3-5 dB.

A sampling of the noise reduction typically measured during cruise conditions is shown in Figure 47. The same three pairs of microphones which were used previously are again used. Two sets of data are given for cruise at 30,000 feet with the third set from data at 18,000 feet. These data are expected to differ from that measured on the ground because of the difference in the type of excitation. The type of excitation for the ground data is assumed to be jet noise, while the cruise data should be predominantly turbulent boundary layer excitation. Jet noise is a highly space coherent form of excitation, while turbulent boundary layer is only moderately space coherent. Hence, for

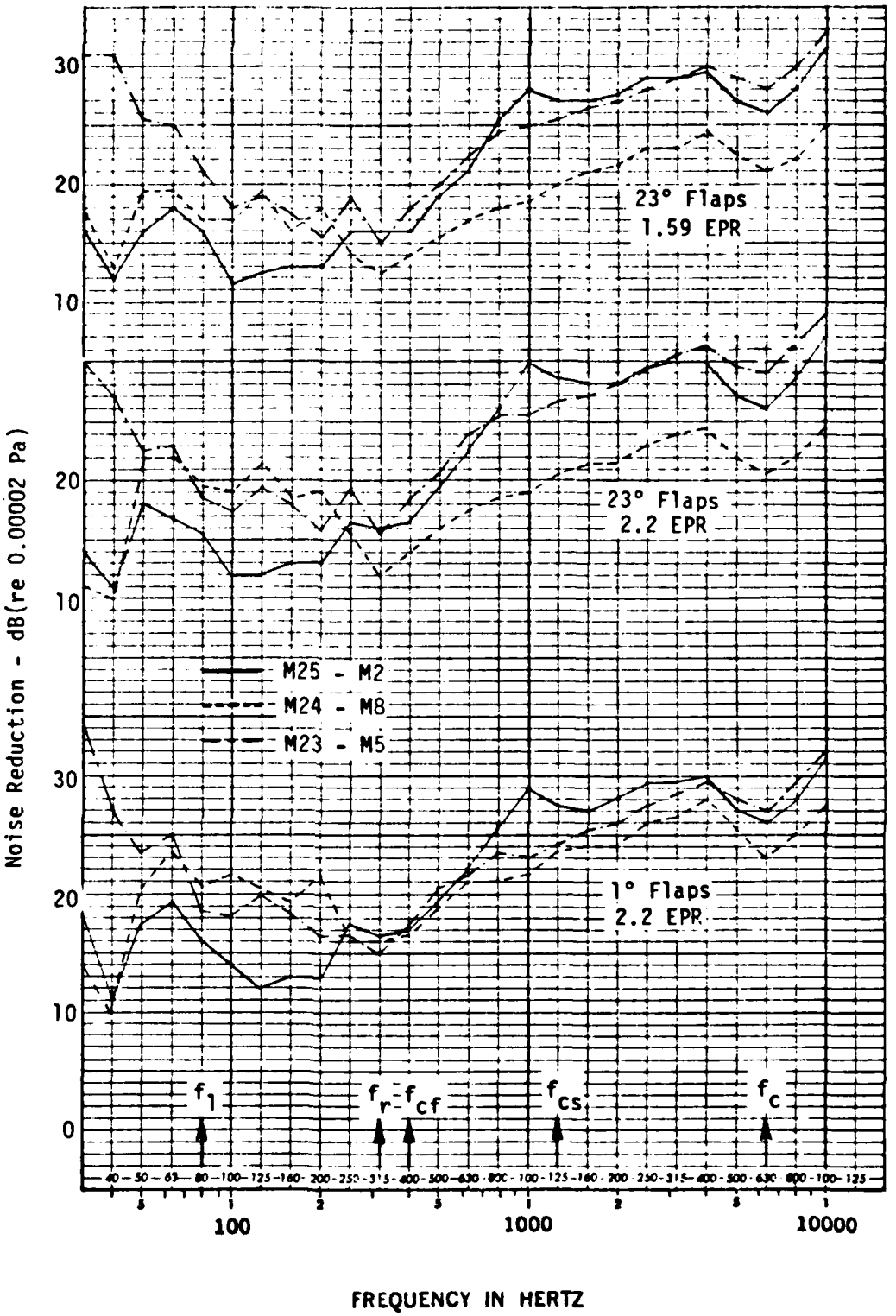

FIGURE 46 NOISE REDUCTION FOR GROUND STATIC OPERATION AT GROUND STATIC

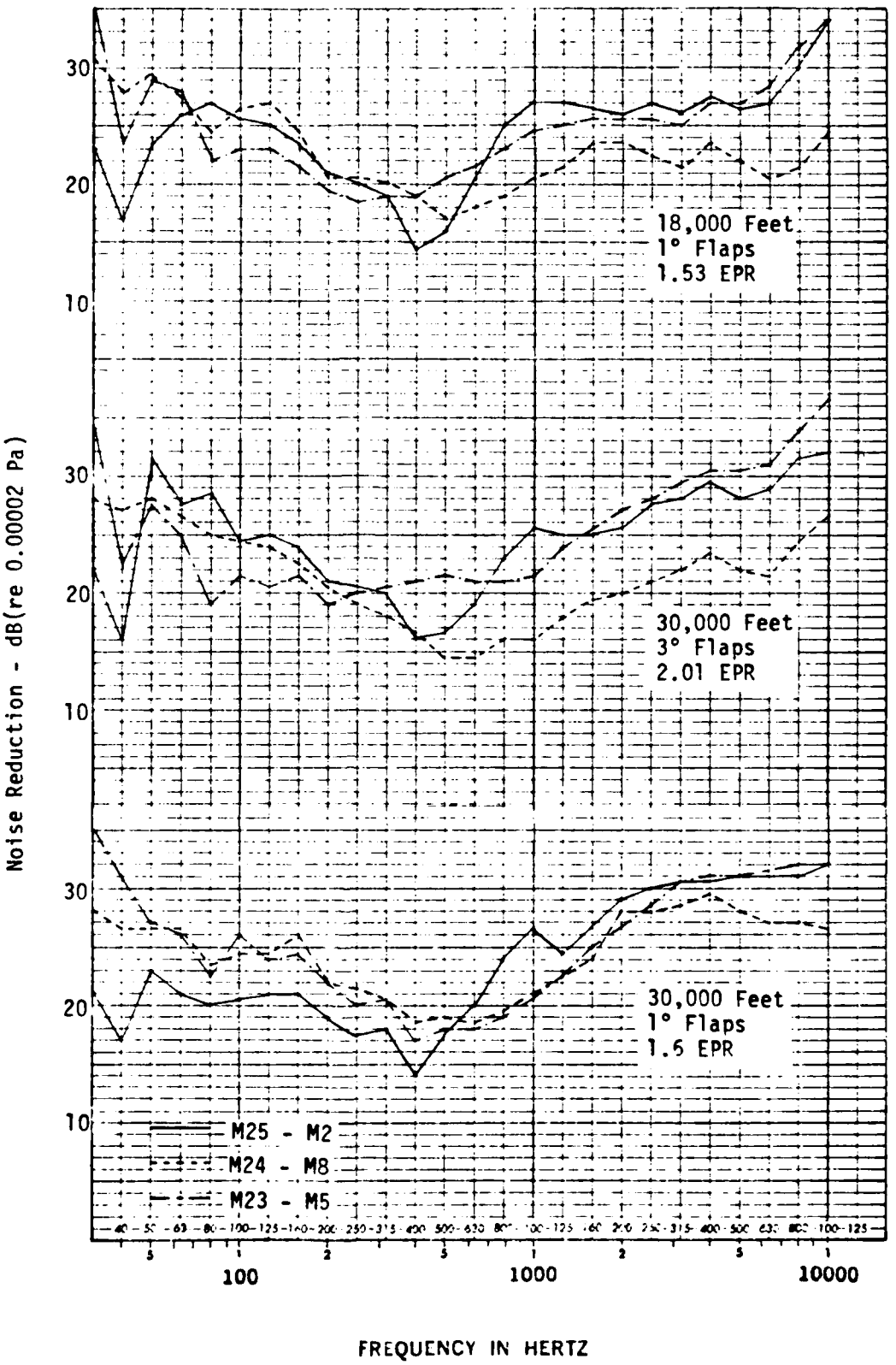

FIGURE 47 MEASURED NOISE REDUCTION FOR CRUISE CONDITIONS AT 18,000 FEET AND 30,000 FEET AND FLIGHT IDLE AT 30,000 FEET

the same external pressure level, jet noise is more efficient at exciting the fuselage structure. A comparison of the typical noise reduction measured on the ground and at 18,000 and 30,000 feet altitude cruise is shown in Figure 48. Both the level and the spectrum shape are altered. The noise reduction at cruise is higher below the region of the ring frequency (approximately 315 Hz), this being attributed to the less well correlated turbulent boundary layer excitation. The external flow at cruise affected the "dips" at the coincidence frequencies by smoothing them out. Flow provides a modest decrease in the mass law region (400-2000 Hz). It is interesting to note that part of the difference in the curves is that due to the mismatch between the atmospheric properties at the different altitudes. A direct impedance mismatch ($\rho_{ex}\ c_{ex}/\rho_{in}\ c_{in}$) would result in about 5 dB of this difference. These observations tend to corroborate the mathematical model of Koval (Ref. 15).

The effect of airspeed on the noise reduction of the sidewall is shown in Figure 49. The data plotted are for cruise conditions at 18,000 feet. Both sets of data show similar trends. The higher speed data generally dominate in the resonance region up through the coincidence frequencies and the lower speed data dominate in the stiffness-controlled region below resonance.

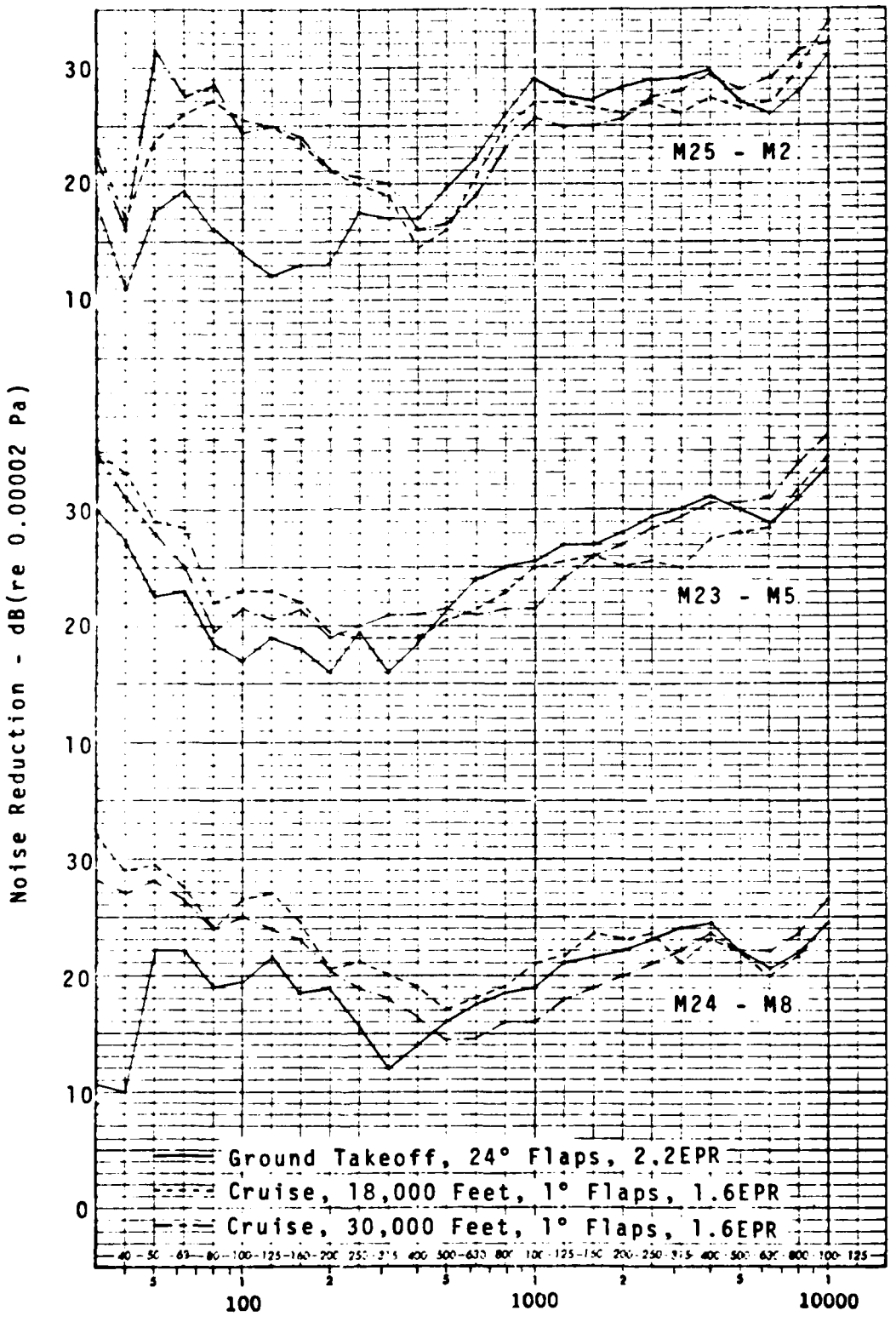

FIGURE 48 COMPARISON OF NOISE REDUCTION ON THE GROUND AND AT CRUISE

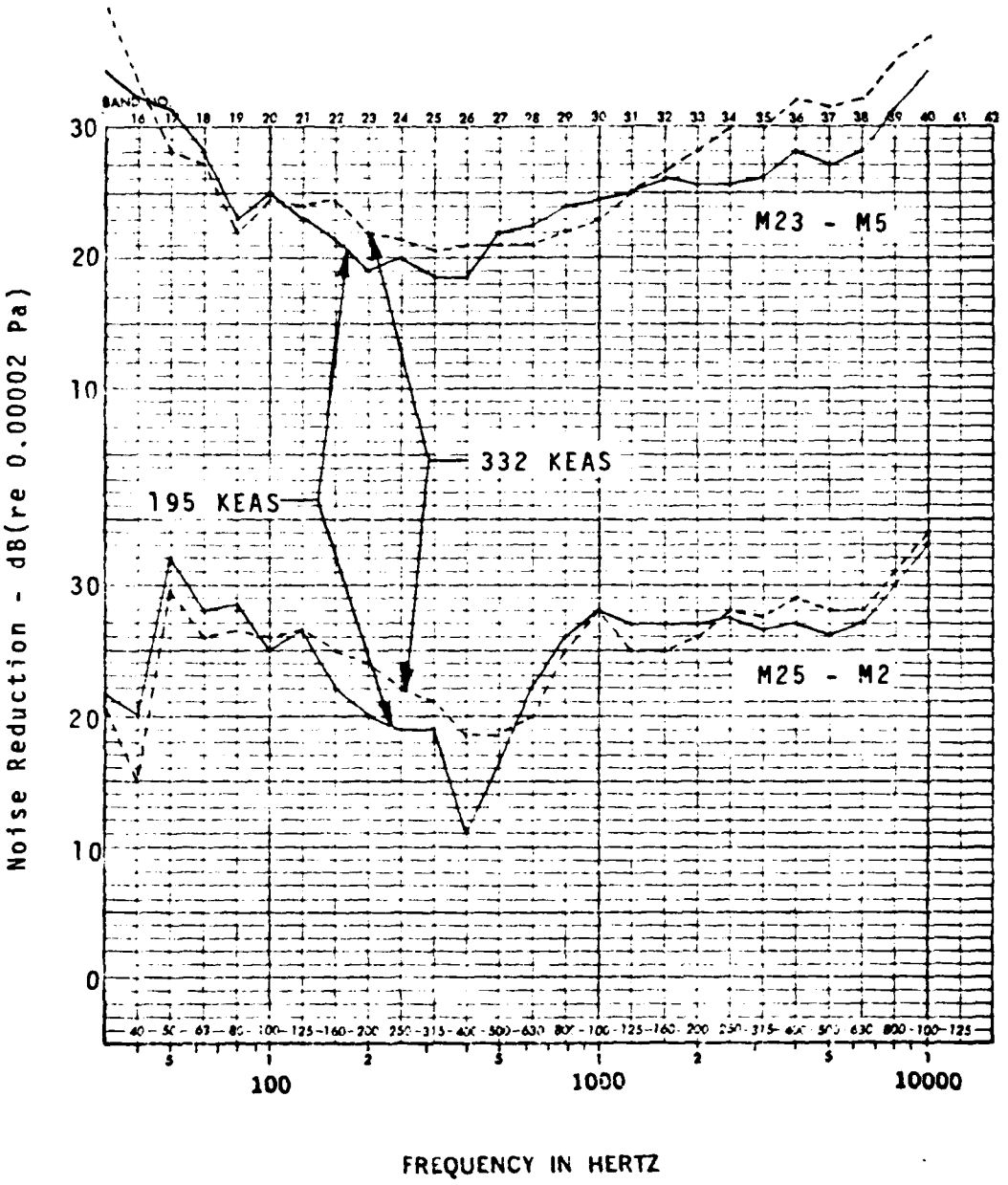

FIGURE 49 EFFECT OF AIRSPEED ON NOISE REDUCTION AT 18,000 FOOT ALTITUDE

VII. CONCLUSIONS

Analysis of the data acquired on the YC-15 aircraft has resulted in a characterization of the noise field, both exterior fuselage and cabin interior of this airplane.

The maximum exterior fuselage noise levels occur on fuselage areas close to and aft of the engine exhaust streams where the exhaust flow appears to impinge or scrub on the fuselage. Maximum cabin noise levels occur close to end aft of the engine exhaust streams, consistent with the portions of the fuselage sidewall closest to the engine exhausts. Inboard engines dominate the noise over the outboard engines.

The cabin sidewall noise levels are similar to the center aisle levels except in the frequencies below 250 hertz. The low frequency differences are conjectured to be due to interior cabin standing waves. Cabin noise appears to be controlled by noise propagating through the sidewall.

Jet exhaust noise controls the exterior fuselage and aft cabin noise during normal flight, no flaps operation. This source of noise dominates those fuselage areas close to or aft of the engine exhaust.

Fuselage sidewall vibration correlated with the exterior fuselage noise. Cabin noise correlated with cabin wall vibration. Not unexpectedly, the cabin noise was simply related to the exterior fuselage noise.

APPENDIX

DATA ACQUISITION AND REDUCTION SYSTEM

The data acquisition system for the interior acoustic tests is diagrammed in Figure 3. Three basic transducer types were used to measure exterior acoustic loads, local fuselage vibrations, and interior noise levels. Endevco Corporation Model 2150 M4A high intensity piezoelectric microphones and Endevco Model 2760A charge amplifiers were used for the acquisition of the exterior acoustic loads data. The microphones and charge amplifiers exhibited a frequency response that was flat within ± 5% and less than ± 35° phase shift from 2 Hz to 20 KHz. Fuselage vibration was measured with Bolt, Beranek, and Newman Inc. (BBN) Model 501 piezoelectric accelerometers with internal preamplifier and mating power supply (Model P-10) and the Intech Inc. Model 2538 voltage amplifier. Each accelerometer and signal conditioner had a frequency response that was flat within ± 5% over a frequency range of 8 Hz to 20 KHz. Interior noise equipment consisted of Bruel and Kjaer (B&K) Type 4134 one-half inch diameter condenser microphone cartridges, B&K Type 2615 microphone preamplifiers, and B&K Type 226-16 power supplies and signal conditioners. This system provided a frequency response that was flat within ± 1 dB over a range of 20 Hz to 20 KHz.

The mounting system for the flush-mounted exterior microphones is shown in Figure 4. They were mounted so that the diaphragm of each exterior microphone was flush with the exterior skin of the aircraft. The gap between the microphone and the fuselage skin was sealed with a sealant to provide both pressure seal and isolation from the aircraft sidewall. The interior microphones were either clamped to the aircraft structure or mounted on tethered tripod stands. The accelerometers were either bonded directly to the aircraft structure or screwed into mountings that were bonded to the structure with dental cement.

The transducers were located as shown in Figure 5 (except for Microphone 9, the forward exterior flush-mounted microphone location) and listed in Table 1. The accelerometers were mounted one panel below the microphones where possible, in order to locate the accelerometers in the proximity of the flush-mounted microphones and reduce the effects of the microphone mounts.

The data recording system consisted of two Honeywell Model 5600C instrumentation recorders. The recorders had frequency response that was flat within ± 1 dB over a frequency range of 0 to 10 KHz at a tape speed of 30 in/sec.

Calibration signals were recorded on the data channels to provide reference signals for data reduction purposes. These calibrations were performed during preflight checkout and before and after each test sequence. Data channels had 1 KHz and 10 KHz reference signals applied simultaneously to all channels to provide phase reference to account for tape recorder and tape reproducer head stack alignment. All channels were calibrated with pink noise (constant energy per octave bandwidth) for the determination of frequency response characteristics. Vibration channels were calibrated at 100 Hz with voltages that were equivalent to the output signal of each accelerometer when vibrated by an electro-mechanical shaker. The acoustic data channels were calibrated with a B&K Type 4220 pistonphone providing 124 dB re 20μPa at 250 Hz. Thirty seconds

of ambient and/or system noise were recorded on magnetic tape prior to starting and after the day's tests. These measurements determined the background level of the acquisition system for each channel.

Data processing was performed in two places: The Douglas Acoustics and Vibration Data Center at Long Beach, California; and later by the Flight Dynamics Laboratory, Structures and Dynamics Division at Wright-Patterson AFB, Ohio.

The basic data from Douglas Data Center were processed and printed with the Flight and Laboratory Development Sigma 7 Computer Program G4SE. Averaging time for data processing was 10 seconds for most cases. All acoustic data were corrected for system frequency response and pressure response characteristics, and all vibration data were corrected for system frequency response. The data were reduced by passing the recorded signals through a General Radio Model 1952 Universal Filter with a bandpass of 40-11,200 Hz and a Bruel & Kjaer Type 2107 Frequency Analyzer using the linear weighting network. These data were recorded as time history charts on a Bruel and Kjaer Type 2305 Level Recorder containing a logarithmic potentiometer. The Program G4SE output is a tabular listing of one-third octave-band, octave-band, A-weighted, and overall levels. One third octave band data and A-weighted levels for most of the test conditions are contained in Reference 8.

The magnetic tapes which were processed at Wright-Patterson AFB were played back on a Honeywell 96 Record/Reproduce System. All analyses were obtained using a General Radio 1921/1926 one-third octave band analyzer. This analyzer was interfaced with an ITI 4900 A/D System. All analyses were processed by a Raytheon 704 Computer, which was interfaced with a Gould 4800 High Speed Plotter.

REFERENCES

1. Warnix and Hines, "YC-15 Interior Noise Measurements-Technical Discussion," Air Force Flight Dynamics Laboratory, AFFDL-TR-76-140, March 1981.

2. Yee, "Flight Effects on Fan Inlet Noise (YC-15 Flight Data for NASA AMST Experiments)," McDonnell-Douglas Corp., Report MDC J-7193, February 1977.

3. Warnix, "Acoustic Absorption Characteristics of the Douglas YC-15" McDonnell-Douglas Corp., Report MDC J-7208, August 1977.

4. Stuart, "YC-15 EBF Aero-Acoustic Loads and Thermal Environment Measurements," McDonnell-Douglas Corp., Report MDC J-7190, February 1977.

5. Peck, "YC-15 Externally Blown Flap Noise," Air Force-Wright Aeronautical Laboratories, AFWAL-TM-82-161-FIBE, February 1982.

6. "Flight Tests Plans - YC-15 Ground and Flight Data Acquisition for NASA and Air Force Flight Dynamics Laboratory: Interior Noise, EBF Aero-Acoustic Loads, and Thermal Environment, and Engine Inlet Acoustics," McDonnell-Douglas Corp., Report MDC J-6055, April 1976.

7. "Ground and Flight Test Plan - YC-15 Interior Noise Measurements," McDonnell-Douglas Corp., Report MDC J-6047, August 1975.

8. Warnix and Lockman, "YC-15 Interior Noise Measurements in Data," McDonnell-Douglas Corp., Report MDC J-7199, December 1976.

9. Ungar, et al, "A Guide for Estimation of Aeroacoustic Loads on Flight Vehicle Surfaces," Air Force Flight Dynamics Laboratory, AFFDL-TR-76-91, Vol. I, February 1977.

10. Lowson, "Prediction of Boundary Layer Pressure Fluctuations," Air Force Flight Dynamics Laboratory, AFFDL-TR-67-167, April 1968.

11. Bartel and Schneider, "A Method for Predicting Acoustically Induced Vibration in Transport Aircraft," Air Force Flight Dynamics Laboratory, AFFDL-TR-74-74, Appendix I, September 1974.

12. Beranek, Noise and Vibration Control, McGraw-Hill Book Co., 1971.

13. Miller and Faulkner, "Prediction of Aircraft Interior Noise Using the Statistical Energy Analysis Method," ASME Paper 81-DET-102, September 1981.

14. Franken and Kerwin, "Methods of Flight Vehicle Noise Prediction," WADC-TR-58-343, November 1958.

15. Koval, "On Sound Transmission into a Thin Cylindrical Shell under Flight Conditions," Journal of Sound and Vibration, 48 (2), pp. 265-275, 1976.

END

DATE
FILMED

9 — 83

DTIC